89001599

MAY 07 1992

DOE/CNWRA TRANSMITTAL 91010

Mr. John P. Roberts, Acting Associate Director
for Systems and Compliance
Office of Civilian Radioactive Waste Management
U.S. Department of Energy, RW-30
Washington, D. C. 20585

Dear Mr. Roberts:

SUBJECT: Transmittal of Center for Nuclear Waste Regulatory Analyses (CNWRA) Report No. CNWRA 91-010 - "Sensitivity and Uncertainty Analyses Applied to One-Dimensional Transport in a Layered Fractured Rock"

Enclosed for your information is the recently released report regarding the above stated subject.

Should you have any questions regarding this matter you may contact me at (301) 504-3391.

Sincerely,
/S/
Joseph J. Holonich, Director
Repository Licensing and Quality
Assurance Project Directorate
Division of High-Level Waste Management
Office of Nuclear Material Safety
and Safeguards

Enclosure: On shelf.
As stated

cc w/encls:
R. Loux, NV
S. Bradhurst, Nye County, NV
D. Bechtel, Clark County, NV
P. Niedzielski-Eichner, Nye County, NV
V. Poe, Mineral County, NV
R. Williams, Lander County, NV
L. Vaughan II, Esmeralda County, NV
T. J. Hickey, Nevada Legislative Committee
C. Gertz, DOE/NV
M. Baughman, Lincoln County, NV
D. Weigel, GAO
C. Thistlethwaite, Inyo County, CA
F. Sperry, White Pine County, NV
P. Goicoechea, Eureka County, NV
C. Shank, Churchill County, NV

DISTRIBUTION w/o enclosure

CNWRA	NMSS R/F	HLPD R/F	LSS
LPDR	ACNW	PDR	Central File
BJYoungblood, HLWM	JLinehan, HLWM	MFederline, HLHP	RBallard, HLGE
On-Site Reps	JHolonich, HLPD	AG r/f	

*See previous concurrence

OFC :HLPD	:HLHP	:HLPD	:
NAME:Gareia	MFederline	JHolonich	:
Date: 5/7/92	:5/6/92	5/7/92	

426.1
WM-1
NH16

9205130277 920507
PDR WASTE
WM-1 PDR

OFFICIAL RECORD COPY

CNWRA 91-010

SENSITIVITY AND UNCERTAINTY ANALYSES APPLIED TO ONE-DIMENSIONAL TRANSPORT IN A LAYERED FRACTURED ROCK

PART 1: ANALYTIC SOLUTIONS AND LOCAL SENSITIVITIES

Prepared for

Nuclear Regulatory Commission
Contract NRC-02-88-005

Prepared by

Center for Nuclear Waste Regulatory Analyses
San Antonio, Texas

August 1991

CNWRA 91-010

SENSITIVITY AND UNCERTAINTY ANALYSES APPLIED TO ONE-DIMENSIONAL TRANSPORT IN A LAYERED FRACTURED ROCK

PART 1: ANALYTIC SOLUTIONS AND LOCAL SENSITIVITIES

Prepared for

Nuclear Regulatory Commission
Contract NRC-02-88-005

Prepared by

A. B. Gureghian
Y.-T. Wu
B. Sagar

Center for Nuclear Waste Regulatory Analyses
San Antonio, Texas

and

R. B. Codell

Nuclear Regulatory Commission
Office of Nuclear Materials Safety & Safeguards

August 1991

TABLE OF CONTENTS

TABLE OF CONTENTS (Continued)

LIST OF FIGURES

LIST OF FIGURES (Continued)

LIST OF TABLES

LIST OF TABLES (Continued)

LIST OF TABLES (Continued)

LIST OF TABLES (Continued)

ACKNOWLEDGMENTS

Several people assisted in the preparation of this report. The authors would like to express their appreciation for their efforts which greatly helped the document to reach its final form.

In particular, we would like to thank Drs. W. C. Patrick and R. Ababou for their reviews, Mr. A. Johnson and Ms. L. Tweedy for their graphical contributions, Messrs. E. Perez and D. Saathoff, of the Computer and Telecommunication Center, and Mrs. M. A. Gruhlke, who assisted in the coordination and production of this document.

EXECUTIVE SUMMARY

Mathematical models have become essential tools in performance assessment investigations, for estimating the potential impact of radionuclide migration out of a HLW geologic repository to the biosphere. These models involve a mathematical description of hydro-geochemical and geophysical processes, and their predictive capabilities are usually commensurate with our understanding of the various classes of geologic media: porous and fractured rock. Currently, the candidate HLW disposal site is one which is located in fractured tuff. Since this geological medium is poorly understood because of its inherent structural uncertainties and currently there is a limited ability to quantitatively describe geological processes in that medium, the use of simplified mathematical models for a conservative probabilistic assessment of performance is appropriate. Moreover, in spite of their limitations the high degree of precision of analytical models coupled with their computational efficiency have induced many investigators worldwide (Rosinger and Tremaine (1978), Hodgkinson and Maul (1985), Rasmuson and Neretnieks (1986), and Burkholder et al., (1976)) to adopt these for addressing some of the critical issues inherent to the containment characteristics of potential radioactive waste disposal sites.

This report is presented in two parts.

Part 1 reports the derivation and verification of the closed form analytical solutions of the one-dimensional non-dispersive and isothermal transport of a radionuclide in a layered system of saturated planar fractures coupled with diffusion into the adjacent saturated rock matrix. In addition to matrix diffusion effects as reported by Grisak et al., (1981, 1980) and Neretnieks (1980) (see also Gureghian (1990a) for a comprehensive list of references) on the one hand, and non-zero initial conditions in both fracture and rock as illustrated by Gureghian (1990b) on the other, three new features associated with 1) the layered nature of the rock matrix, 2) the length dependency of fracture aperture, and 3) periodicity aspect of radionuclides released from the source have been implemented in these new solutions.

Part 2 evaluates and demonstrates the use of several sensitivity and uncertainty analysis methods using the analytical model developed in Part 1.

The mathematical model "MULTFRAC" associated with Part 1 of this report includes two modules. The first module predicts the space-time dependent concentration of a decaying species migrating within the fracture network and the surrounding rock matrix layers, including the cumulative mass at an arbitrary observation point within the fracture. Note that the steady unidirectional flow of water through the fracture is normal to the rock matrix layers. Moreover, the material properties of individual fracture and rock matrix layers assumed to be fully saturated, are homogeneous and isotropic. The second module predicts the analytical and numerical local sensitivities i.e., the first order derivatives of the concentration and cumulative mass with respect to the dependent variables. These are basic requirements for parameter estimation or sampling design in the case of the concentration, and for uncertainty analysis of cumulative releases of a typical species from the repository at a typical point in time along the fracture as illustrated in Part 2 of this report.

The analytical solutions are based on the Laplace transform method where the domains of radionuclide migration in both fractures and rock layers are one-dimensional and of the semi infinite type, implying in this instance that radionuclide diffusion from the fractures wall to the rock matrix may extend to infinity. The sorption phenomena in both fracture and rock matrix layers are described by a linear equilibrium sorption isotherm. Two types of radionuclide release modes are considered: the continuously decaying and the periodically fluctuating decaying source, which may in turn be subject to step and band release modes. The initial concentrations in the fracture and rock matrix layers may be assigned spatially varying values in the case of the first whereas uniform ones may be implemented in both cases.

The verification of the new analytical solutions pertaining to solute transport in fracture and rock matrix was performed by means of several well established numerical evaluation methods of Laplace inversion integral proposed by Talbot (1979), Durbin (1974), and Stefhest (1970). Two test cases involving the migration of Np-237 and Cm-245, in a five-layered fractured rock system were investigated. An evaluation of some of these inversion methods over the range of investigated parameters have also been reported. On the other hand, the verification of the analytical solutions for the local sensitivities of the concentration and cumulative mass in the fracture with respect to the parameters of the system was performed by means of numerical differentiation techniques based on the finite-difference method of approximation.

APPLICATIONS

The deterministic solutions presented in Part I of this report are primarily related to performance assessment investigations of potential nuclear waste repository sites restricted to typical scenario analyses associated with long term migration of radionuclides in an idealized fractured rock system. The new predictive capabilities imbedded in the derived solutions are expected to improve the confidence of the investigator performing sensitivity and uncertainty analyses based on this model.

The model MULTFRAC was written in VAX FORTRAN Version 4.8 using the G floating point option (REAL*16). The computation was executed on a VAX 8700 under VMS Version 4.7

1. INTRODUCTION

For more than a decade analytical solutions have played an important role in assessing the impact of burying radioactive waste in permeable porous media (Gureghian (1987), Gureghian and Jansen (1985, 1983), van Genuchten (1982), Pigford et al., (1980), Hadermann (1980), Burkholder et al., (1976), Rosinger and Tremaine (1978), Lester et al., (1975), and Shamir and Harleman (1966)), and fractured rock masses (Gureghian (1990(a,b), Ahn et al., (1986, 1985), Chen (1986), Hodgkinson and Maul (1985), Sudicky and Frind (1984), Grisak and Pickens (1981), Kanki et al., (1981), Chambré et al., (1982), Sudicky and Frind (1982), Tang et al., (1981), and Neretnieks (1980)).

In order to cope with the heterogeneity problem currently witnessed in geologic media, a new analytical solution of radionuclide transport through an idealized saturated fractured rock system composed of n number of parallel fractured rock layers is developed. Typically each layer is assumed to be characterized by constant parameters.

In this instance the geometry of the cross section of such a fractured rock network corresponds to a series of connected parallel line segments of different thicknesses (see Figure 1.1). Computationally viable closed form analytical solutions which satisfy some of the requirements of Part 2 of this report (i.e., the section dealing with the uncertainties issues) are developed after assuming that transport through the fractures is predominantly caused by advection and that matrix diffusion may extend to infinity. In a single layer situation, the solution with zero dispersion in the fracture has been shown by Ahn et.al.,(1985) to yield close enough results to the one with non-zero dispersion contingent to it satisfying a criterion which will be subsequently reported. Furthermore, the solution corresponding to the infinite rock matrix diffusion case (i.e., single fracture) was proven by Gureghian (1990a) to yield similar results to the finite diffusion one (i.e., parallel fractures), as long as the resulting Fourier number, a dimensionless parameter, was less than or equal to 0.1

With the assumption that migration within the fracture is solely by advection, the mass flux F at the exit or entry face of a typical fracture layer i of unit width may be written as

$$F_i^{\pm} = [2b_i u_i A_i]^{\pm} \qquad (1.1)$$

where

A_i	is the concentration in the fracture (ML^{-3})
u_i	is the average fluid velocity in the fracture (LT^{-1})
$2b_i$	is the thickness of the fracture (L)
+	is the symbol of an entry face
-	is the symbol of an exit face

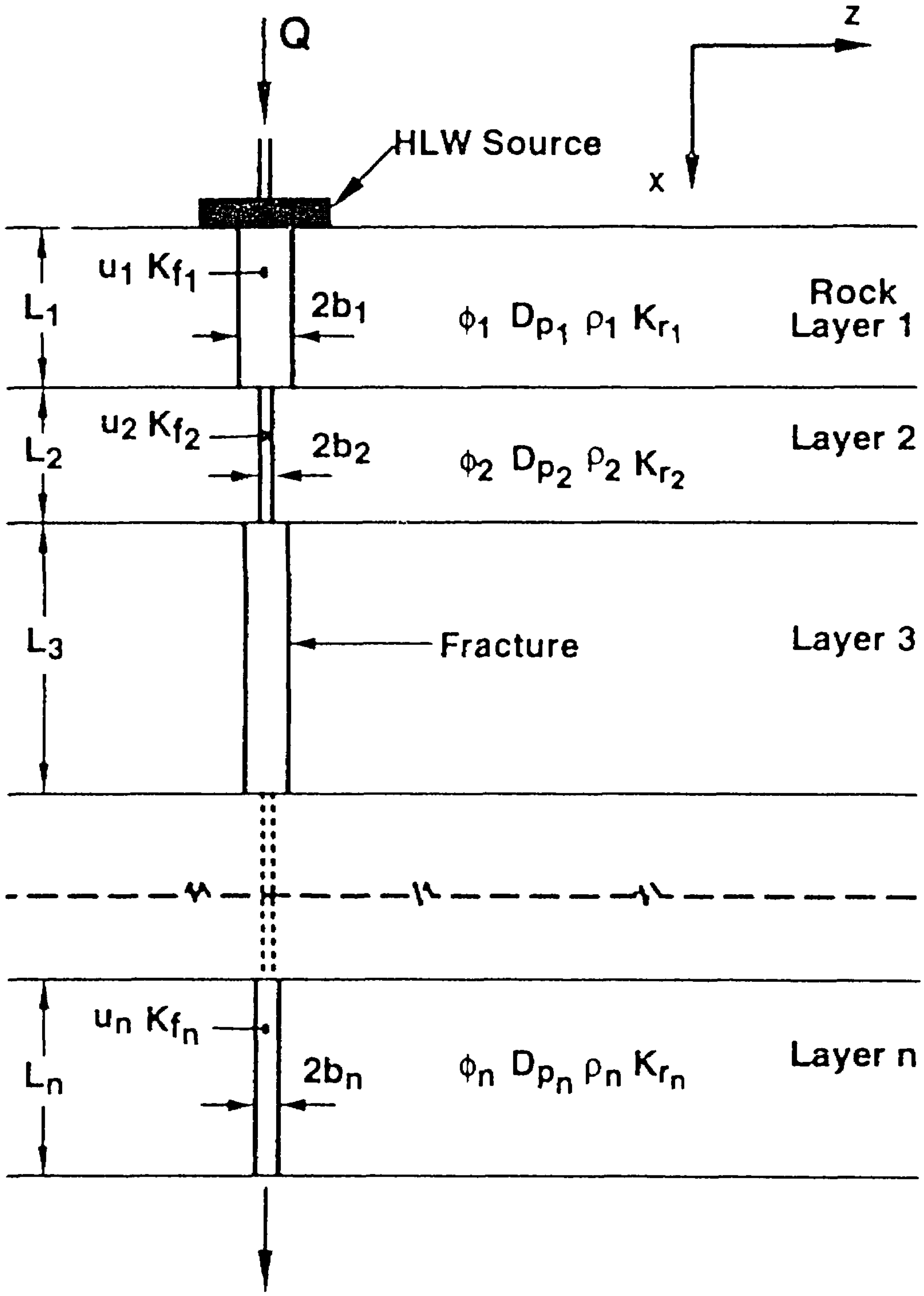

Figure 1-1. Description of Migration Pathways in a System of Homogeneous Layers of Fractured Rock. (See Appendix F for definition of symbols.)

Note that in Equation (1-1) it is assumed that transport occurs under isothermal conditions and the fluid density is constant and that concentrations are small such that these do not affect the properties of the fluid or rock. In addition, the transfer of fluid through the fracture walls is assumed negligible.

At the interface of two consecutive fracture layers $i-1$ and i, the steady-state continuity equation for fluid is given by

$$[u_{i-1} b_{i-1}]^{+} = [u_i b_i]^{-} \qquad (1\text{-}2)$$

and from the mass conservation relation of the solute we have

$$F_{i-1}^{+} = F_i^{-} \qquad (1\text{-}3)$$

with the notion that the flow rate within a typical fracture segment is constant under steady-state flow conditions, substituting Equations (1-1) and (1-2) into Equation (1-3) yields

$$A_{i-1}^{+} = A_i^{-} \qquad (1\text{-}4)$$

which guarantees a continuity of concentration at the interface between fracture layers.

2. ANALYTICAL CONCENTRATIONS AND CUMULATIVE MASS

2.1. GOVERNING EQUATIONS

The governing one-dimensional equation describing the non-dispersive movement of a typical nuclide in the ith layer of the fracture and rock matrix respectively (Neretnieks, 1980) is given by

(a) Fracture

$$R_i \frac{\partial A_i}{\partial t} + u_i \frac{\partial A_i}{\partial x} + \lambda R_i A_i + \frac{J_i}{b_i} = 0, \quad x_{i-1} < x < x_i \tag{2.1}$$

(b) Rock Matrix

$$R_i^{\prime} \frac{\partial B_i}{\partial t} - D_{p_i} \frac{\partial^2 B_i}{\partial z^2} + \lambda R_i^{\prime} B_i = 0 \tag{2.2}$$

$$t > 0, \; x > 0, \; z \geq b_i, \; i = 1,2,3,\ldots,n$$

where

R_i	is the retardation in the fracture
λ	is the first-order rate constant for decay (T^{-1})
J_i	is the diffusive rate of radionuclide at surface of fracture per unit area of fracture surface ($ML^{-2}T^{-1}$)
$R_i^{\prime}$	is the retardation factor in the rock matrix
B_i	is the concentration in the rock matrix (ML^{-3})
D_{p_i}	is the pore diffusivity (L^2T^{-1})
x	is the spatial coordinate in the fracture (L)
z	is the spatial coordinate in the rock matrix (L)
t	is the time (T)
i	is the index related to the particular layer of fracture and surrounding rock matrix
n	is the total number of fractured rock layers

A complete list of symbols and their meanings is given in Appendix F.

The diffusive rate of a nuclide into the ith layer of the rock matrix is assumed to obey Fick's law of diffusion written as

$$J_i = D_{ei} \frac{\partial B_i}{\partial z} |_{z = b_i} \qquad (2\text{-}3)$$

where D_{ei} is the effective diffusivity in the typical section of the rock matrix (see Neretnieks, 1980) defined as

$$D_{ei} = \phi_i D_{pi} \qquad (2\text{-}4)$$

where

Φ_i	is the rock porosity
D_{pi}	is the pore diffusivity (i.e., $D_{pi} = D_d g_{fi}$) (L^2T^{-1})
D_d	is the molecular diffusion of nuclide in water (L^2T^{-1})
g_{fi}	is the geometric factor (δ_{di} / τ_i^2) where
δ_{di}	is constrictivity for diffusion (L^0)
τ_i	is tortuosity of rock matrix (L^0)

The retardation factor in the ith layer of the fracture (R_i) and the rock matrix (R_i^l), respectively (see Neretnicks et al., 1982), are given by:

$$R_i = 1 + \frac{K_{fi}}{b_i} \qquad (2\text{-}5)$$

$$R_i^l = 1 + [(1-\Phi_i)/\Phi_i] \rho_{ri} K_{ri} \qquad (2\text{-}6)$$

where

ρ_{ri}	is the bulk rock density (ML^{-3})
K_{fi}	is the surface distribution coefficient in the fracture (L)
K_{ri}	is the distribution coefficient in the rock matrix (L^3M^{-1})

2.1.1. Initial and Boundary Conditions

The set of differential equations, Equations (2-1) and (2-2), are subject to the initial conditions:

$$A_i(x,0) = a_{1i} + a_{2i} e^{-\alpha_i x_i}, \quad x_{i-1} < x \le x_i \qquad (2\text{-}7)$$

where

$$\chi_i = \begin{cases} x, & i = 1 \\ x - x_{i-1} = x - \sum_{j=1}^{i-1} L_j, & i > 1 \end{cases} \tag{2-8}$$

$$B_i(x,z,0) = b_{1i},\ x_{i-1} < x \le x_i,\ x > 0,\ z \ge b_i \tag{2-9}$$

where a_{1i}, a_{2i}, b_{1i} (all ML^{-3}), and α_i (L^{-1}) are constant for each layer i of the fracture rock system and time invariant, and independent of boundary conditions in the fracture and rock matrix. The boundary conditions in the fracture are given by

$$A_1(0,t) = \bar{A}(t),\ t > 0 \tag{2-10}$$

$$\frac{\partial A_n(\infty,t)}{\partial x} = 0,\ t > 0 \tag{2-11}$$

where $\bar{A}(t)$ is the concentration at the source.

For the ith layer of the rock matrix, the corresponding boundary conditions are

$$B_i(x,b_i,t) = A_i(x,t),\quad t > 0,\ x > 0,\ x_{i-1} < x \le x_i \tag{2-12}$$

$$\frac{\partial B_i(x,\infty,t)}{\partial z} = 0,\quad t > 0,\ x > 0,\ x_{i-1} < x \le x_i \tag{2-13}$$

2.1.2. Concentrations of the Source

For a step release mode, the concentration of a typical nuclide at the source $\bar{A}(t)$ decaying either continuously or subject to periodical fluctuations are given by

(a) Exponentially Decaying Source

$$\bar{A}(t) = A^0 e^{-\lambda t},\ t > 0 \tag{2-14}$$

(b) Periodically Fluctuating Source with Exponential Decay

$$\bar{A}(t) = A^0 e^{-\lambda t}[\nu_a - \nu_b \sin\omega t],\ t>0 \tag{2-15}$$

where A^0 is the concentration of the species at time equals zero, ν_a and ν_b are constants which sum corresponds to one, with $\nu_b \leq \nu_a$, and the time period T_p of a complete cycle of variation is $2\pi/\omega$. These source types are illustrated in Figure 2-1.

For a band release mode, the boundary condition at the fracture inlet may be written as

$$A_1(0,t) = \bar{A}(t)[U(t) - U(t-T)],\ t>0 \tag{2-16}$$

where T is the leaching time and U(t-T) is the Heaviside function defined as

$$U(t-T) = \begin{cases} 1, & t>T \\ \frac{1}{2}, & t=T \\ 0, & t<T \end{cases} \tag{2-17}$$

The general form of the solutions for the band release mode in the ith layer of the fracture and rock matrix based on a boundary condition given by Equation (2-16) and which uses the superposition method (Foglia et al. (1979)) may be written as:

$$\begin{aligned} {}^bA_i(x,t) &= A_i\left(x,t;\ \bar{A}(t), A_i(x,0), B_i(x,z,0)\right) \\ &- e^{-\lambda T} A_i\left(x,t-T;\ \bar{A}(t-T)\right) U(t-T) \end{aligned} \tag{2-18}$$

$$\begin{aligned} {}^bB_i(x,z,t) &= B_i\left(x,z,t;\ \bar{A}(t),\ A_i(x,0),\ B_i(x,z,0)\right) \\ &- e^{-\lambda T} B_i\left(x,z,t-T;\ \bar{A}(t-T)\right) U(t-T) \end{aligned} \tag{2-19}$$

where ${}^bA_i(x,t)$ and ${}^bB_i(x,z,t)$ correspond to the band-release solutions.

At the interface of two consecutive fracture layers we have:

$$A_i(x,t) = A_{i-1}(x,t),\quad i>1 \tag{2-20}$$

2.1.3. Solution of Transport Equations for the Rock Matrix and Fracture

2.1.3.1. Rock Matrix

The Laplace transformation of Equation (2-2) with its associated initial and boundary condition Equations (2-9), (2-12), and (2-13) may be written as

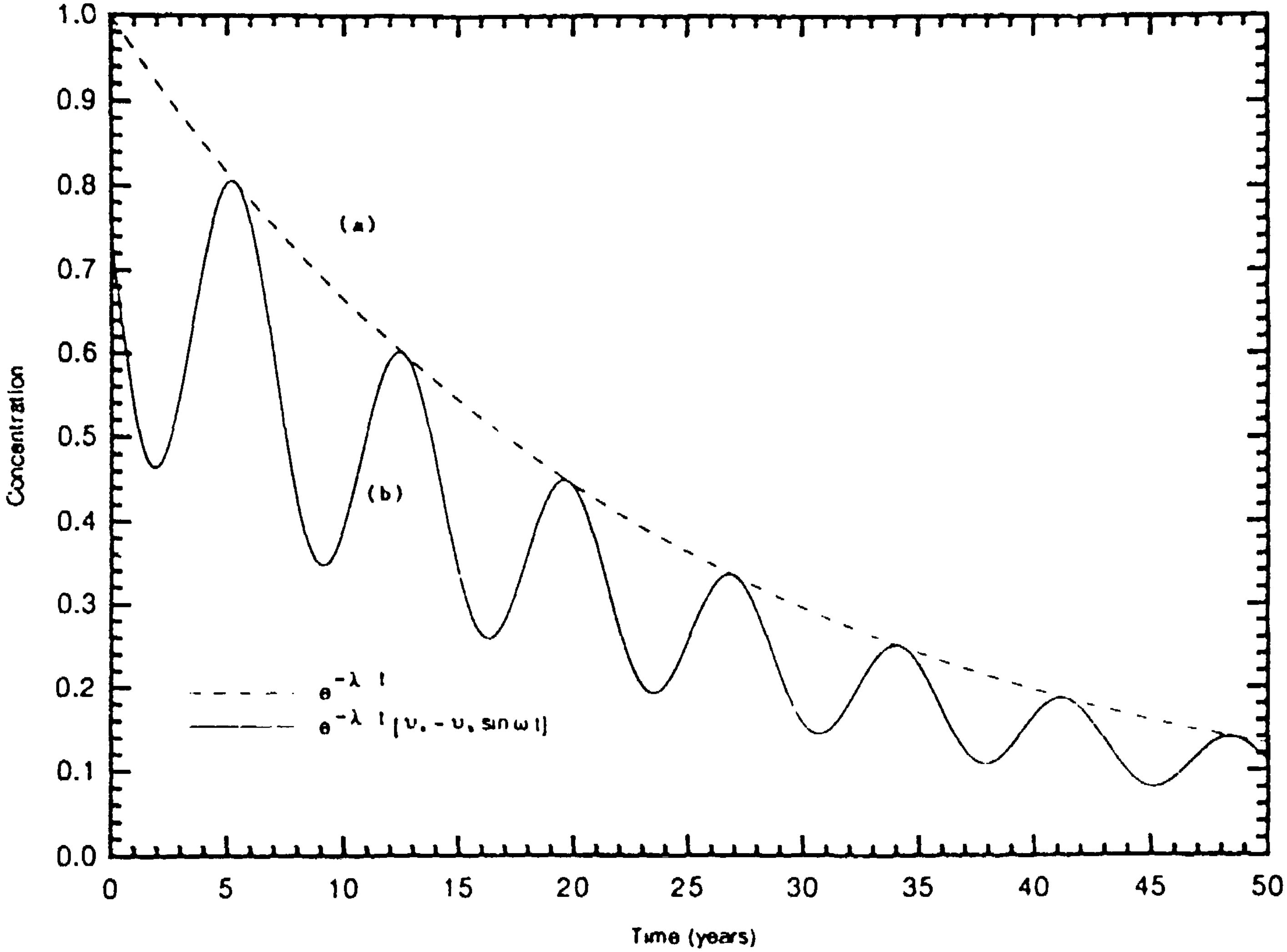

Figure 2-1. Source Models: (a) Exponentially decaying, and (b) Periodically fluctuating decaying.

$$D_{pi}\frac{d^2\overline{B}_i}{dz^2} - R_i' (s + \lambda)\overline{B}_i = -R_i' b_{1i} \qquad (2\text{-}21)$$

with

$$\overline{B}_i(x,b_i,s) = \overline{A}_i(x,s) \qquad (2\text{-}22a)$$

and

$$\frac{\partial \overline{B}_i(x,\infty,s)}{\partial z} = 0 \qquad (2\text{-}22b)$$

where

$$\overline{B}_i = \int_0^\infty B_i e^{-st} dt \qquad (2\text{-}23)$$

The general solution of Equation (2-21) yielding the concentration in the ith layer of the rock matrix is given by

$$\overline{B}_i(x,z,s) = \left(\overline{A}_i - \frac{b_{1i}}{s + \lambda}\right) e^{-r_{bi}(z-b_i)} + \frac{b_{1i}}{s + \lambda} \qquad (2\text{-}24)$$

with

$$r_{bi} = c_{ri}(s + \lambda)^{1/2} \qquad (2\text{-}25)$$

and

$$c_{ri} = (R'_i/D_{pi})^{1/2} \qquad (2\text{-}26)$$

Note that the inverse Laplace transform of B_i might be sought once A_i is identified as shown in the subsequent section.

The Laplace transform of the diffusive flux Equation (2-3) prevailing at the interface of the fracture and rock matrix within a typical layer i is given by

$$\bar{J}_i = -\phi_i D_{pi} \frac{\partial \bar{B}_i(x,b_i,s)}{\partial z} = \phi_i D_{pi} r_{bi} \left(\bar{A}_i(x,s) - \frac{b_{1i}}{s + \lambda} \right) \tag{2-27}$$

Note that r_{bi} in the above equation is given by Equation (2-25).

2.1.3.2. *Fracture*

After proper substitution of the transform of the diffusive flux given by Equation (2-27) into the Laplace transformation of Equation (2-1)

$$u_i \frac{d\bar{A}_i}{dx} + \left[R_i(s + \lambda) + c_A(s + \lambda)^{1/2} \right] \bar{A}_i = R_i(a_{1i} + a_{2i} e^{-a_{3i} x}) + \frac{c_A b_{1i}}{(s + \lambda)^{1/2}} \tag{2-28}$$

with

$$c_A = \frac{\phi_i}{b_i} \left(R_i' D_{pi} \right)^{1/2} \tag{2-29}$$

Note that the initial condititions given by Equation (2-7) are included into Equation (2-28) by virtue of Theorem (A.1-4) of Appendix A.

Similarly, the boundary conditions given by Equations (2-14) and (2-15) are obtained using the appropriate Laplace transforms given in Appendix A. Hence,

(a) Exponentially Decaying Source

$$\bar{A}_1(0,s) = \frac{A^0}{s + \lambda} \tag{2-30}$$

(b) Periodically Fluctuating Decaying Source

$$\bar{A}_1(0,s) = A^0 \left[\frac{v_a}{s + \lambda} - \frac{v_b \omega}{(s + \lambda)^2 + \omega^2} \right] \tag{2-31}$$

2.1.3.2.1. *First Layer*

The solution of Equation (2-28) for the first layer (i.e., with i set to one), subject to its initial and boundary conditions given by Equations (2-7), (2-10), and (2-11), may be written as

$$\bar{A}_1(x,s) = \left[\bar{F}_0 - \bar{F}'_1\right] e^{-r_{ai}\eta_1} + \bar{F}_1 \qquad (2\text{-}32)$$

where

$$\bar{F}_0 = \bar{A}_1(0,s) \qquad (2\text{-}33a)$$

$$\bar{F}'_i = \sum_{j=1}^{3} f_{ji}(s) \qquad (2\text{-}33b)$$

$$\bar{F}_i = \sum_{\substack{j=1 \\ j\neq 2}}^{4} f_{ji}(s) \qquad (2\text{-}33c)$$

with

$$f_{1i}(s) = \frac{R_i a_{1i}}{r_{ai}} \qquad (2\text{-}34a)$$

$$f_{2i}(s) = \frac{R_i a_{2i}}{r_{ai} - p_i} \qquad (2\text{-}34b)$$

$$f_{3i}(s) = \frac{c_{fi} b_i}{r_{ci}} \qquad (2\text{-}34c)$$

$$f_{4i}(x,s) = f_{2i}(s)\, e^{-\alpha_i x_i} \qquad (2\text{-}34d)$$

and

$$r_{ai} = R_i(s + \lambda) + c_{fi}(s + \lambda)^{1/2} \qquad (2\text{-}35a)$$

$$p_i = u_i \alpha_i \qquad (2\text{-}35b)$$

$$r_{ci} = r_{ai}(s + \lambda)^{1/2} \qquad (2\text{-}35c)$$

$$\bar{\eta}_i = \frac{L_i}{u_i} \qquad (2\text{-}35d)$$

$$\eta_i = \frac{\chi_i}{u_i} \qquad (2\text{-}35e)$$

Note that subscript i refers to a typical layer and χ_i given by Equation (2-8) corresponds to the distance within the portion of the fracture network stretching between the exit face of layer i-1 and the location of the observation point in layer i.

2.1.3.2.2. Second Layer

With the assumption that the upstream boundary condition of the second layer will correspond to the prevailing concentration at the downstream end of the first layer (see Equation (1-4)), we may write

$$\bar{A}_2(0,s) = \bar{A}_1(L_1,s) \qquad (2\text{-}36)$$

hence the solution of Equation (2-28), related to the second fracture layer, may be written as

$$\overline{A_2}(x,s) = (\overline{F_0} - \overline{F'_1})e^{-(r_{a1}\bar{\eta}_1 + r_{a2}\eta_2)} + (\overline{F_1} - \overline{F'_2})e^{-r_{a2}\eta_2} + \bar{F}_2 \qquad (2\text{-}37)$$

2.1.3.2.3. Nth Layer

Applying successively the above approach to the subsequent portions of the fracture layers, the solution of Equation (2-28) corresponding to the nth layer may be written as

$$\bar{A}_n(x,s) = (\bar{F}_0 - \overline{F'_1})e^{-r_{an}\eta_n}\prod_{i=1}^{n-1} e^{-r_{ai}\bar{\eta}_i}$$

$$+ \sum_{i=2}^{n} (\bar{F}_{i-1} - \overline{F'_i})e^{-r_{an}\eta_n}\prod_{j=i}^{n-1} e^{-r_{aj}\bar{\eta}_j} + \bar{F}_n \qquad (2\text{-}38)$$

Using the following notations

$$\theta_{mn} = \sum_{i=m}^{n-1} c_{fi}\bar{\eta}_i + c_{fn}\eta_n \tag{2-39}$$

$$\gamma_{mn} = \sum_{i=m}^{n-1} R_i\bar{\eta}_i + R_n\eta_n \tag{2-40}$$

$$g_{mn}(x,s) = e^{-r_n\eta_n}\prod_{i=m}^{n-1} e^{-r_i\bar{\eta}_i} = e^{-\gamma_{mn}(s+\lambda) - \theta_{mn}(s+\lambda)^{1/2}} \tag{2-41}$$

the inverse Laplace transform of Equation (2-38) yielding the closed form solution of the concentration of a typical species in the nth fracture layer is obtained by means of the various theorems and Laplace transforms reported in Table A of Appendix A. This may be written as

$$A_n(x,t) = F_{0_{1n}}(x,t) - \sum_{i=1}^{n} F'_{iin}(x,t) + \sum_{i=2}^{n} F_{i-1in}(x,t) + F_n(x,t) \tag{2-42}$$

The various components of the above equation correspond to

$$F_{0_{1n}}(x,t) = L^{-1}[\bar{F}_0 \cdot g_{1n}(x,s)] \tag{2-43a}$$

$$F'_{imn}(x,t) = \sum_{j=1}^{3} L^{-1} f_{ji}(s) \cdot g_{mn}(x,s) \tag{2-43b}$$

$$F_{imn}(x,t) = \sum_{\substack{j=1 \\ j\neq 2}}^{3} L^{-1} f_{ji}(s) \cdot g_{mn}(s) + L^{-1} f_{4i}(x,s) \cdot g_{mn}(x,s) \tag{2-43c}$$

$$F_n(x,t) = \sum_{\substack{j=1 \\ j\neq 2}}^{3} L^{-1} f_{jn}(s) + L^{-1} f_{4n}(x,s) \tag{2-43d}$$

where $\bar{F}_0$, $f_{jn}(s)$, and $g_{mn}(x,s)$ are given by Equations (2-33a), (2-34), and (2-41) respectively

The components of functions $F_{01n}(x,t)$, $F'_{mn}(x,t)$, $F_{mn}(x,t)$ and $F_n(x,t)$ are now given by:

(a) Exponentially Decaying Source

$$F_{0_{1n}}(x,t) = L^{-1}\left[\bar{F}_0 \cdot g_{1n}(x,s)\right] = A^0 e^{-\lambda t}\, erfc\left[\frac{\theta_{1n}}{2(t-\gamma_{1n})^{1/2}}\right] U(t-\gamma_{1n}) \tag{2-44a}$$

(b) Periodically Fluctuating Source with Exponential Decay

$$F_{0_{1n}}(x,t) = L^{-1}\left[\bar{F}_0 \cdot g_{1n}(x,s)\right] = A^0 e^{-\lambda t}\left[v_a\, erfc\left[\frac{\theta_{1n}}{2(t-\gamma_{1n})^{1/2}}\right] - \frac{v_b}{4i}\left\{E(t-\gamma_{1n},\theta_{1n},i\omega) - E(t-\gamma_{1n},\theta_{1n},-i\omega)\right\}\right] U(t-\gamma_{1n}) \tag{2-44b}$$

The reader may refer to Appendix A, Equation (A.2-3) for a full definition of function $E(\cdot)$. Note that the second member of the above equation, which includes a combination of exponential and complementary error functions with complex arguments, has been shown to yield a real number (see Appendix B, Section B.3).

The inverse Laplace transforms of the the right hand side of Equations (2-43b), (2-43c) and (2-43d) are given by

$$L^{-1}\left[f_{1i}(s)\cdot g_{mn}(x,s)\right] = e^{-\lambda t}\, a_{1i}\, \exp\left[\frac{\theta_{mn} c_{fi}}{R_i}\right] \exp\left[\left(\frac{c_{fi}}{R_i}\right)^2 (t-\gamma_{mn})\right] \cdot erfc\left[\frac{c_{fi}}{R_i}(t-\gamma_{mn})^{1/2} + \frac{\theta_{mn}}{2\,(t-\gamma_{mn})^{1/2}}\right] U(t-\gamma_{mn}) \tag{2-45a}$$

$$L^{-1}\left[f_{2i}(s)\cdot g_{mn}(x,s)\right] = \sum_{j=1}^{2} (-1)^j\, e^{-\lambda t} \frac{a_{2i}\, \beta_{ji}}{q_i} \exp\left[\beta_{ji}\theta_{mn} + \beta_{ji}^2 (t-\gamma_{mn})\right] \cdot erfc\left[\beta_{ji}(t-\gamma_{mn})^{1/2} + \frac{\theta_{mn}}{2\,(t-\gamma_{mn})^{1/2}}\right] U(t-\gamma_{mn}) \tag{2-45b}$$

$$L^{-1}\left[f_{3i}(s)\cdot g_{mn}(x,s)\right] = e^{-\lambda t} b_i \left[erfc\left(\frac{\theta_{mn}}{2(t-\gamma_{mn})^{1/2}}\right) - \exp\left[\frac{\theta_{mn} c_{fi}}{R_i}\right]\cdot \right. \tag{2-45c}$$

$$\left. \exp\left[\left(\frac{c_{fi}}{R_i}\right)^2 (t-\gamma_{mn})\right] erfc\left[\frac{c_{fi}}{R_i}(t-\gamma_{mn})^{1/2} + \frac{\theta_{mn}}{2(t-\gamma_{mn})^{1/2}}\right]\right] U(t-\gamma_{mn})$$

$$L^{-1}\left[f_{4i}(x,s)\cdot g_{mn}(x,s)\right] = e^{-\pi_i x_i} L^{-1}\left[f_{2i}(s)\cdot g_{mn}(x,s)\right] \tag{2-45d}$$

$$L^{-1}\left[f_{1i}(s)\right] = e^{-\lambda t} a_{1i} \exp\left[\left(\frac{c_{fi}}{R_i}\right)^2 t\right] erfc\left[\frac{c_{fi}}{R_i} t^{1/2}\right] \tag{2-46a}$$

$$L^{-1}\left[f_{4i}(x,s)\right] = \sum_{j=1}^{2} (-1)^j \frac{a_{2i} e^{-\pi_i x_i} \beta_{ji}}{q_i} e^{-(\lambda - \beta_{ji}^2)t} erfc(\beta_{ji} t^{1/2}) \tag{2-46b}$$

$$L^{-1}\left[f_{3i}(s)\right] = e^{-\lambda t} b_{1i}\left[1 - \exp\left[\left(\frac{c_{fi}}{R_i}\right)^2 t\right] erfc\left[\frac{c_{fi}}{R_i} t^{1/2}\right]\right] \tag{2-46c}$$

with

$$q_i = 2\left[\left(\frac{c_{fi}}{2R_i}\right)^2 + \frac{p_i}{R_i}\right]^{1/2} \tag{2-47}$$

and

$$\beta_{1i} = \frac{c_{fi}}{2R_i} - \frac{q_i}{2} \qquad (2\text{-}48a)$$

$$\beta_{2i} = \frac{c_{fi}}{2R_i} + \frac{q_i}{2} \qquad (2\text{-}48b)$$

Note that β_{1i} and β_{2i} have dimensions of $t^{-1/2}$.

Grouping the components of $F^{l}_{imn}(x,t)$, $F_{imn}(x,t)$, and $F_n(x,t)$, one may then write

$$F'_{imn}(x,t) = {}_1H_{imn}(x,t) + {}_2H_{imn}(x,t) \qquad (2\text{-}49)$$

$$F_{imn}(x,t) = {}_1H_{imn}(x,t) + e^{-\varepsilon_i x_i}\,{}_2H_{imn}(x,t) \qquad (2\text{-}50)$$

where

$$\begin{aligned} {}_1H_{imn}(x,t) = e^{-\lambda t}\Bigg[& b_{1i}\,erfc\left[\frac{\theta_{mn}}{2(t-\gamma_{mn})^{1/2}}\right] + (a_{1i} - b_{1i})\exp\left[\frac{\theta_{mn}c_{fi}}{R_i}\right]\cdot \\ & \exp\left[\left(\frac{c_{fi}}{R_i}\right)^2 (t-\gamma_{mn})\right] erfc\left[\frac{c_{fi}}{R_i}(t-\gamma_{mn})^{1/2} + \frac{\theta_{mn}}{2(t-\gamma_{mn})^{1/2}}\right]\Bigg] U(t-\gamma_{mn}) \end{aligned} \qquad (2\text{-}51)$$

and

$$
{}_2H_{lmn}(x,t) = e^{-\lambda t}\sum_{j=1}^{2}(-1)^j\frac{a_{2l}\beta_{jl}}{q_l}\exp[\beta_{jl}\theta_{mn} + \beta_{jl}^2(t - \gamma_{mn})]\cdot
$$

$$
erfc\left[\beta_{jl}(t - \gamma_{mn})^{1/2} + \frac{\theta_{mn}}{2(t - \gamma_{mn})^{1/2}}\right]U(t - \gamma_{mn}) \tag{2-52}
$$

$$
F_n(x,t) = \sum_{i=1}^{2}(-1)^i\,\frac{a_{2n}\beta_{in}e^{-a_n x_n}}{q_n}e^{-(\lambda - \beta_{in}^2)t}erfc(\beta_{in}t^{1/2}) +
$$

$$
e^{-\lambda t}\left[b_{1n} + (a_{1n} - b_{1n})\exp\left[\left(\frac{c_{fn}}{R_n}\right)^2 t\right]erfc\left[\frac{c_{fn}}{R_n}t^{1/2}\right]\right] \tag{2-53}
$$

Note that the evaluation of expressions involving products of exponential and complementary error functions are presented in Appendix B.

2.1.3.3. *Rock Matrix*

Substitution of Equation (2-38) in Equation (2-24) gives the Laplace transform solution of the concentration in the nth layer of the rock matrix

$$
\overline{B}_n(x,z,s) = \left[\overline{F}_0 - \overline{F'}_1\right]e^{-[r_{an}\eta_n + r_{bn}(z - b_n)]}\prod_{i=1}^{n-1}e^{-r_{ai}\bar{\eta}_i} +
$$

$$
\sum_{i=2}^{n}\left(\overline{F}_{i-1} - \overline{F'}_i\right)e^{-[r_{an}\eta_n + r_{bn}(z - b_n)]}\prod_{j=i}^{n-1}e^{-r_{aj}\bar{\eta}_j} + \tag{2-54}
$$

$$
\overline{F}_n e^{-r_{bn}(z - b_n)} + \frac{b_{1n}}{s + \lambda}\left(1 - e^{-r_{bn}(z - b_n)}\right)
$$

The inverse Laplace transform of the above equation yielding the closed form solution of the concentration in the nth layer of the rock matrix is then obtained by means of the various theorems and Laplace transforms reported in Appendix A. This may be written as

$$B_n(x,z,t) = G_{0_{1n}}(x,z,t) - \sum_{i=1}^{n} G'_{iin}(x,z,t) + \sum_{i=2}^{n} G_{i-1in}(x,z,t) + G_n(x,z,t) \tag{2-55}$$

The components of functions $G_{01n}(x, z, t)$, $G'_{imn}(x,z,t)$, $G_{mn}(x, z, t)$ and $G_n(x, z, t)$ are now given by:

(a) Exponentially Decaying Source

$$G_{0_{1n}}(x,z,t) = A^0 e^{-\lambda t}\, erfc\left[\frac{\theta'_{1n}}{2(t - \gamma_{1n})^{1/2}}\right] U(t - \gamma_{1n}) \tag{2-56a}$$

(b) Periodically Fluctuating Source with Exponential Decay

$$G_{0_{1n}}(x,z,t) = L^{-1}|\bar{F}_0 \cdot g_{1n}(x,s)| = A^0 e^{-\lambda t}\left[\nu_a\, erfc\left[\frac{\theta'_{1n}}{2(t - \gamma_{1n})^{1/2}}\right] - \frac{\nu_b}{4i}\left[E(t-\gamma_{1n},\theta'_{1n},i\omega) - E\left(t-\gamma_{1n},\theta'_{1n},-i\omega\right)\right]\right] U(t - \gamma_{1n}) \tag{2-56b}$$

where function $E(\cdot)$ is given in Appendix A, Equation (A.2-3).

$$G'_{imn}(x,z,t) = {}_1H'_{imn}(x,z,t) + {}_2H'_{imn}(x,z,t) \tag{2-57a}$$

$$G_{imn}(x,z,t) = {}_1H'_{imn}(x,z,t) + e^{-\alpha_i x_i}\, {}_2H'_{imn}(x,z,t) \tag{2-57b}$$

where

$$
{}_1H'_{imn}(x,t) = e^{-\lambda t}\left[b_{1i}\,erfc\left[\frac{\theta'_{mn}}{2(t-\gamma_{mn})^{1/2}}\right] + (a_{1i} - b_{1i})\exp\left[\frac{\theta'_{mn}c_{fi}}{R_i}\right]\cdot \right.
$$

$$
\left.\exp\left[\left(\frac{c_{fi}}{R_i}\right)^2 (t-\gamma_{mn})\right] erfc\left[\frac{c_{fi}}{R_i}(t-\gamma_{mn})^{1/2} + \frac{\theta'_{mn}}{2(t-\gamma_{mn})^{1/2}}\right]\right] U(t-\gamma_{mn}) \tag{2-58}
$$

$$
{}_2H'_{imn}(x,z,t) = e^{-\lambda t}\sum_{j=1}^{2}(-1)^j\frac{a_{2i}\beta_{ji}}{q_i}\exp[\beta_{ji}\theta'_{mn} + \beta_{ji}^2(t-\gamma_{mn})]\cdot
$$

$$
erfc\left[\beta_{ji}(t-\gamma_{mn})^{1/2} + \frac{\theta'_{mn}}{2(t-\gamma_{mn})^{1/2}}\right] U(t-\gamma_{mn}) \tag{2-59}
$$

$$
F_n(x,z,t) = e^{-\lambda t}\sum_{i=1}^{2}(-1)^i\,\frac{a_{2n}\beta_{in}e^{-\alpha_n x_n}}{q_n}\exp\left[\beta_{in}^2 t + \beta_{in}c_{rn}(z-b_n)\right]\cdot
$$

$$
erfc\left[\beta_{in}t^{1/2}) + \frac{c_{rn}(z-b_n)}{2t^{1/2}}\right] + e^{-\lambda t}\left[b_{1n} + (a_{1n} - b_{1n})\exp\left[c_{rn}(z-b_n)\frac{c_{fn}}{R_n}\right]\cdot\right. \tag{2-60}
$$

$$
\left.\exp\left[\left(\frac{c_{fn}}{R_n}\right)^2 t\right] erfc\left[\frac{c_{fn}}{R_n}t^{1/2} + \frac{c_{rn}(z-b_n)}{2t^{1/2}}\right]\right]
$$

$$
\theta'_{mn} = \theta_{mn} + c_{rn}\,(z - b_n) \tag{2-61}
$$

2.2. CUMULATIVE MASS

The cumulative mass per unit width at any point within the fracture is given by

$$M(x,t) = \int_0^t q_n 2b_n A_n(x,\tau)\,d\tau = q_n 2b_n \left[Q_{0_{1n}}(x,t) - \sum_{l=1}^{n} Q'_{lln}(x,t) \right. \tag{2-62}$$

$$\left. + \sum_{l=2}^{n} Q_{l-1ln}(x,t) + Q_n(x,t) \right]$$

where $A_n(x,t)$ the concentration in the fracture is given by Equation (2-42). In the above equation the components of functions $Q_{01n}(x,t)$, $Q'_{lln}(x,t)$, $Q_{lln}(x,t)$ and $Q_n(x,t)$ are evaluated based on the various integrals derived in Appendix C and are given by

(a) Exponentially Decaying Source

$$Q_{0_{1n}}(x,t) = \int_{\gamma_{1n}}^{t} F_{0_{1n}}(\tau)\,d\tau = A^0 I_1(t,\lambda,\frac{\theta_{1n}}{2},\gamma_{1n})\,U(t-\gamma_{1n}) \tag{2-63a}$$

(b) Periodically Fluctuating Source with Exponential Decay

$$Q_{0_{1n}}(x,t) = \int_{\gamma_{1n}}^{t} F_{0_{1n}}(\tau)\,d\tau = \tag{2-63b}$$

$$A^0 \left[\nu_a I_1(t,\lambda,\frac{\theta_{1n}}{2},\gamma_{1n}) - \nu_b \omega I_4(t,\theta_{1n},i\omega,\lambda,\gamma_{1n}) \right] U(t-\gamma_{1n})$$

$$Q^l_{imn}(x,t) = \int_{\gamma_{mn}}^{t} F^l_{imn}(x,\tau)d\tau = {}_1Q^l_{imn}(x,t) + {}_2Q^l_{imn}(x,t) \tag{2-64a}$$

$$Q_{imn}(x,t) = \int_{\gamma_{mn}}^{t} F_{imn}(x,\tau)d\tau = {}_1Q^l_{imn}(x,t) + e^{-a_i x_i}\,{}_2Q^l_{imn}(x,t) \tag{2-64b}$$

where

$$
{}_1Q'_{imn}(x,t) = \int_{\gamma_{mn}}^{t} {}_1H_{imn}(x,\tau)d\tau = \left[b_{1i} I_1(t,\lambda,\frac{\theta_{mn}}{2},\gamma_{mn}) \right. \tag{2-65}
$$

$$
\left. + (a_{1i} - b_{1i})\exp\left[\frac{c_{fi}}{R_i}\left(\theta_{mn} - \frac{c_{fi}\gamma_{mn}}{R_i}\right)\right] I_2\left(t,\left(\frac{c_{fi}}{R_i}\right)^2 - \lambda, \frac{c_{fi}}{R_i}, \frac{\theta_{mn}}{2}, \gamma_{mn}\right)\right] U(t-\gamma_{mn})
$$

$$
{}_2Q'_{imn}(x,t) = \int_{\gamma_{mn}}^{t} {}_2H_{imn}(x,\tau)d\tau = \sum_{j=1}^{2} (-1)^j \frac{a_{2i}\beta_{ji}}{q_i} \exp[\beta_{ji}(\theta_{mn} - \beta_{ji}\gamma_{mn})] \cdot \tag{2-66}
$$

$$
I_2\left(t,(\beta_{ji}^2 - \lambda),\beta_{ji},\frac{\theta_{mn}}{2},\gamma_{mn}\right) U(t-\gamma_{mn})
$$

$$
Q_n(x,t) = \int_0^t F_n(x,t) = \sum_{i=1}^{2} (-1)^i \frac{a_{2n}\beta_{in}}{q_n} e^{-\kappa_n x_n} I_3\left(0,t,(\beta_{in}^2 - \lambda),\beta_{in}\right) \tag{2-67}
$$

$$
+ \left[\frac{b_{1n}}{\lambda}(1 - e^{-\lambda t}) + (a_{1n} - b_{1n}) I_3\left(0,t,\left(\left(\frac{c_{fn}}{R_n}\right)^2 - \lambda\right),\frac{c_{fn}}{R_n}\right)\right]
$$

More explicitly, using the definitions of I_1 through I_4 reported in Appendix C, Equations (2-63) through (2-67) may be written as

(a) Exponentially Decaying Source

$$
Q_{0_{1n}}(x,t) = A_1^0 \left\{ -\frac{e^{-\lambda t}}{\lambda} erfc\left[\frac{\theta_{1n}}{2(t-\gamma_{1n})^{1/2}}\right] + \right. \tag{2-68a}
$$

$$
\frac{e^{-\lambda\gamma_{1n}}}{2\lambda}\left[e^{\theta_{1n}\sqrt{\lambda}} erfc\left[\frac{\theta_{1n}}{2(t-\gamma_{1n})^{1/2}} + \sqrt{\lambda(t-\gamma_{1n})}\right] + \right.
$$

$$
\left.\left. e^{-\theta_{1n}\sqrt{\lambda}} erfc\left[\frac{\theta_{1n}}{2(t-\gamma_{1n})^{1/2}} - \sqrt{\lambda(t-\gamma_{1n})}\right]\right]\right\} U(t-\gamma_{1n})
$$

(b) Periodically Fluctuating Source with Exponential Decay

$$
\begin{aligned}
Q_{0_{1n}}(x,t) = A^0 \Bigg[& -\nu_a \frac{e^{-\lambda t}}{\lambda} erfc\left[\frac{\theta_{1n}}{2(t-\gamma_{1n})^{1/2}}\right] + \\
& \frac{e^{-\lambda\gamma_{1n}}}{2\lambda}\Bigg[e^{\theta_{1n}\sqrt{\lambda}} erfc\left[\frac{\theta_{1n}}{2(t-\gamma_{1n})^{1/2}} + \sqrt{\lambda(t-\gamma_{1n})}\right] + \\
& e^{-\theta_{1n}\sqrt{\lambda}} erfc\left[\frac{\theta_{1n}}{2(t-\gamma_{1n})^{1/2}} - \sqrt{\lambda(t-\gamma_{1n})}\right]\Bigg] \\
& -\nu_b\omega\Bigg\{\frac{1}{4i\omega}\Bigg[-\frac{e^{-(\lambda-i\omega)t}}{\lambda-i\omega} E_1(t-\gamma_{1n},\theta_{1n},i\omega) + \frac{e^{-(\lambda+i\omega)t}}{\lambda+i\omega} E_2(t-\gamma_{1n},\theta_{1n},-i\omega)\Bigg] \\
& + \frac{e^{-\lambda\gamma_{1n}}(\lambda\sin(i\omega\gamma_{1n}) + i\omega\cos(i\omega\gamma_{1n}))}{2i\omega(\lambda^2-\omega^2)} \\
& \Bigg[e^{\theta_{1n}\sqrt{\lambda}} erfc\left(\frac{\theta_{1n}}{2(t-\gamma_{1n})^{1/2}} + \sqrt{\lambda(t-\gamma_{1n})}\right) \\
& + e^{-\theta_{1n}\sqrt{\lambda}} erfc\left(\frac{\theta_{1n}}{2(t-\gamma_{1n})^{1/2}} - \sqrt{\lambda(t-\gamma_{1n})}\right)\Bigg]\Bigg\}\Bigg] U(t-\gamma_{1n})
\end{aligned}
\tag{2-68b}
$$

where functions $E_1(\cdot)$ and $E_2(\cdot)$ in the above equation are given by Equations (C.4-3) of Appendix C, and:

$$
{}_1Q'_{imn}(x,t) = b_{1i}\Bigg\{ -\frac{e^{-\lambda t}}{\lambda}\, erfc\left[\frac{\theta_{mn}}{2(t-\gamma_{mn})^{1/2}}\right] +
$$

$$
\frac{e^{-\lambda\gamma_{mn}}}{2\lambda}\left[e^{\theta_{mn}\sqrt{\lambda}}\, erfc\left[\frac{\theta_{mn}}{2(t-\gamma_{mn})^{1/2}} + \sqrt{\lambda(t-\gamma_{mn})}\right] + \right.
$$

$$
\left. e^{-\theta_{mn}\sqrt{\lambda}}\, erfc\left[\frac{\theta_{mn}}{2(t-\gamma_{1n})^{1/2}} - \sqrt{\lambda(t-\gamma_{mn})}\right]\right]\Bigg\} U(t \quad \gamma_{mn})
$$

$$
+\frac{(a_{1i}-b_{1i})}{\left(\frac{c_{fi}}{R_i}\right)^2 - \lambda}\Bigg\{ \exp\left[\frac{c_{fi}}{R_i}\left(\theta_{mn} - \frac{c_{fi}\gamma_{mn}}{R_i}\right)\right] \exp\left[\left(\left(\frac{c_{fi}}{R_i}\right)^2 - \lambda\right)t\right] \cdot
$$

$$
erfc\left[\frac{\theta_{mn}}{2(t-\gamma_{mn})^{1/2}} + \frac{c_{fi}}{R_i}(t-\gamma_{mn})^{1/2}\right] - \tag{2-69}
$$

$$
\frac{\exp(-\lambda\gamma_{mn})}{2}\left[e^{\theta_{mn}\sqrt{\lambda}}\, erfc\left[\frac{\theta_{mn}}{2(t-\gamma_{mn})^{1/2}} + \sqrt{\lambda(t-\gamma_{mn})}\right]\left(\frac{c_{fi}}{R_i\sqrt{\lambda}} + 1\right) - \right.
$$

$$
\left. e^{-\theta_{mn}\sqrt{\lambda}}\, erfc\left[\frac{\theta_{mn}}{2(t-\gamma_{mn})^{1/2}} - \sqrt{\lambda(t-\gamma_{mn})}\right]\left(\frac{c_{fi}}{R_i\sqrt{\lambda}} - 1\right)\right]\Bigg\} U(t-\gamma_{mn})
$$

$$
{}_2Q'_{imn}(x,t) = \sum_{j=1}^{2} (-1)^j a_{2i} \frac{\beta_{ji}}{q_i} \Big\{ \exp\left[\beta_{ji}(\theta_{mn} - \beta_{ji}\gamma_{mn})\right] \cdot
$$

$$
\frac{e^{(\beta_{ji}^2 - \lambda)t}}{\beta_{ji}^2 - \lambda} \; erfc\left[\beta_{ji}(t - \gamma_{mn})^{1/2} + \frac{\theta_{mn}}{2(t - \gamma_{mn})^{1/2}}\right]
$$

$$
- \frac{\exp(-\lambda\gamma_{mn})}{2(\beta_{ji}^2 - \lambda)} \left[e^{\theta_{mn}\sqrt{\lambda}} erfc\left[\frac{\theta_{mn}}{2(t-\gamma_{mn})^{1/2}} + \sqrt{\lambda(t - \gamma_{mn})}\right]\left(\frac{\beta_{ji}}{\sqrt{\lambda}} + 1\right) - \right. \tag{2-70}
$$

$$
\left. e^{-\theta_{mn}\sqrt{\lambda}} erfc\left[\frac{\theta_{mn}}{2(t-\gamma_{mn})^{1/2}} - \sqrt{\lambda(t-\gamma_{mn})}\right]\left(\frac{\beta_{ji}}{\sqrt{\lambda}} - 1\right) \right] \Big\} U(t - \gamma_{mn})
$$

$$
Q_n(x,t) = \sum_{j=1}^{2} (-1)^j \frac{a_{2n}\beta_{jn}}{q_n} e^{-a_n x_n} \frac{1}{(\beta_{jn}{}^2 - \lambda)} \left[e^{(\beta_{jn}^2 - \lambda)t} erfc(\beta_{jn}\sqrt{t}) + \right.
$$

$$
\left. \frac{\beta_{jn}}{\sqrt{\lambda}} erf\left[(\lambda t)^{1/2}\right] - 1 \right]
$$

$$
+ \frac{b_{1n}}{\lambda}(1 - e^{-\lambda t}) + \frac{(a_{1n} - b_{1n})}{\left[\left(\frac{c_{fn}}{R_n}\right)^2 - \lambda\right]} \left[\exp\left[\left(\left(\frac{c_{fn}}{R_n}\right)^2 - \lambda\right)t\right] \cdot \right. \tag{2-71}
$$

$$
\left. erfc\left[\frac{c_{fn}}{R_n} t^{1/2}\right] + \frac{c_{fn}}{\sqrt{\lambda}R_n} erf\left[(\lambda t)^{1/2}\right] - 1 \right]
$$

Note that when the exponential term in the model describing the initial concentration distribution in the fracture (see Equation (2-7)) is taken into account, overflow problems are likely to be encountered when the value of the time parameter becomes excessively large. This state of affairs is inherent to the presence of parameter β_{ii} (see, for example, Equation (2-52)), which by virtue of being negative (i.e., when subscript i corresponds to 1, see Equation (2-48a)), tends to freeze the complementary function at a constant value of approximately 2 (i.e., when its argument becomes less than or equal to -3), whilst the exponential term will increase positively with increasing values of time. To mitigate the incumbent overflow problem, the solution is optimized through an iterative process intended to estimate an acceptable upper limit for the magnitude of the exponential argument. Consequently, exponential terms witnessing β_{1i} in their list of arguments are ignored (i.e., set automatically to zero) when the preset limit is exceeded. Computationally, this is achieved after initializing the significant absolute limit of the exponential argument, initially to a value corresponding to 30, the latter affecting exclusively the specific components of the solutions which include parameter β_{1i}. The computation is reiterated after halving the value of the exponential argument, and the absolute relative error in the computed results is subsequently estimated. This process is continued until when, in two successive iterations, the preset convergence criteria (i.e., 1% relative error) is said to be satisfied. For the test cases reported herein a maximum of three iterations were proven sufficient to provide an optimized value of the exponential argument and yield a highly accurate solution.

2.3. DISCUSSIONS OF RESULTS

The analytical solutions presented in this section of the report were verified by comparison with three approximate methods of Laplace inversion integral as proposed by Talbot (1979), Durbin (1974), as modified by Piessens and Huysmans (1984) and Stefhest (1970). All three methods apply to the case where the source term corresponds to a continuous exponentially decaying one, in which instance the required inversion of the Laplace transform is strictly confined to the real domain. However, when a periodically fluctuating and decaying source term is adopted, then only the first two of these methods are useful for evaluating the Laplace transform inversion in the complex domain. Note that in the case of Stefhest's algorithm, 36 summation points were found to produce almost oscillation-free solutions.

As far as the calculation of the analytical solution related to the cumulative mass (i.e., the time integrated solution of the concentration at a typical point along the longitudinal axis of the fracture) is concerned, this is performed by numerically integrating solutions of the Laplace-transformed equation of the concentration in the fracture. This integration is performed using a composite Gauss-Legendre quadrature scheme, where 40 integration points were found adequate to yield a convergent quadrature for the investigated test cases.

The two test cases reported subsequently refer to the one-dimensional transport of two radionuclides: Np-237 (i.e., long half-life) and Cm-245 (short half-life), in a heterogeneous saturated fractured rock system composed of five layers (the last extending to infinity), with piecewise constant parameters. In the first test case, the imposed source term corresponds to an exponentially decaying function (see Equation (2-14)). This is substituted by a periodically fluctuating and decaying one (see Equation (2-15)) in the second, respectively. In both cases, the steady flow rate of water per unit width of fracture corresponds to 0.1 m^2/yr. Two types of solute release modes at the source were investigated namely: step and band. Note that the flow domain in both fracture and rock layers are assigned non-zero initial concentrations (see Equations (2-7) and (2-9)).

2.3.1. Case 1 Results

This test case examines the spatial and temporal variation of the concentration of Np-237, as well as the cumulative release of mass from the fracture. In addition, the spatial variation of the concentration in the rock matrix is also investigated. The input data pertaining to this test case is presented in Table 2-1.

Figure 2-2(a) shows the spatial relative concentration profiles of Np-237 calculated in the fracture layers at simulation times of 10^3, 5×10^3 and 5×10^4 years. A comparison of our results with the ones obtained from the three numerical inversion algorithms (see Tables 2-2(a) through 2-2(c)) show that these are in excellent agreement. Note that in this test case, the observation times were selected in a manner to allow an evaluation of the accuracy of our solution for both release modes of the radionuclide at the source, it may be added that in the case of the intermediate observation time, the source strength is reduced by half from its original value (see Equation (2-17)).

Figure 2-2(b) shows the temporal relative concentration of Np-237 observed in the fracture at three different observation points: 100, 200, and 500 meters downstream from the source, located in the second, third and fifth layer, respectively, for a band release. Up to the leaching time of 5×10^3 years, the shape of the profiles bears a close similarity with those of a step release. Past the leaching time, the relative concentrations profiles show a rapid change of their gradient from positive to negative and concentrations decrease with time to a value lying within close range to the initial concentrations of the various fracture layers of interest. A comparison of our results with the three numerical ones (see Tables 2-3(a) through 2-3(c)) show that with the exception of a portion of the results yielded by Talbot's solution, these are in excellent agreement. Note that in this instance, the adoption of three recommended[1] values of the constants required by Talbot's algorithm, seems to have restricted the accuracy of the latter to simulation times greater than 30, 80 and 100 years. Therefore, it appears that the three constants in Talbot's algorithm seem to be correlated with the independent variables, rendering their selection problem dependent.

Figure 2-2(c) depicts the time-dependent evolution of the cumulative mass (per unit width of the fracture) profile at three different observation points in the fracture as in the previous example. Because of its computational viability Stefhest's algorithm is selected from this point on as the benchmark. A comparison of our analytical solution results with those

---

[1] D. Hodgkinson, personal communication.

yielded by Stefhest's solution (see Tables 2-4(a) through 2-4(c)) indicates excellent agreement. Note that all three profiles tend to become asymptotic to three specific values of the cumulative mass namely, 4.903×10^2, 4.7×10^2, and 4.309×10^2 (UA/m)[2]. The latter may be easily computed from Equation (2-62) after setting the value of the independent variable t equal to infinity.

Figure 2-2(d) shows the concentration profiles in the rock matrix at three positions downstream from the source (i.e., x = 100m, 200m, and 500m) for a step release. Comparison of our analytical results against those yielded by the Stefhest's solution method (see Tables 2-5(a) through 2-5(c)) indicate an excellent agreement. Note that at their downstream end, all three profiles tend to become asymptotic to a concentration value slightly in excess of the residual concentration prevailing in their respective layers.

Figure 2-2(e) shows the concentration profiles in the rock matrix at three positions downstream from the source (i.e., x = 100m , 200m, and 500m) and for a simulation time of 5×10^4 years, for a band release with a leaching time corresponding to 5×10^3 years. Past the leaching time, the contaminant in a typical rock layer close to the source would begin to exhibit a higher concentration than in the fracture, which would then initiate its diffusion back into the fracture. Indeed a quick reference to Figure 2-2(e) shows that the gradient of the concentration profiles at the fracture rock interface tends to decrease with increasing distances from the source. As in the preceding case, results reported in Tables 2-6(a) through 2-6(c) show excellent agreement between the analytical and the numerical solutions.

---

[2] UA: Arbitrary Units of Activity/meter.

Table 2-1. INPUT PARAMETERS FOR CASE I EXPONENTIALLY DECAYING SOURCE

SPECIES	Np-237
$T_{1/2}$	2.3×10^6 yr
Release Mode:	
Step	NA
Band Leaching Time	5×10^3 yr
A°	1.0*
Q	0.1 (m^3/yr)
ν_a	NA
ν_b	NA
T_p	NA

LAYER	L(m)	b (m)	u (m/yr)	Φ
1	50.0	5.0E-03	10.0	0.01
2	75.0	4.0E-03	12.5	0.008
3	100.0	3.0E-03	16.666	0.006
4	150.0	2.0E-03	25.0	0.004
5	∞	1.5E-03	33.333	0.002

LAYER	ρ (g/cm^3)	D_p (m^2/yr)	K_f (m)	K_r (cm^3/g)
1	2.0	0.01	5.0E-03	0.5
2	2.3	0.02	8.0E-03	0.6978
3	2.6	0.06	2.7E-02	1.158
4	2.65	0.05	1.0E-02	1.059
5	2.7	0.03	3.0E-03	0.741

Table 2-1. INPUT PARAMETERS FOR CASE 1 EXPONENTIALLY DECAYING SOURCE (Continued)

LAYER	a_1^*	a_2^*	α (m^{-1})	b_1^*
1	1.50E-04	-0.50E-04	0.02	1.00E-05
2	2.00E-04	-0.25E-05	0.02	1.75E-05
3	1.75E-04	-0.20E-05	0.02	1.25E-05
4	2.00E-04	-0.15E-05	0.02	1.05E-05
5	1.50E-04	0.20E-05	0.02	1.05E-05

* (arbitrary units of activity/L^3)

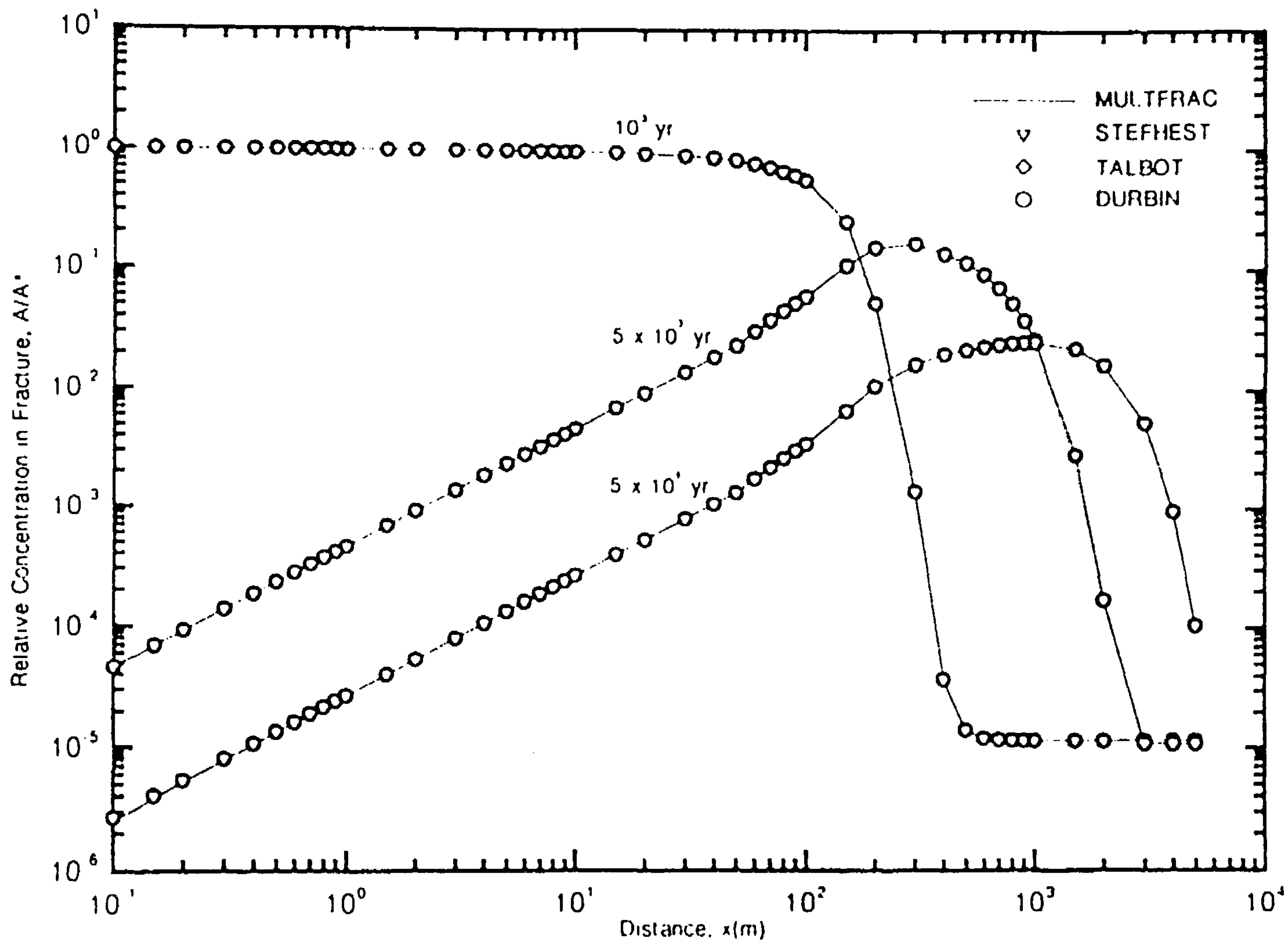

Figure 2-2(a). Relative concentration of Np-237 vs. d nce in the fracture at different times t = 1,000, 5,000, and 50,000 years (Exponentially decaying source and step and band release).

Table 2-2(a). CASE 1 RESULTS: CONCENTRATION OF Np-237 IN THE FRACTURE AT TIME t = 1,000 YEARS (EXPONENTIALLY DECAYING SOURCE AND STEP RELEASE MODE)

DISTANCE (m)	MULTFRAC	STEFHEST	TALBOT	DURBIN
1.000E-01	9.993E-01	9.993E-01	9.993E-01	9.993E-01
1.500E-01	9.992E-01	9.992E-01	9.992E-01	9.992E-01
2.000E-01	9.990E-01	9.990E-01	9.990E-01	9.990E-01
3.000E-01	9.986E-01	9.986E-01	9.986E-01	9.986E-01
4.000E-01	9.983E-01	9.983E-01	9.983E-01	9.983E-01
5.000E-01	9.979E-01	9.979E-01	9.979E-01	9.979E-01
6.000E-01	9.976E-01	9.976E-01	9.976E-01	9.976E-01
7.000E-01	9.972E-01	9.972E-01	9.972E-01	9.972E-01
8.000E-01	9.968E-01	9.968E-01	9.968E-01	9.968E-01
9.000E-01	9.965E-01	9.965E-01	9.965E-01	9.965E-01
1.000E+00	9.961E-01	9.961E-01	9.961E-01	9.961E-01
1.500E+00	9.943E-01	9.943E-01	9.943E-01	9.943E-01
2.000E+00	9.926E-01	9.926E-01	9.926E-01	9.926E-01
3.000E+00	9.890E-01	9.890E-01	9.890E-01	9.890E-01
4.000E+00	9.854E-01	9.854E-01	9.854E-01	9.854E-01
5.000E+00	9.819E-01	9.819E-01	9.819E-01	9.819E-01
6.000E+00	9.783E-01	9.783E-01	9.783E-01	9.783E-01
7.000E+00	9.747E-01	9.747E-01	9.747E-01	9.747E-01
8.000E+00	9.711E-01	9.711E-01	9.711E-01	9.711E-01
9.000E+00	9.676E-01	9.676E-01	9.676E-01	9.676E-01
1.000E+01	9.640E-01	9.640E-01	9.640E-01	9.640E-01
1.500E+01	9.461E-01	9.462E-01	9.462E-01	9.462E-01
2.000E+01	9.283E-01	9.283E-01	9.283E-01	9.283E-01
3.000E+01	8.927E-01	8.927E-01	8.927E-01	8.927E-01
4.000E+01	8.572E-01	8.572E-01	8.572E-01	8.572E-01
5.000E+01	8.219E-01	8.219E-01	8.219E-01	8.219E-01
6.000E+01	7.550E-01	7.662E-01	7.662E-01	7.662E-01
7.000E+01	7.061E-01	7.116E-01	7.116E-01	7.116E-01
8.000E+01	6.558E-01	6.582E-01	6.582E-01	6.582E-01
9.000E+01	6.056E-01	6.064E-01	6.064E-01	6.064E-01
1.000E+02	5.564E-01	5.564E-01	5.564E-01	5.564E-01
1.500E+02	2.491E-01	2.490E-01	2.490E-01	2.490E-01
2.000E+02	5.308E-02	5.308E-02	5.308E-02	5.308E-02
3.000E+02	1.400E-03	1.400E-03	1.400E-03	1.400E-03
4.000E+02	3.744E-05	3.761E-05	3.761E-05	3.761E-05
5.000E+02	1.409E-05	1.411E-05	1.411E-05	1.413E-05

Table 2-2(a). CASE 1 RESULTS: CONCENTRATION OF Np-237 IN THE FRACTURE AT TIME t = 1,000 YEARS (EXPONENTIALLY DECAYING SOURCE AND STEP RELEASE MODE) (Continued)

DISTANCE (m)	MULTFRAC	STEFHEST	TALBOT	DURBIN
6.000E+02	1.201E-05	1.202E-05	1.202E-05	1.204E-05
7.000E+02	1.171E-05	1.171E-05	1.171E-05	1.174E-05
8.000E+02	1.159E-05	1.159E-05	1.159E-05	1.161E-05
9.000E+02	1.154E-05	1.154E-05	1.154E-05	1.156E-05
1.000E+03	1.152E-05	1.152E-05	1.152E-05	1.155E-05
1.500E+03	1.152E-05	1.152E-05	1.152E-05	1.154E-05
2.000E+03	1.152E-05	1.152E-05	1.152E-05	1.154E-05
3.000E+03	1.152E-05	1.152E-05	1.152E-05	1.154E-05
4.000E+03	1.152E-05	1.152E-05	1.152E-05	1.154E-05
5.000E+03	1.152E-05	1.152E-05	1.152E-05	1.154E-05

Table 2-2(b). CASE 1 RESULTS: CONCENTRATION OF Np-237 IN THE FRACTURE AT TIME t = 5,000 YEARS (EXPONENTIALLY DECAYING SOURCE AND BAND RELEASE MODE)

DISTANCE (m)	MULTFRAC	STEFHEST	TALBOT	DURBIN
1.000E-01	4.612E-05	4.660E-05	4.660E-05	4.660E-05
1.500E-01	6.943E-05	6.990E-05	6.990E-05	6.990E-05
2.000E-01	9.273E-05	9.320E-05	9.320E-05	9.320E-05
3.000E-01	1.393E-04	1.398E-04	1.398E-04	1.398E-04
4.000E-01	1.859E-04	1.864E-04	1.864E-04	1.864E-04
5.000E-01	2.325E-04	2.330E-04	2.330E-04	2.330E-04
6.000E-01	2.791E-04	2.796E-04	2.796E-04	2.796E-04
7.000E-01	3.257E-04	3.262E-04	3.262E-04	3.262E-04
8.000E-01	3.723E-04	3.728E-04	3.728E-04	3.728E-04
9.000E-01	4.189E-04	4.194E-04	4.194E-04	4.194E-04
1.000E+00	4.655E-04	4.660E-04	4.660E-04	4.660E-04
1.500E+00	6.986E-04	6.990E-04	6.990E-04	6.990E-04
2.000E+00	9.316E-04	9.321E-04	9.321E-04	9.321E-04
3.000E+00	1.398E-03	1.398E-03	1.398E-03	1.398E-03
4.000E+00	1.864E-03	1.864E-03	1.864E-03	1.864E-03
5.000E+00	2.330E-03	2.330E-03	2.330E-03	2.330E-03
6.000E+00	2.796E-03	2.797E-03	2.797E-03	2.797E-03
7.000E+00	3.262E-03	3.263E-03	3.263E-03	3.263E-03
8.000E+00	3.728E-03	3.729E-03	3.729E-03	3.729E-03
9.000E+00	4.195E-03	4.195E-03	4.195E-03	4.195E-03

Table 2-2(b). CASE 1 RESULTS: CONCENTRATION OF Np-237 IN THE FRACTURE AT TIME t = 5,000 YEARS (EXPONENTIALLY DECAYING SOURCE AND BAND RELEASE MODE) (Continued)

DISTANCE (m)	MULTFRAC	STEFHEST	TALBOT	DURBIN
1.000E+01	4.661E-03	4.661E-03	4.661E-03	4.661E-03
1.500E+01	6.992E-03	6.992E-03	6.992E-03	6.992E-03
2.000E+01	9.322E-03	9.323E-03	9.323E-03	9.323E-03
3.000E+01	1.398E-02	1.398E-02	1.398E-02	1.398E-02
4.000E+01	1.863E-02	1.863E-02	1.863E-02	1.863E-02
5.000E+01	2.327E-02	2.327E-02	2.327E-02	2.327E-02
6.000E+01	3.064E-02	3.064E-02	3.064E-02	3.064E-02
7.000E+01	3.796E-02	3.796E-02	3.796E-02	3.796E-02
8.000E+01	4.520E-02	4.520E-02	4.520E-02	4.520E-02
9.000E+01	5.234E-02	5.234E-02	5.234E-02	5.234E-02
1.000E+02	5.938E-02	5.938E-02	5.938E-02	5.938E-02
1.500E+02	1.080E-01	1.080E-01	1.080E-01	1.080E-01
2.000E+02	1.525E-01	1.525E-01	1.525E-01	1.525E-01
3.000E+02	1.642E-01	1.642E-01	1.642E-01	1.642E-01
4.000E+02	1.352E-01	1.352E-01	1.352E-01	1.352E-01
5.000E+02	1.135E-01	1.135E-01	1.135E-01	1.135E-01
6.000E+02	9.129E-02	9.129E-02	9.129E-02	9.129E-02
7.000E+02	7.056E-02	7.056E-02	7.056E-02	7.056E-02
8.000E+02	5.256E-02	5.256E-02	5.256E-02	5.257E-02
9.000E+02	3.784E-02	3.784E-02	3.784E-02	3.784E-02
1.000E+03	2.638E-02	2.638E-02	2.638E-02	2.638E-02
1.500E+03	2.836E-03	2.836E-03	2.836E-03	2.837E-03
2.000E+03	1.703E-04	1.703E-04	1.703E-04	1.702E-04
3.000E+03	1.087E-05	1.087E-05	1.087E-05	1.089E-05
4.000E+03	1.079E-05	1.079E-05	1.079E-05	1.081E-05
5.000E+03	1.079E-05	1.079E-05	1.079E-05	1.081E-05

TABLE 2-2(c). CASE 1 RESULTS: CONCENTRATION OF Np-237 IN THE FRACTURE AT TIME t = 50,000 YEARS (EXPONENTIALLY DECAYING SOURCE AND STEP RELEASE MODE)

DISTANCE (m)	MULTFRAC	STEFHEST	TALBOT	DURBIN
1.000E-01	2.479E-06	2.689E-06	2.689E-06	2.689E-06
1.500E-01	3.824E-06	4.034E-06	4.034E-06	4.034E-06
2.000E-01	5.169E-06	5.379E-06	5.379E-06	5.379E-06
3.000E-01	7.859E-06	8.068E-06	8.068E-06	8.068E-06
4.000E-01	1.055E-05	1.076E-05	1.076E-05	1.076E-05

Table 2-2(c). CASE 1 RESULTS: CONCENTRATION OF Np-237 IN THE FRACTURE AT TIME t = 50,000 YEARS (EXPONENTIALLY DECAYING SOURCE AND STEP RELEASE MODE) (Continued)

DISTANCE (m)	MULTFRAC	STEFHEST	TALBOT	DURBIN
5.000E-01	1.324E-05	1.345E-05	1.345E-05	1.345E-05
6.000E-01	1.593E-05	1.614E-05	1.614E-05	1.614E-05
7.000E-01	1.862E-05	1.883E-05	1.883E-05	1.883E-05
8.000E-01	2.131E-05	2.151E-05	2.151E-05	2.151E-05
9.000E-01	2.400E-05	2.420E-05	2.420E-05	2.420E-05
1.000E+00	2.669E-05	2.689E-05	2.689E-05	2.689E-05
1.500E+00	4.013E-05	4.034E-05	4.034E-05	4.034E-05
2.000E+00	5.358E-05	5.379E-05	5.379E-05	5.379E-05
3.000E+00	8.048E-05	8.068E-05	8.068E-05	8.068E-05
4.000E+00	1.074E-04	1.076E-04	1.076E-04	1.076E-04
5.000E+00	1.343E-04	1.345E-04	1.345E-04	1.345E-04
6.000E+00	1.612E-04	1.614E-04	1.614E-04	1.614E-04
7.000E+00	1.881E-04	1.883E-04	1.883E-04	1.883E-04
8.000E+00	2.150E-04	2.152E-04	2.152E-04	2.152E-04
9.000E+00	2.419E-04	2.420E-04	2.420E-04	2.420E-04
1.000E+01	2.688E-04	2.689E-04	2.689E-04	2.689E-04
1.500E+01	4.032E-04	4.034E-04	4.034E-04	4.034E-04
2.000E+01	5.377E-04	5.379E-04	5.379E-04	5.379E-04
3.000E+01	8.066E-04	8.068E-04	8.068E-04	8.068E-04
4.000E+01	1.075E-03	1.076E-03	1.076E-03	1.076E-03
5.000E+01	1.344E-03	1.344E-03	1.344E-03	1.344E-03
6.000E+01	1.774E-03	1.774E-03	1.774E-03	1.774E-03
7.000E+01	2.203E-03	2.203E-03	2.203E-03	2.203E-03
8.000E+01	2.632E-03	2.632E-03	2.632E-03	2.632E-03
9.000E+01	3.060E-03	3.060E-03	3.060E-03	3.060E-03
1.000E+02	3.486E-03	3.486E-03	3.486E-03	3.486E-03
1.500E+02	6.700E-03	6.700E-03	6.700E-03	6.700E-03
2.000E+02	1.082E-02	1.082E-02	1.082E-02	1.082E-02
3.000E+02	1.656E-02	1.656E-02	1.656E-02	1.656E-02
4.000E+02	2.018E-02	2.018E-02	2.018E-02	2.018E-02
5.000E+02	2.174E-02	2.174E-02	2.174E-02	2.174E-02
6.000E+02	2.300E-02	2.300E-02	2.300E-02	2.300E-02
7.000E+02	2.398E-02	2.398E-02	2.398E-02	2.398E-02
8.000E+02	2.467E-02	2.467E-02	2.467E-02	2.467E-02
9.000E+02	2.508E-02	2.508E-02	2.508E-02	2.508E-02
1.000E+03	2.521E-02	2.521E-02	2.521E-02	2.521E-02
1.500E+03	2.248E-02	2.248E-02	2.248E-02	2.248E-02
2.000E+03	1.642E-02	1.642E-02	1.642E-02	1.642E-02

Table 2-2(c). CASE 1 RESULTS: CONCENTRATION OF Np-237 IN THE FRACTURE AT TIME t = 50,000 YEARS (EXPONENTIALLY DECAYING SOURCE AND STEP RELEASE MODE) (Continued)

DISTANCE (m)	MULTFRAC	STEFHEST	TALBOT	DURBIN
3.000E+03	5.311E-03	5.311E-03	5.311E-03	5.311E-03
4.000E+03	9.475E-04	9.475E-04	9.475E-04	9.474E-04
5.000E+03	1.046E-04	1.046E-04	1.046E-04	1.046E-04

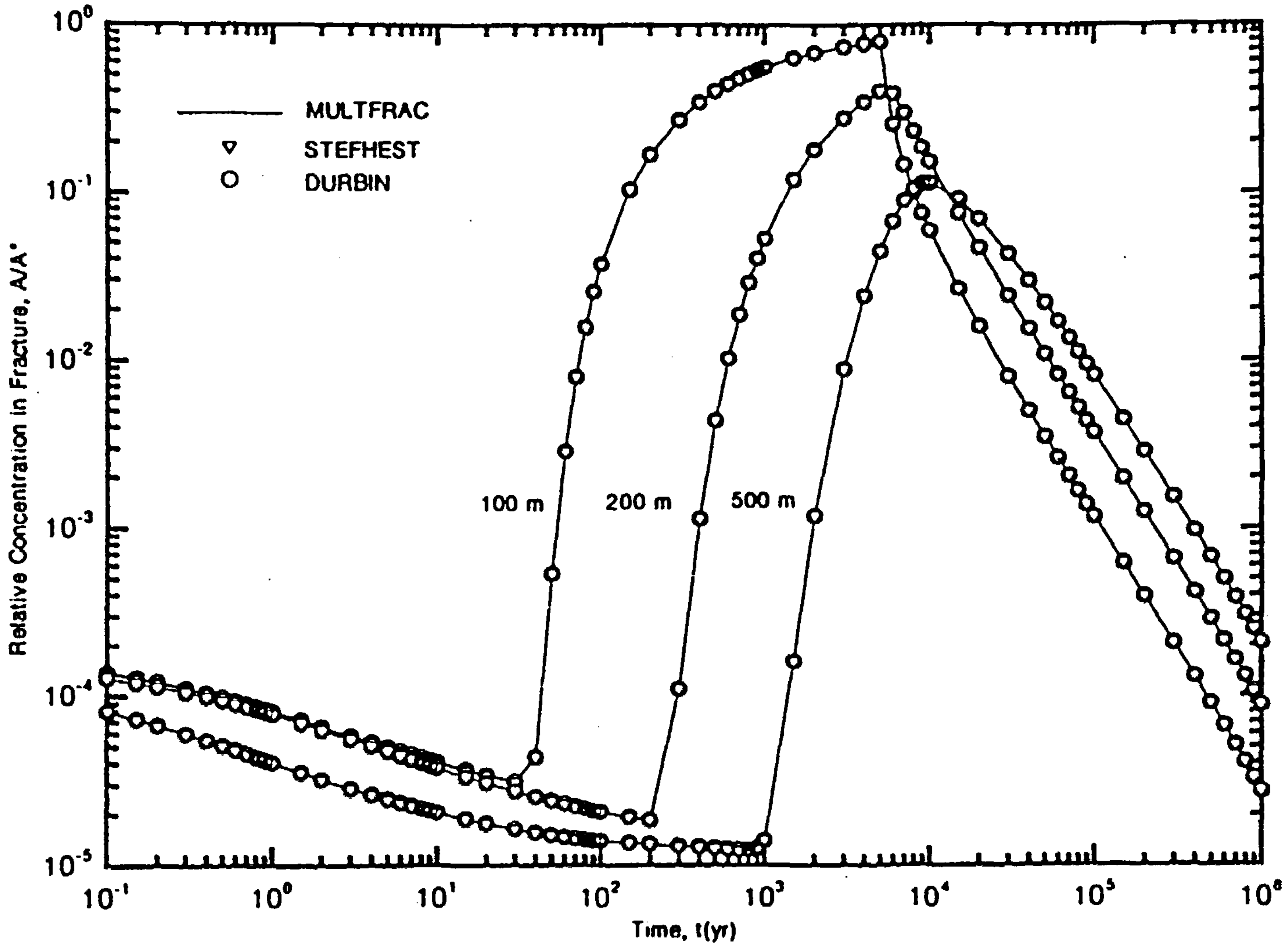

Figure 2-2(b). Relative concentration of Np-237 in the fracture vs. time at different positions x = 100 meters, 200 meters, and 500 meters (Exponentially decaying source).

Table 2-3(a). CASE 1 RESULTS: CONCENTRATION OF Np-237 IN THE FRACTURE LAYER 2, AT DISTANCE x = 100 METERS (EXPONENTIALLY DECAYING SOURCE AND STEP RELEASE MODE)

TIME t(yr)	MULTFRAC	STEHFEST	TALBOT	DURBIN
1.000E-01	1.370E-04	1.370E-04	3.453+248	1.370E-04
1.500E-01	1.278E-04	1.278E-04	-1.309+258	1.278E-04
2.000E-01	1.209E-04	1.209E-04	-1.006+263	1.209E-04
3.000E-01	1.109E-04	1.109E-04	-1.457+232	1.109E-04
4.000E-01	1.037E-04	1.037E-04	-3.245+266	1.037E-04
5.000E-01	9.806E-05	9.806E-05	2.308+235	9.807E-05
6.000E-01	9.353E-05	9.353E-05	1.153+253	9.354E-05
7.000E-01	8.975E-05	8.975E-05	8.592+213	8.976E-05
8.000E-01	8.652E-05	8.652E-05	2.367+243	8.653E-05
9.000E-01	8.371E-05	8.371E-05	1.139+213	8.372E-05
1.000E+00	8.124E-05	8.124E-05	-1.166+254	8.125E-05
1.500E+00	7.215E-05	7.215E-05	1.420+223	7.216E-05
2.000E+00	6.617E-05	6.617E-05	-3.639+234	6.618E-05
3.000E+00	5.850E-05	5.850E-05	-1.693+237	5.848E-05
4.000E+00	5.362E-05	5.362E-05	-3.822+167	5.360E-05
5.000E+00	5.016E-05	5.016E-05	-1.900+125	5.014E-05
6.000E+00	4.753E-05	4.753E-05	-1.166E+97	4.752E-05
7.000E+00	4.546E-05	4.546E-05	3.444+168	4.544E-05
8.000E+00	4.376E-05	4.376E-05	-5.676+136	4.375E-05
9.000E+00	4.234E-05	4.234E-05	1.595+112	4.232E-05
1.000E+01	4.113E-05	4.113E-05	-5.187E+93	4.111E-05
1.500E+01	3.694E-05	3.694E-05	7.614E+34	3.693E-05
2.000E+01	3.440E-05	3.439E-05	4.816E+05	3.439E-05
3.000E+01	3.129E-05	3.111E-05	3.122E-05	3.131E-05
4.000E+01	4.396E-05	4.359E-05	4.372E-05	4.373E-05
5.000E+01	5.396E-04	5.394E-04	5.392E-04	5.389E-04
6.000E+01	2.886E-03	2.885E-03	2.885E-03	2.885E-03
7.000E+01	7.987E-03	7.987E-03	7.987E-03	7.987E-03
8.000E+01	1.580E-02	1.580E-02	1.580E-02	1.580E-02
9.000E+01	2.580E-02	2.580E-02	2.580E-02	2.580E-02
1.000E+02	3.739E-02	3.739E-02	3.739E-02	3.739E-02
1.500E+02	1.042E-01	1.042E-01	1.042E-01	1.042E-01
2.000E+02	1.682E-01	1.682E-01	1.682E-01	1.682E-01
3.000E+02	2.702E-01	2.702E-01	2.702E-01	2.702E-01
4.000E+02	3.443E-01	3.443E-01	3.443E-01	3.443E-01
5.000E+02	4.003E-01	4.003E-01	4.003E-01	4.003E-01
6.000E+02	4.444E-01	4.444E-01	4.444E-01	4.444E-01
7.000E+02	4.800E-01	4.800E-01	4.800E-01	4.800E-01

Table 2-3(a). CASE 1 RESULTS: CONCENTRATION OF Np-237 IN THE FRACTURE LAYER 2, AT DISTANCE x = 100 METERS (EXPONENTIALLY DECAYING SOURCE AND STEP RELEASE MODE) (Continued)

TIME t(yr)	MULTFRAC	STEFHEST	TALBOT	DURBIN
8.000E+02	5.097E-01	5.097E-01	5.097E-01	5.097E-01
9.000E+02	5.348E-01	5.348E-01	5.348E-01	5.348E-01
1.000E+03	5.564E-01	5.564E-01	5.564E-01	5.564E-01
1.500E+03	6.322E-01	6.322E-01	6.322E-01	6.322E-01
2.000E+03	6.789E-01	6.789E-01	6.789E-01	6.789E-01
3.000E+03	7.355E-01	7.355E-01	7.355E-01	7.355E-01
4.000E+03	7.697E-01	7.697E-01	7.697E-01	7.697E-01
5.000E+03	7.932E-01	7.932E-01	7.932E-01	7.932E-01
6.000E+03	2.550E-01	2.550E-01	2.550E-01	2.550E-01
7.000E+03	1.462E-01	1.462E-01	1.462E-01	1.462E-01
8.000E+03	1.005E-01	1.005E-01	1.005E-01	1.005E-01
9.000E+03	7.528E-02	7.528E-02	7.528E-02	7.528E-02
1.000E+04	5.938E-02	5.938E-02	5.938E-02	5.938E-02
1.500E+04	2.650E-02	2.650E-02	2.650E-02	2.650E-02
2.000E+04	1.583E-02	1.583E-02	1.583E-02	1.583E-02
3.000E+04	7.972E-03	7.972E-03	7.972E-03	7.972E-03
4.000E+04	4.986E-03	4.986E-03	4.986E-03	4.986E-03
5.000E+04	3.486E-03	3.486E-03	3.486E-03	3.486E-03
6.000E+04	2.610E-03	2.610E-03	2.610E-03	2.610E-03
7.000E+04	2.046E-03	2.046E-03	2.046E-03	2.046E-03
8.000E+04	1.658E-03	1.658E-03	1.658E-03	1.658E-03
9.000E+04	1.378E-03	1.378E-03	1.378E-03	1.378E-03
1.000E+05	1.168E-03	1.168E-03	1.168E-03	1.168E-03
1.500E+05	6.188E-04	6.188E-04	6.188E-04	6.188E-04
2.000E+05	3.936E-04	3.936E-04	3.936E-04	3.936E-04
3.000E+05	2.067E-04	2.067E-04	2.067E-04	2.067E-04
4.000E+05	1.300E-04	1.300E-04	1.300E-04	1.300E-04
5.000E+05	9.011E-05	9.013E-05	9.013E-05	9.013E-05
6.000E+05	6.647E-05	6.649E-05	6.649E-05	6.649E-05
7.000E+05	5.116E-05	5.118E-05	5.118E-05	5.118E-05
8.000E+05	4.063E-05	4.064E-05	4.064E-05	4.064E-05
9.000E+05	3.304E-05	3.305E-05	3.305E-05	3.305E-05
1.000E+06	2.738E-05	2.739E-05	2.739E-05	2.739E-05

Table 2-3(b). CASE 1 RESULTS: CONCENTRATION OF Np-237 IN THE FRACTURE LAYER 3, AT DISTANCE x = 200 METERS (EXPONENTIALLY DECAYING SOURCE AND BAND RELEASE MODE)

TIME t(yr)	MULTFRAC	STEFHEST	TALBOT	DURBIN
1.000E-01	1.266E-04	1.266E-04	3.773+263	1.266E-04
1.500E-01	1.189E-04	1.189E-04	-2.483+248	1.189E-04
2.000E-01	1.131E-04	1.131E-04	-6.383+224	1.131E-04
3.000E-01	1.045E-04	1.045E-04	1.549+232	1.045E-04
4.000E-01	9.819E-05	9.819E-05	-3.547+269	9.821E-05
5.000E-01	9.321E-05	9.321E-05	-1.915+271	9.323E-05
6.000E-01	8.913E-05	8.913E-05	-9.269+254	8.914E-05
7.000E-01	8.568E-05	8.568E-05	-7.268+257	8.569E-05
8.000E-01	8.270E-05	8.270E-05	4.472+262	8.272E-05
9.000E-01	8.010E-05	8.010E-05	3.029+267	8.011E-05
1.000E+00	7.779E-05	7.779E-05	-6.074+236	7.780E-05
1.500E+00	6.915E-05	6.915E-05	1.481+256	6.916E-05
2.000E+00	6.334E-05	6.334E-05	-5.650+263	6.332E-05
3.000E+00	5.574E-05	5.574E-05	5.634+226	5.572E-05
4.000E+00	5.081E-05	5.081E-05	-7.401+231	5.080E-05
5.000E+00	4.728E-05	4.728E-05	2.485+213	4.726E-05
6.000E+00	4.458E-05	4.458E-05	-2.428+255	4.456E-05
7.000E+00	4.243E-05	4.243E-05	1.182+214	4.241E-05
8.000E+00	4.066E-05	4.066E-05	1.540+183	4.064E-05
9.000E+00	3.918E-05	3.918E-05	-2.004+216	3.916E-05
1.000E+01	3.790E-05	3.790E-05	-2.717+231	3.789E-05
1.500E+01	3.349E-05	3.349E-05	-1.524+152	3.348E-05
2.000E+01	3.079E-05	3.079E-05	-3.934+163	3.078E-05
3.000E+01	2.753E-05	2.753E-05	-2.499+110	2.751E-05
4.000E+01	2.555E-05	2.555E-05	3.674E+61	2.554E-05
5.000E+01	2.420E-05	2.420E-05	9.401E+32	2.428E-05
6.000E+01	2.319E-05	2.319E-05	2.380E+13	2.326E-05
7.000E+01	2.240E-05	2.240E-05	1.140E+00	2.248E-05
8.000E+01	2.177E-05	2.177E-05	2.176E-05	2.184E-05
9.000E+01	2.124E-05	2.124E-05	2.124E-05	2.131E-05
1.000E+02	2.080E-05	2.080E-05	2.080E-05	2.086E-05
1.500E+02	1.928E-05	1.928E-05	1.928E-05	1.934E-05
2.000E+02	1.856E-05	1.856E-05	1.856E-05	1.853E-05
3.000E+02	1.101E-04	1.102E-04	1.102E-04	1.102E-04
4.000E+02	1.144E-03	1.144E-03	1.144E-03	1.144E-03
5.000E+02	4.388E-03	4.388E-03	4.388E-03	4.388E-03
6.000E+02	1.032E-02	1.032E-02	1.032E-02	1.032E-02

Table 2-3(b). CASE 1 RESULTS: CONCENTRATION OF Np-237 IN THE FRACTURE LAYER 3, AT DISTANCE x = 200 METERS (EXPONENTIALLY DECAYING SOURCE AND BAND RELEASE MODE) (Continued)

TIME t(yr)	MULTFRAC	STEFHEST	TALBOT	DURBIN
7.000E+02	1.869E-02	1.869E-02	1.869E-02	1.869E-02
8.000E+02	2.896E-02	2.896E-02	2.896E-02	2.896E-02
9.000E+02	4.058E-02	4.058E-02	4.058E-02	4.058E-02
1.000E+03	5.308E-02	5.308E-02	5.308E-02	5.308E-02
1.500E+03	1.190E-01	1.190E-01	1.190E-01	1.190E-01
2.000E+03	1.796E-01	1.796E-01	1.796E-01	1.796E-01
3.000E+03	2.761E-01	2.761E-01	2.761E-01	2.761E-01
4.000E+03	3.469E-01	3.469E-01	3.469E-01	3.469E-01
5.000E+03	4.009E-01	4.009E-01	4.009E-01	4.009E-01
6.000E+03	3.905E-01	3.905E-01	3.905E-01	3.905E-01
7.000E+03	2.988E-01	2.988E-01	2.988E-01	2.988E-01
8.000E+03	2.314E-01	2.314E-01	2.314E-01	2.314E-01
9.000E+03	1.853E-01	1.853E-01	1.853E-01	1.853E-01
1.000E+04	1.525E-01	1.525E-01	1.525E-01	1.525E-01
1.500E+04	7.499E-02	7.499E-02	7.499E-02	7.499E-02
2.000E+04	4.647E-02	4.647E-02	4.647E-02	4.647E-02
3.000E+04	2.418E-02	2.418E-02	2.418E-02	2.418E-02
4.000E+04	1.535E-02	1.535E-02	1.535E-02	1.535E-02
5.000E+04	1.082E-02	1.082E-02	1.082E-02	1.082E-02
6.000E+04	8.146E-03	8.146E-03	8.146E-03	8.146E-03
7.000E+04	6.410E-03	6.410E-03	6.410E-03	6.410E-03
8.000E+04	5.210E-03	5.210E-03	5.210E-03	5.210E-03
9.000E+04	4.340E-03	4.340E-03	4.340E-03	4.340E-03
1.000E+05	3.685E-03	3.686E-03	3.686E-03	3.686E-03
1.500E+05	1.962E-03	1.962E-03	1.962E-03	1.962E-03
2.000E+05	1.251E-03	1.251E-03	1.251E-03	1.251E-03
3.000E+05	6.588E-04	6.589E-04	6.589E-04	6.589E-04
4.000E+05	4.147E-04	4.147E-04	4.147E-04	4.147E-04
5.000E+05	2.878E-04	2.878E-04	2.878E-04	2.878E-04
6.000E+05	2.124E-04	2.124E-04	2.124E-04	2.124E-04
7.000E+05	1.635E-04	1.635E-04	1.635E-04	1.635E-04
8.000E+05	1.299E-04	1.299E-04	1.299E-04	1.299E-04
9.000E+05	1.056E-04	1.057E-04	1.057E-04	1.057E-04
1.000E+06	8.755E-05	8.757E-05	8.757E-05	8.757E-05

Table 2-3(c). CASE 1 RESULTS: CONCENTRATION OF Np-237 IN THE FRACTURE LAYER 5, AT DISTANCE x = 500 METERS (EXPONENTIALLY DECAYING SOURCE AND BAND RELEASE MODE)

TIME t(yr)	MULTFRAC	STEFHEST	TALBOT	DURBIN
1.000E-01	8.014E-05	8.014E-05	1.068+242	8.016E-05
1.500E-01	7.234E-05	7.234E-05	-5.321+263	7.235E-05
2.000E-01	6.687E-05	6.687E-05	-7.510+213	6.689E-05
3.000E-01	5.943E-05	5.943E-05	3.313+254	5.942E-05
4.000E-01	5.443E-05	5.443E-05	5.954+235	5.441E-05
5.000E-01	5.074E-05	5.074E-05	-1.736+248	5.073E-05
6.000E-01	4.787E-05	4.787E-05	-4.745+270	4.786E-05
7.000E-01	4.555E-05	4.555E-05	1.094+267	4.554E-05
8.000E-01	4.362E-05	4.362E-05	-4.012+268	4.361E-05
9.000E-01	4.199E-05	4.199E-05	3.677+251	4.197E-05
1.000E+00	4.057E-05	4.057E-05	5.799+260	4.056E-05
1.500E+00	3.559E-05	3.559E-05	4.358+244	3.557E-05
2.000E+00	3.248E-05	3.248E-05	9.867+243	3.246E-05
3.000E+00	2.866E-05	2.866E-05	4.827+261	2.865E-05
4.000E+00	2.632E-05	2.632E-05	-4.553+259	2.631E-05
5.000E+00	2.471E-05	2.471E-05	5.079+253	2.479E-05
6.000E+00	2.350E-05	2.350E-05	6.143+248	2.358E-05
7.000E+00	2.256E-05	2.256E-05	4.573+246	2.264E-05
8.000E+00	2.180E-05	2.180E-05	-2.746+234	2.187E-05
9.000E+00	2.116E-05	2.116E-05	1.214+234	2.123E-05
1.000E+01	2.062E-05	2.062E-05	4.457+246	2.069E-05
1.500E+01	1.879E-05	1.879E-05	4.433+213	1.885E-05
2.000E+01	1.768E-05	1.768E-05	1.464+203	1.774E-05
3.000E+01	1.637E-05	1.637E-05	-2.484+193	1.642E-05
4.000E+01	1.559E-05	1.559E-05	1.093+182	1.563E-05
5.000E+01	1.507E-05	1.507E-05	4.421+128	1.511E-05
6.000E+01	1.471E-05	1.471E-05	-7.477E+92	1.475E-05
7.000E+01	1.444E-05	1.444E-05	-1.793E+67	1.448E-05
8.000E+01	1.424E-05	1.425E-05	-1.223E+48	1.428E-05
9.000E+01	1.409E-05	1.409E-05	8.463E+33	1.413E-05
1.000E+02	1.396E-05	1.397E-05	1.263E+21	1.401E-05
1.500E+02	1.356E-05	1.358E-05	1.358E-05	1.361E-05
2.000E+02	1.332E-05	1.334E-05	1.334E-05	1.337E-05
3.000E+02	1.299E-05	1.301E-05	1.301E-05	1.304E-05
4.000E+02	1.275E-05	1.278E-05	1.278E-05	1.281E-05
5.000E+02	1.258E-05	1.261E-05	1.261E-05	1.264E-05
6.000E+02	1.245E-05	1.248E-05	1.248E-05	1.251E-05
7.000E+02	1.236E-05	1.238E-05	1.238E-05	1.241E-05

Table 2-3(c). CASE 1 RESULTS: CONCENTRATION OF Np-237 IN THE FRACTURE LAYER 5, AT DISTANCE x = 500 METERS (EXPONENTIALLY DECAYING SOURCE AND BAND RELEASE MODE) (Continued)

TIME t(yr)	MULTFRAC	STEFHEST	TALBOT	DURBIN
8.000E+02	1.233E-05	1.236E-05	1.236E-05	1.238E-05
9.000E+02	1.263E-05	1.266E-05	1.266E-05	1.263E-05
1.000E+03	1.409E-05	1.411E-05	1.411E-05	1.413E-05
1.500E+03	1.619E-04	1.619E-04	1.619E-04	1.619E-04
2.000E+03	1.192E-03	1.193E-03	1.193E-03	1.189E-03
3.000E+03	8.880E-03	8.880E-03	8.880E-03	8.881E-03
4.000E+03	2.425E-02	2.425E-02	2.425E-02	2.425E-02
5.000E+03	4.458E-02	4.458E-02	4.458E-02	4.458E-02
6.000E+03	6.731E-02	6.731E-02	6.731E-02	6.731E-02
7.000E+03	8.959E-02	8.959E-02	8.959E-02	8.959E-02
8.000E+03	1.051E-01	1.051E-01	1.051E-01	1.051E-01
9.000E+03	1.123E-01	1.123E-01	1.123E-01	1.123E-01
1.000E+04	1.135E-01	1.135E-01	1.135E-01	1.135E-01
1.500E+04	9.175E-02	9.175E-02	9.175E-02	9.175E-02
2.000E+04	6.929E-02	6.929E-02	6.929E-02	6.929E-02
3.000E+04	4.287E-02	4.287E-02	4.287E-02	4.287E-02
4.000E+04	2.946E-02	2.946E-02	2.946E-02	2.946E-02
5.000E+04	2.174E-02	2.174E-02	2.174E-02	2.174E-02
6.000E+04	1.685E-02	1.685E-02	1.685E-02	1.685E-02
7.000E+04	1.354E-02	1.354E-02	1.354E-02	1.354E-02
8.000E+04	1.118E-02	1.118E-02	1.118E-02	1.118E-02
9.000E+04	9.420E-03	9.420E-03	9.420E-03	9.420E-03
1.000E+05	8.075E-03	8.075E-03	8.075E-03	8.075E-03
1.500E+05	4.420E-03	4.420E-03	4.420E-03	4.420E-03
2.000E+05	2.857E-03	2.858E-03	2.858E-03	2.858E-03
3.000E+05	1.525E-03	1.525E-03	1.525E-03	1.525E-03
4.000E+05	9.664E-04	9.665E-04	9.665E-04	9.665E-04
5.000E+05	6.733E-04	6.733E-04	6.733E-04	6.733E-04
6.000E+05	4.982E-04	4.982E-04	4.982E-04	4.982E-04
7.000E+05	3.843E-04	3.844E-04	3.844E-04	3.844E-04
8.000E+05	3.057E-04	3.057E-04	3.057E-04	3.057E-04
9.000E+05	2.489E-04	2.489E-04	2.489E-04	2.489E-04
1.000E+06	2.064E-04	2.065E-04	2.065E-04	2.065E-04

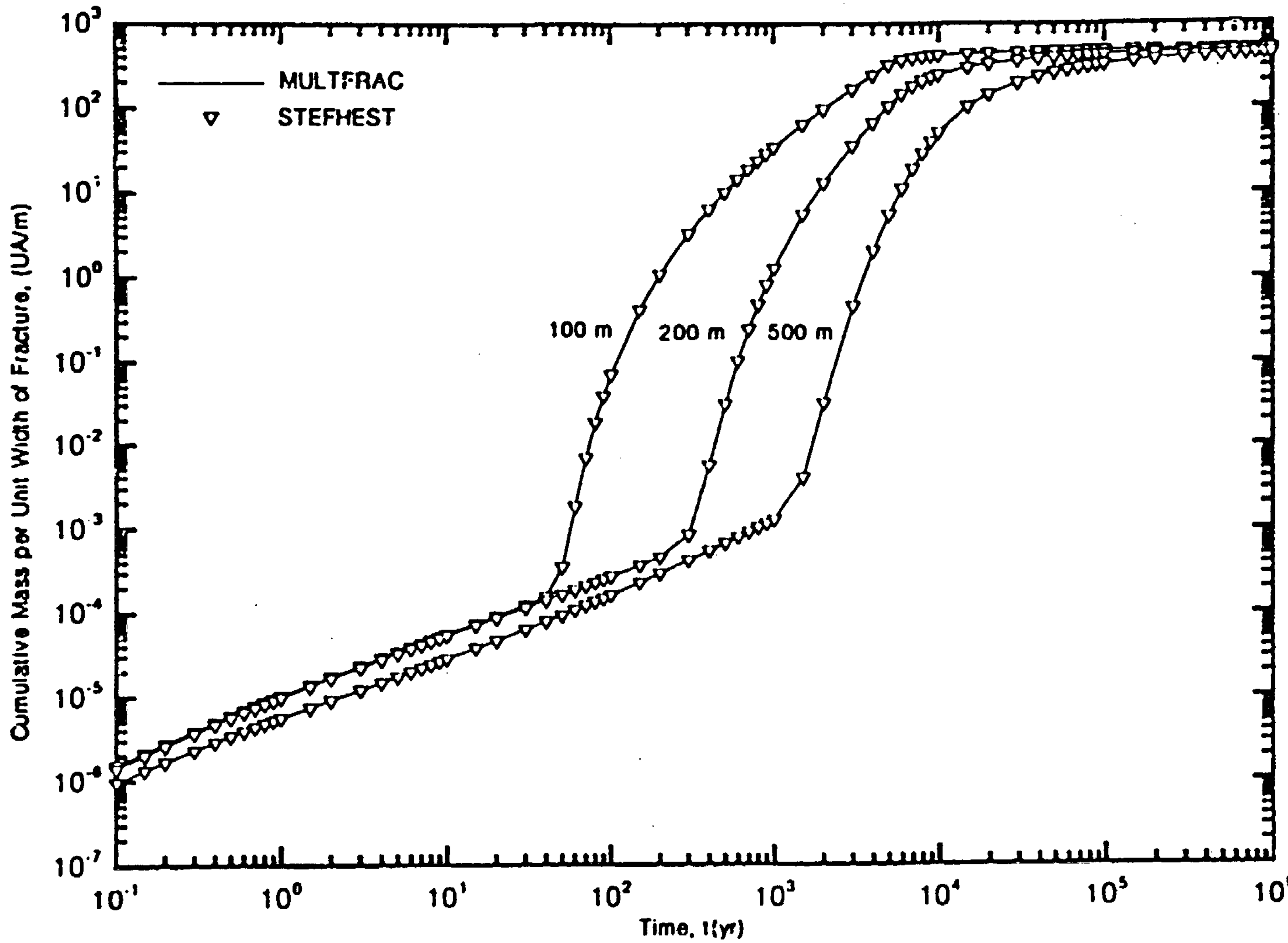

Figure 2-2(c). Cumulative mass of Np-237 per unit in the fracture vs. time at different positions x = 100, 200, and 500 meters (Exponentially decaying source and band release mode).

Table 2-4(a). CASE 1 RESULTS: CUMULATIVE MASS OF Np-237 IN THE FRACTURE AT DISTANCE x = 100 METERS (EXPONENTIALLY DECAYING SOURCE AND BAND RELEASE MODE)

TIME (yr)	MULTFRAC	STEFHEST
1.000E-01	1.543E-06	1.543E-06
1.500E-01	2.204E-06	2.204E-06
2.000E-01	2.825E-06	2.825E-06
3.000E-01	3.980E-06	3.980E-06
4.000E-01	5.051E-06	5.051E-06
5.000E-01	6.059E-06	6.059E-06
6.000E-01	7.016E-06	7.016E-06
7.000E-01	7.932E-06	7.932E-06
8.000E-01	8.813E-06	8.813E-06
9.000E-01	9.664E-06	9.664E-06
1.000E+00	1.049E-05	1.049E-05
1.500E+00	1.430E-05	1.430E-05
2.000E+00	1.775E-05	1.775E-05
3.000E+00	2.395E-05	2.395E-05
4.000E+00	2.954E-05	2.954E-05
5.000E+00	3.472E-05	3.472E-05
6.000E+00	3.960E-05	3.960E-05
7.000E+00	4.425E-05	4.425E-05
8.000E+00	4.871E-05	4.870E-05
9.000E+00	5.301E-05	5.301E-05
1.000E+01	5.718E-05	5.718E-05
1.500E+01	7.660E-05	7.659E-05
2.000E+01	9.439E-05	9.438E-05
3.000E+01	1.271E-04	1.270E-04
4.000E+01	1.594E-04	1.594E-04
5.000E+01	3.594E-04	3.594E-04
6.000E+01	1.863E-03	1.863E-03
7.000E+01	7.060E-03	7.060E-03
8.000E+01	1.874E-02	1.874E-02
9.000E+01	3.939E-02	3.939E-02
1.000E+02	7.087E-02	7.087E-02
1.500E+02	4.223E-01	4.223E-01
2.000E+02	1.107E+00	1.107E+00
3.000E+02	3.326E+00	3.326E+00
4.000E+02	6.417E+00	6.417E+00
5.000E+02	1.015E+01	1.015E+01
6.000E+02	1.438E+01	1.438E+01

Table 2-4(a). CASE 1 RESULTS: CUMULATIVE MASS OF Np-237 IN THE FRACTURE AT DISTANCE x = 100 METERS (EXPONENTIALLY DECAYING SOURCE AND BAND RELEASE MODE) (Continued)

TIME (yr)	MULTFRAC	STEFHEST
7.000E+02	1.901E+01	1.901E+01
8.000E+02	2.397E+01	2.397E+01
9.000E+02	2.919E+01	2.919E+01
1.000E+03	3.465E+01	3.465E+01
1.500E+03	6.454E+01	6.454E+01
2.000E+03	9.740E+01	9.740E+01
3.000E+03	1.684E+02	1.684E+02
4.000E+03	2.438E+02	2.438E+02
5.000E+03	3.220E+02	3.220E+02
6.000E+03	3.676E+02	3.676E+02
7.000E+03	3.867E+02	3.867E+02
8.000E+03	3.988E+02	3.988E+02
9.000E+03	4.075E+02	4.075E+02
1.000E+04	4.142E+02	4.141E+02
1.500E+04	4.338E+02	4.338E+02
2.000E+04	4.440E+02	4.440E+02
3.000E+04	4.551E+02	4.551E+02
4.000E+04	4.614E+02	4.613E+02
5.000E+04	4.656E+02	4.655E+02
6.000E+04	4.686E+02	4.685E+02
7.000E+04	4.709E+02	4.709E+02
8.000E+04	4.728E+02	4.727E+02
9.000E+04	4.743E+02	4.743E+02
1.000E+05	4.755E+02	4.755E+02
1.500E+05	4.798E+02	4.798E+02
2.000E+05	4.822E+02	4.823E+02
3.000E+05	4.851E+02	4.852E+02
4.000E+05	4.867E+02	4.868E+02
5.000E+05	4.878E+02	4.879E+02
6.000E+05	4.886E+02	4.887E+02
7.000E+05	4.891E+02	4.893E+02
8.000E+05	4.896E+02	4.897E+02
9.000E+05	4.900E+02	4.901E+02
1.000E+06	4.903E+02	4.904E+02

Table 2-4(b). CASE 1 RESULTS: CUMULATIVE MASS OF Np-237 IN THE FRACTURE AT DISTANCE x = 200 METERS (EXPONENTIALLY DECAYING SOURCE AND BAND RELEASE MODE)

TIME (yr)	MULTFRAC	STEFHEST
1.000E-01	1.404E-06	1.404E-06
1.500E-01	2.016E-06	2.016E-06
2.000E-01	2.596E-06	2.596E-06
3.000E-01	3.682E-06	3.682E-06
4.000E-01	4.694E-06	4.694E-06
5.000E-01	5.650E-06	5.650E-06
6.000E-01	6.561E-06	6.561E-06
7.000E-01	7.434E-06	7.434E-06
8.000E-01	8.276E-06	8.276E-06
9.000E-01	9.090E-06	9.090E-06
1.000E+00	9.879E-06	9.879E-06
1.500E+00	1.354E-05	1.354E-05
2.000E+00	1.684E-05	1.684E-05
3.000E+00	2.276E-05	2.276E-05
4.000E+00	2.807E-05	2.807E-05
5.000E+00	3.297E-05	3.297E-05
6.000E+00	3.756E-05	3.756E-05
7.000E+00	4.190E-05	4.190E-05
8.000E+00	4.606E-05	4.605E-05
9.000E+00	5.005E-05	5.004E-05
1.000E+01	5.390E-05	5.390E-05
1.500E+01	7.164E-05	7.164E-05
2.000E+01	8.767E-05	8.766E-05
3.000E+01	1.167E-04	1.166E-04
4.000E+01	1.431E-04	1.431E-04
5.000E+01	1.680E-04	1.679E-04
6.000E+01	1.916E-04	1.916E-04
7.000E+01	2.144E-04	2.144E-04
8.000E+01	2.365E-04	2.364E-04
9.000E+01	2.580E-04	2.579E-04
1.000E+02	2.790E-04	2.789E-04
1.500E+02	3.788E-04	3.787E-04
2.000E+02	4.730E-04	4.728E-04
3.000E+02	8.643E-04	8.640E-04
4.000E+02	5.753E-03	5.753E-03
5.000E+02	3.122E-02	3.122E-02
6.000E+02	1.026E-01	1.026E-01
7.000E+02	2.458E-01	2.458E-01

Table 2-4(b). CASE 1 RESULTS: CUMULATIVE MASS OF Np-237 IN THE FRACTURE AT DISTANCE x = 200 METERS (EXPONENTIALLY DECAYING SOURCE AND BAND RELEASE MODE) (Continued)

TIME (yr)	MULTFRAC	STEFHEST
8.000E+02	4.827E-01	4.827E-01
9.000E+02	8.295E-01	8.294E-01
1.000E+03	1.297E+00	1.297E+00
1.500E+03	5.598E+00	5.598E+00
2.000E+03	1.310E+01	1.310E+01
3.000E+03	3.614E+01	3.614E+01
4.000E+03	6.747E+01	6.747E+01
5.000E+03	1.050E+02	1.050E+02
6.000E+03	1.460E+02	1.460E+02
7.000E+03	1.803E+02	1.803E+02
8.000E+03	2.066E+02	2.066E+02
9.000E+03	2.273E+02	2.273E+02
1.000E+04	2.441E+02	2.441E+02
1.500E+04	2.972E+02	2.972E+02
2.000E+04	3.266E+02	3.266E+02
3.000E+04	3.600E+02	3.600E+02
4.000E+04	3.792E+02	3.792E+02
5.000E+04	3.920E+02	3.920E+02
6.000E+04	4.014E+02	4.014E+02
7.000E+04	4.086E+02	4.086E+02
8.000E+04	4.144E+02	4.144E+02
9.000E+04	4.192E+02	4.192E+02
1.000E+05	4.232E+02	4.232E+02
1.500E+05	4.365E+02	4.366E+02
2.000E+05	4.444E+02	4.444E+02
3.000E+05	4.534E+02	4.534E+02
4.000E+05	4.586E+02	4.586E+02
5.000E+05	4.621E+02	4.620E+02
6.000E+05	4.646E+02	4.645E+02
7.000E+05	4.664E+02	4.664E+02
8.000E+05	4.679E+02	4.679E+02
9.000E+05	4.690E+02	4.690E+02
1.000E+06	4.700E+02	4.700E+02

Table 2-4(c). CASE 1 RESULTS: CUMULATIVE MASS OF Np-237 IN THE FRACTURE AT DISTANCE x = 500 METERS (EXPONENTIALLY DECAYING SOURCE AND BAND RELEASE MODE)

TIME (yr)	MULTFRAC	STEFHEST
1.000E-01	9.712E-07	9.712E-07
1.500E-01	1.351E-06	1.351E-06
2.000E-01	1.698E-06	1.698E-06
3.000E-01	2.327E-06	2.327E-06
4.000E-01	2.895E-06	2.895E-06
5.000E-01	3.420E-06	3.420E-06
6.000E-01	3.913E-06	3.913E-06
7.000E-01	4.379E-06	4.379E-06
8.000E-01	4.825E-06	4.825E-06
9.000E-01	5.253E-06	5.253E-06
1.000E+00	5.666E-06	5.665E-06
1.500E+00	7.558E-06	7.558E-06
2.000E+00	9.254E-06	9.254E-06
3.000E+00	1.229E-05	1.229E-05
4.000E+00	1.503E-05	1.503E-05
5.000E+00	1.758E-05	1.758E-05
6.000E+00	1.999E-05	1.999E-05
7.000E+00	2.229E-05	2.229E-05
8.000E+00	2.451E-05	2.450E-05
9.000E+00	2.665E-05	2.665E-05
1.000E+01	2.874E-05	2.874E-05
1.500E+01	3.855E-05	3.854E-05
2.000E+01	4.765E-05	4.763E-05
3.000E+01	6.461E-05	6.459E-05
4.000E+01	8.056E-05	8.053E-05
5.000E+01	9.588E-05	9.583E-05
6.000E+01	1.108E-04	1.107E-04
7.000E+01	1.253E-04	1.252E-04
8.000E+01	1.397E-04	1.396E-04
9.000E+01	1.538E-04	1.537E-04
1.000E+02	1.679E-04	1.677E-04
1.500E+02	2.366E-04	2.364E-04
2.000E+02	3.039E-04	3.036E-04
3.000E+02	4.355E-04	4.351E-04
4.000E+02	5.644E-04	5.638E-04
5.000E+02	6.913E-04	6.906E-04
6.000E+02	8.167E-04	8.158E-04
7.000E+02	9.410E-04	9.400E-04

Table 2-4(c). CASE 1 RESULTS: CUMULATIVE MASS OF Np-237 IN THE FRACTURE AT DISTANCE x = 500 METERS (EXPONENTIALLY DECAYING SOURCE AND BAND RELEASE MODE) (Continued)

TIME (yr)	MULTFRAC	STEFHEST
8.000E+02	1.065E-03	1.063E-03
9.000E+02	1.189E-03	1.188E-03
1.000E+03	1.321E-03	1.320E-03
1.500E+03	4.087E-03	4.086E-03
2.000E+03	3.215E-02	3.215E-02
3.000E+03	4.659E-01	4.659E-01
4.000E+03	2.068E+00	2.068E+00
5.000E+03	5.480E+00	5.480E+00
6.000E+03	1.106E+01	1.106E+01
7.000E+03	1.894E+01	1.894E+01
8.000E+03	2.875E+01	2.875E+01
9.000E+03	3.968E+01	3.968E+01
1.000E+04	5.101E+01	5.101E+01
1.500E+04	1.031E+02	1.031E+02
2.000E+04	1.430E+02	1.430E+02
3.000E+04	1.975E+02	1.975E+02
4.000E+04	2.330E+02	2.330E+02
5.000E+04	2.583E+02	2.583E+02
6.000E+04	2.774E+02	2.774E+02
7.000E+04	2.925E+02	2.925E+02
8.000E+04	3.048E+02	3.048E+02
9.000E+04	3.150E+02	3.150E+02
1.000E+05	3.238E+02	3.238E+02
1.500E+05	3.535E+02	3.535E+02
2.000E+05	3.713E+02	3.713E+02
3.000E+05	3.921E+02	3.920E+02
4.000E+05	4.042E+02	4.042E+02
5.000E+05	4.122E+02	4.123E+02
6.000E+05	4.180E+02	4.181E+02
7.000E+05	4.224E+02	4.224E+02
8.000E+05	4.258E+02	4.259E+02
9.000E+05	4.286E+02	4.286E+02
1.000E+06	4.309E+02	4.309E+02

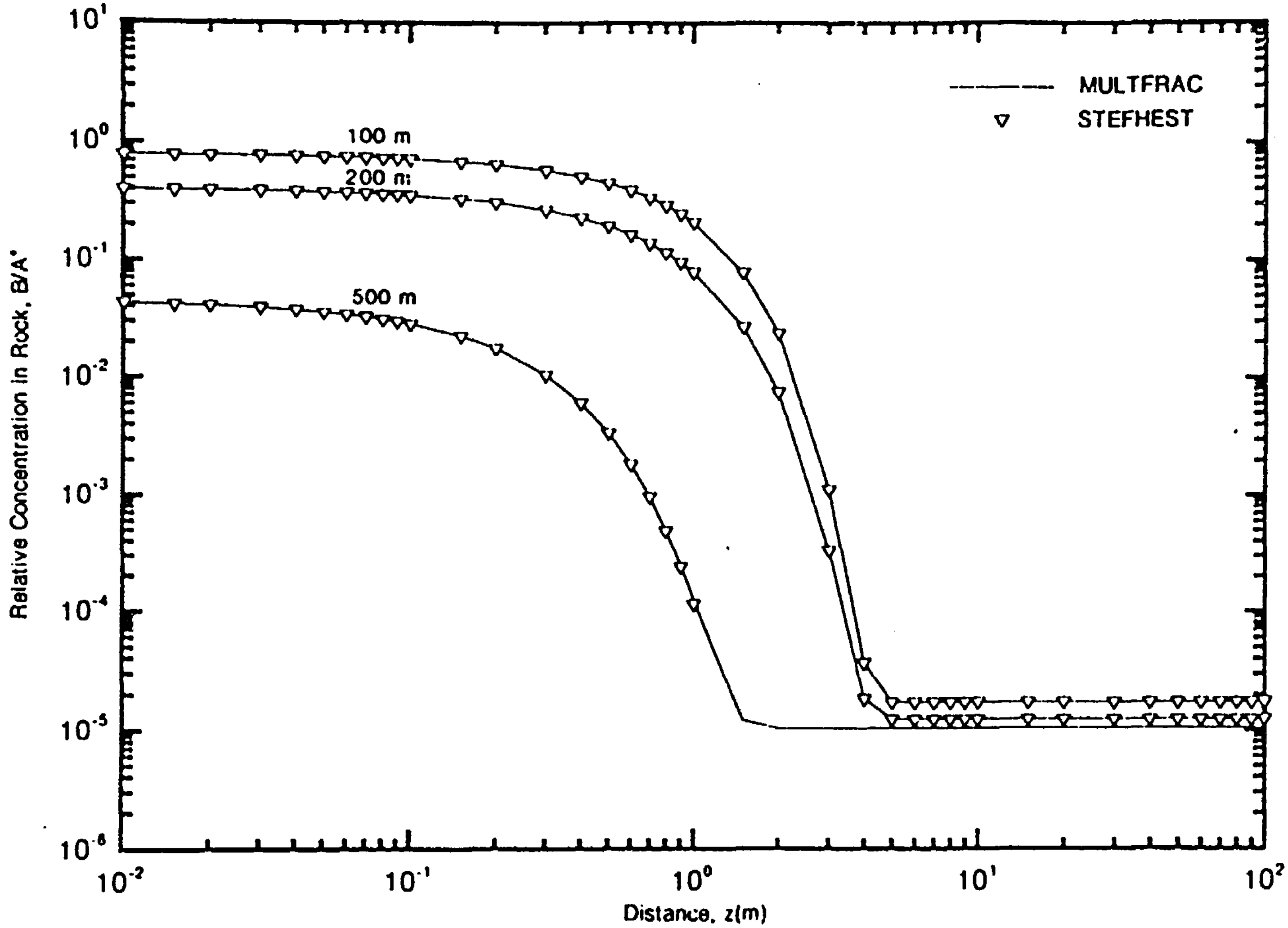

Figure 2-2(d). Relative concentration of Np-237 in rock vs. distance z at time T = 5,000 years and distances from the source x = 100, 200 and 500 meters (Exponentially decaying source and step release mode).

Table 2-5(a). CASE 1 RESULTS: CONCENTRATION OF Np-237 IN THE ROCK MATRIX LAYER 2, AT DISTANCE x = 100 METERS AND TIME t = 5,000 YEARS (EXPONENTIALLY DECAYING SOURCE AND STEP RELEASE MODE)

DISTANCE z(m)	MULTFRAC	STEFHEST
1.000E-02	7.886E-01	7.886E-01
1.500E-02	7.847E-01	7.847E-01
2.000E-02	7.809E-01	7.809E-01
3.000E-02	7.732E-01	7.732E 01
4.000E-02	7.656E-01	7.656E-01
5.000E-02	7.579E-01	7.579E-01
6.000E-02	7.503E-01	7.503E-01
7.000E-02	7.428E-01	7.428E-01
8.000E-02	7.352E-01	7.352E-01
9.000E-02	7.277E-01	7.277E-01
1.000E-01	7.202E-01	7.202E-01
1.500E-01	6.831E-01	6.831E-01
2.000E-01	6.467E-01	6.467E-01
3.000E-01	5.765E-01	5.765E-01
4.000E-01	5.101E-01	5.101E-01
5.000E-01	4.480E-01	4.480E-01
6.000E-01	3.904E-01	3.904E-01
7.000E-01	3.375E-01	3.375E-01
8.000E-01	2.895E-01	2.895E-01
9.000E-01	2.463E-01	2.463E-01
1.000E+00	2.078E-01	2.078E-01
1.500E+00	7.774E-02	7.832E-02
2.000E+00	2.371E-02	2.374E-02
3.000E+00	1.117E-03	1.117E-03
4.000E+00	3.739E-05	3.739E-05
5.000E+00	1.761E-05	1.761E-05
6.000E+00	1.747E-05	1.747E-05
7.000E+00	1.747E-05	1.747E-05
8.000E+00	1.747E-05	1.747E-05
9.000E+00	1.747E-05	1.747E-05
1.000E+01	1.747E-05	1.747E-05

Table 2-5(b). CASE 1 RESULTS: CONCENTRATION OF Np-237 IN THE ROCK MATRIX LAYER 3, AT DISTANCE x = 200 METERS AND TIME t = 5,000 YEARS (EXPONENTIALLY DECAYING SOURCE AND STEP RELEASE MODE)

DISTANCE z(m)	MULTFRAC	STEFHEST
1.000E-02	3.973E-01	3.973E-01
1.500E-02	3.947E-01	3.947E-01
2.000E-02	3.922E-01	3.922E-01
3.000E-02	3.871E-01	3.871E-01
4.000E-02	3.821E-01	3.821E-01
5.000E-02	3.771E-01	3.771E-01
6.000E-02	3.722E-01	3.722E-01
7.000E-02	3.673E-01	3.673E-01
8.000E-02	3.624E-01	3.624E-01
9.000E-02	3.576E-01	3.576E-01
1.000E-01	3.528E-01	3.528E-01
1.500E-01	3.295E-01	3.295E-01
2.000E-01	3.072E-01	3.072E-01
3.000E-01	2.657E-01	2.657E-01
4.000E-01	2.283E-01	2.283E-01
5.000E-01	1.947E-01	1.947E-01
6.000E-01	1.649E-01	1.649E-01
7.000E-01	1.387E-01	1.387E-01
8.000E-01	1.158E-01	1.158E-01
9.000E-01	9.604E-02	9.604E-02
1.000E+00	7.904E-02	7.904E-02
1.500E+00	2.671E-02	2.671E-02
2.000E+00	7.473E-03	7.473E-03
3.000E+00	3.370E-04	3.370E-04
4.000E+00	1.884E-05	1.884E-05
5.000E+00	1.254E-05	1.254E-05
6.000E+00	1.248E-05	1.248E-05
7.000E+00	1.248E-05	1.248E-05
8.000E+00	1.248E-05	1.248E-05
9.000E+00	1.248E-05	1.248E-05
1.000E+01	1.248E-05	1.248E-05

Table 2-5(c). CASE 1 RESULTS: CONCENTRATION OF Np-237 IN THE ROCK MATRIX LAYER 5, AT DISTANCE x = 500 METERS AND TIME t = 5,000 YEARS (EXPONENTIALLY DECAYING SOURCE AND STEP RELEASE MODE)

DISTANCE z(m)	MULTFRAC	STEFHEST
1.000E-02	4.293E-02	4.294E-02
1.500E-02	4.199E-02	4.200E-02
2.000E-02	4.107E-02	4.107E-02
3.000E-02	3.927E-02	3.927E-02
4.000E-02	3.754E-02	3.754E-02
5.000E-02	3.588E-02	3.588E-02
6.000E-02	3.428E-02	3.428E-02
7.000E-02	3.274E-02	3.274E-02
8.000E-02	3.126E-02	3.126E-02
9.000E-02	2.983E-02	2.983E-02
1.000E-01	2.847E-02	2.847E-02
1.500E-01	2.242E-02	2.241E-02
2.000E-01	1.752E-02	1.751E-02
3.000E-01	1.045E-02	1.045E-02
4.000E-01	6.045E-03	6.040E-03
5.000E-01	3.390E-03	3.384E-03
6.000E-01	1.844E-03	1.837E-03
7.000E-01	9.744E-04	9.660E-04
8.000E-01	5.011E-04	4.921E-04
9.000E-01	2.523E-04	2.429E-04
1.000E+00	1.259E-04	1.161E-04
1.500E+00	1.223E-05	1.823E-06
2.000E+00	1.625E-06	1.505E-08
3.000E+00	1.048E-05	7.758E-13
4.000E+00	1.048E-05	3.047E-15
5.000E+00	1.048E-05	-9.383E-17

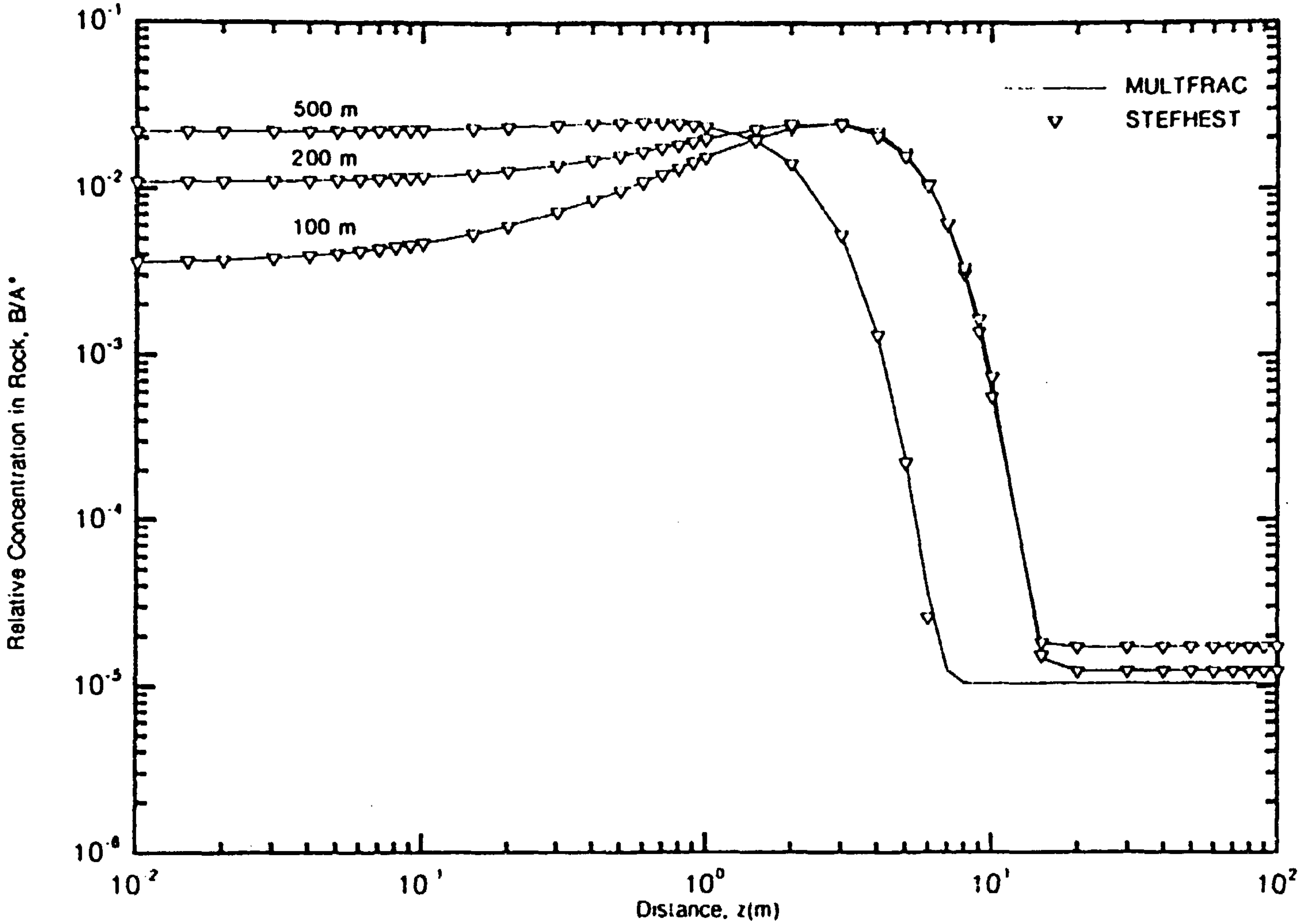

Figure 2-2(e). Relative concentration of Np-237 in rock vs. distance at t = 50,000 years (Exponentially decaying source and band release mode).

Table 2-6(a). CASE 1 RESULTS: CONCENTRATION OF Np-237 IN THE ROCK MATRIX LAYER 2, AT DISTANCE X = 100 METERS AND TIME t = 50,000 YEARS (EXPONENTIALLY DECAYING SOURCE AND BAND RELEASE MODE)

DISTANCE z(m)	MULTFRAC	STEFHEST
1.000E-02	3.566E-03	3.566E-03
1.500E-02	3.633E-03	3.633E-03
2.000E-02	3.699E-03	3.699E-03
3.000E-02	3.832E-03	3.832E-03
4.000E-02	3.965E-03	3.965E-03
5.000E-02	4.098E-03	4.098E-03
6.000E-02	4.230E-03	4.230E-03
7.000E-02	4.363E-03	4.363E-03
8.000E-02	4.495E-03	4.495E-03
9.000E-02	4.627E-03	4.627E-03
1.000E-01	4.759E-03	4.759E-03
1.500E-01	5.416E-03	5.417E-03
2.000E-01	6.070E-03	6.070E-03
3.000E-01	7.361E-03	7.362E-03
4.000E-01	8.630E-03	8.630E-03
5.000E-01	9.872E-03	9.872E-03
6.000E-01	1.108E-02	1.108E-02
7.000E-01	1.226E-02	1.226E-02
8.000E-01	1.340E-02	1.340E-02
9.000E-01	1.450E-02	1.450E-02
1.000E+00	1.555E-02	1.555E-02
1.500E+00	2.008E-02	2.008E-02
2.000E+00	2.321E-02	2.321E-02
3.000E+00	2.505E-02	2.505E-02
4.000E+00	2.203E-02	2.203E-02
5.000E+00	1.649E-02	1.649E-02
6.000E+00	1.070E-02	1.070E-02
7.000E+00	6.101E-03	6.101E-03
8.000E+00	3.077E-03	3.077E-03
9.000E+00	1.383E-03	1.383E-03
1.000E+01	5.603E-04	5.603E-04
1.500E+01	1.825E-05	1.825E-05
2.000E+01	1.724E-05	1.724E-05
3.000E+01	1.719E-05	1.724E-05
4.000E+01	1.724E-05	1.724E-05
5.000E+01	1.724E-05	1.724E-05
6.000E+01	1.724E-05	1.724E-05
7.000E+01	1.724E-05	1.724E-05

Table 2-6(a). CASE 1 RESULTS: CONCENTRATION OF Np-237 IN THE ROCK MATRIX LAYER 2, AT DISTANCE X = 100 METERS AND TIME t = 50,000 YEARS (EXPONENTIALLY DECAYING SOURCE AND BAND RELEASE MODE) (Continued)

DISTANCE z(m)	MULTFRAC	STEFHEST
8.000E+01	1.724E-05	1.724E-05
9.000E+01	1.724E-05	1.724E-05
1.000E+02	1.724E-05	1.724E-05

Table 2-6(b). CASE 1 RESULTS: CONCENTRATION OF Np-237 IN THE ROCK MATRIX LAYER 3, AT DISTANCE x = 200 METERS AND TIME t = 50,000 years (EXPONENTIALLY DECAYING SOURCE AND BAND RELEASE MODE)

DISTANCE z(m)	MULTFRAC	STEFHEST
1.000E-02	1.090E-02	1.090E-02
1.500E-02	1.095E-02	1.095E-02
2.000E-02	1.101E-02	1.101E-02
3.000E-02	1.112E-02	1.112E-02
4.000E-02	1.123E-02	1.123E-02
5.000E-02	1.134E-02	1.134E-02
6.000E-02	1.144E-02	1.144E-02
7.000E-02	1.155E-02	1.155E-02
8.000E-02	1.166E-02	1.166E-02
9.000E-02	1.177E-02	1.177E-02
1.000E-01	1.187E-02	1.187E-02
1.500E-01	1.241E-02	1.241E-02
2.000E-01	1.293E-02	1.293E-02
3.000E-01	1.395E-02	1.395E-02
4.000E-01	1.494E-02	1.494E-02
5.000E-01	1.589E-02	1.589E-02
6.000E-01	1.680E-02	1.680E-02
7.000E-01	1.767E-02	1.767E-02
8.000E-01	1.849E-02	1.849E-02
9.000E-01	1.927E-02	1.927E-02
1.000E+00	2.001E-02	2.001E-02
1.500E+00	2.296E-02	2.296E-02
2.000E+00	2.466E-02	2.466E-02
3.000E+00	2.455E-02	2.455E-02
4.000E+00	2.092E-02	2.092E-02
5.000E+00	1.566E-02	1.566E-02
6.000E+00	1.043E-02	1.043E-02

Table 2-6(b). CASE 1 RESULTS: CONCENTRATION OF Np-237 IN THE ROCK MATRIX LAYER 3, AT DISTANCE x = 200 METERS AND TIME t = 50,000 years (EXPONENTIALLY DECAYING SOURCE AND BAND RELEASE MODE) (Continued)

DISTANCE z(m)	MULTFRAC	STEFHEST
7.000E+00	6.232E-03	6.232E-03
8.000E+00	3.361E-03	3.361E-03
9.000E+00	1.644E-03	1.644E-03
1.000E+01	7.339E-04	7.339E-04
1.500E+01	1.468E-05	1.532E-05
2.000E+01	1.231E-05	1.231E-05
3.000E+01	1.231E-05	1.231E-05
4.000E+01	1.231E-05	1.231E-05
5.000E+01	1.231E-05	1.231E-05
6.000E+01	1.231E-05	1.231E-05
7.000E+01	1.231E-05	1.231E-05
8.000E+01	1.231E-05	1.231E-05
9.000E+01	1.231E-05	1.231E-05
1.000E+02	1.231E-05	1.231E-05

Table 2-6(c). CASE 1 RESULTS: CONCENTRATION OF Np-237 IN THE ROCK MATRIX LAYER 3, AT DISTANCE x = 500 METERS AND TIME t = 50,000 YEARS (EXPONENTIALLY DECAYING SOURCE AND BAND RELEASE MODE)

DISTANCE z(m)	MULTFRAC	STEFHEST
1.000E-02	2.184E-02	2.184E-02
1.500E-02	2.189E-02	2.189E-02
2.000E-02	2.195E-02	2.195E-02
3.000E-02	2.206E-02	2.206E-02
4.000E-02	2.217E-02	2.217E-02
5.000E-02	2.228E-02	2.228E-02
6.000E-02	2.239E-02	2.239E-02
7.000E-02	2.249E-02	2.249E-02
8.000E-02	2.260E-02	2.259E-02
9.000E-02	2.270E-02	2.270E-02
1.000E-01	2.279E-02	2.279E-02
1.500E-01	2.326E-02	2.326E-02
2.000E-01	2.367E-02	2.367E-02
3.000E-01	2.434E-02	2.434E-02
4.000E-01	2.481E-02	2.481E-02
5.000E-01	2.509E-02	2.509E-02
6.000E-01	2.519E-02	2.518E-02

Table 2-6(c). CASE 1 RESULTS: CONCENTRATION OF Np-237 IN THE ROCK MATRIX LAYER 3, AT DISTANCE x = 500 METERS AND TIME t = 50,000 YEARS (EXPONENTIALLY DECAYING SOURCE AND BAND RELEASE MODE) (Continued)

DISTANCE z(m)	MULTFRAC	STEFHEST
7.000E-01	2.510E-02	2.510E-02
8.000E-01	2.485E-02	2.485E-02
9.000E-01	2.445E-02	2.444E-02
1.000E+00	2.390E-02	2.390E-02
1.500E+00	1.966E-02	1.965E-02
2.000E+00	1.425E-02	1.424E-02
3.000E+00	5.357E-03	5.347E-03
4.000E+00	1.341E-03	1.331E-03
5.000E+00	2.350E-04	2.247E-04
6.000E+00	3.646E-05	2.613E-05
7.000E+00	1.245E-05	2.110E-06
8.000E+00	1.046E-05	1.192E-07
9.000E+00	1.035E-05	4.741E-09
1.000E+01	1.034E-05	1.336E-10
1.500E+01	1.034E-05	6.509E-16
2.000E+01	1.034E-05	2.326E-17
3.000E+01	1.034E-05	-6.476E-22
4.000E+01	1.034E-05	-3.892E-26
5.000E+01	1.034E-05	5.217E-30
6.000E+01	1.034E-05	-2.151E-33
7.000E+01	1.034E-05	-3.111E-36
8.000E+01	1.034E-05	-3.367E-39
9.000E+01	1.034E-05	-3.562E-42
1.000E+02	1.034E-05	-3.746E-45

2.3.2 Case 2 Results

This test case examines, as before, the spatial and temporal variation of the concentration of Cm-245, as well as its cumulative mass flux in the fracture. In addition, the spatial variations of the concentration in the rock matrix are also investigated. The source terms correspond now to a periodically fluctuating one with exponential decay, and the assigned residual concentrations are almost one order of magnitude less than their counterparts in the case of Np-237. The input data pertaining to this test case is presented in Table 2-7. Note that the implementation of a periodically decaying source restricts the use of benchmarking algorithms other than Talbot's and Durbin's for reasons presented earlier.

Figure 2-3(a) shows the spatial relative concentration profiles of Cm-245 observed in the fracture layers for simulation times corresponding to 10^1, $5x10^1$ and $5 X10^4$ years. A comparison of our results with the ones obtained from the two numerical inversion algorithms. Tables 2-8(a) through 2-8(c) show that these are in excellent agreement.

Figure 2-3(b) shows the temporal relative concentration of Np-237 observed in the fracture at three different observation points: 100, 200 and 500 meters downstream from the source, located in the second, third and fifth layer respectively, for a band release mode. The observations here are similar to the ones reported for Np-237 except that in the present case the upper tail of the concentration profiles is akin to the assigned initial concentrations of the various fracture layers of interest. A comparison of our results with those yielded by Talbot's and Durbin's algorithms lying within the acceptable range of concentrations (see Tables 2-9(a) through 2-9(c)) seem to indicate good agreement. Note that Talbot's algorithm performance is further reduced in this case, where correct predictions of the concentrations at the three monitoring points seem to be registered only for times greater than 40, 80 and 300 years respectively.

Figure 2-3(c) depicts the time-dependent evolution of the cumulative mass release (per unit width of the fracture) profile at three different observation points in the fracture as in the previous example. Because of its robustness, Durbin's algorithm is selected as the benchmark. A comparison of our analytical solution results with those yielded by Durbin's solution (see Tables 2-10(a) through 2-10(c)) indicate excellent agreement. Note that all three profiles will tend to become asymptotic to three specific values of the cumulative mass namely: 2.175×10^2, 1.237×10^2, and 40.9 (UA/m)[3].

Figures 2-3(d) and 2-3(e) show the concentration profiles in the rock matrix at three position downstream from the source (i.e., x = 100m , 200m, and 500m) for a step release and band release respectively. Comparison of our analytical results against those yielded by the two approximate solution methods (see Tables 2-11(a) through 2-12(c)) indicate excellent agreement.

The assumption of zero dispersive flux in the fracture raises the question of the range of validity of the analytical solutions presented in this report. This matter depends very much on the importance of the hydrodynamic dispersion effects prevailing in the fracture. This matter has been investigated and quantified numerically by Ahn et al., (1985) (i.e., for the case of zero initial concentrations in both fracture and rock) who suggested that hydrodynamic dispersion D (see Bear, 1972) should meet the following criterion

[3] UA: Arbitrary Units of Activity/meter.

$$D_i \leq \frac{10\, u_i^2\, b_i}{\Phi \left(D_{pi} R_i' \right)^{1/2}}$$

in order to validate the use of the zero fracture dispersion solution. The maximum permissible value of D_i for any layer i would correspond to a minimum of 254.0 m^2/yr for Test Case 1, and 245.0 m^2/yr for Test Case 2. Expressed in terms of dispersivity (i.e., D_i/u_i) these would correspond approximately to a value of 16 m in both cases.

Table 2-7. INPUT PARAMETERS FOR CASE 2 PERIODICALLY FLUCTUATING SOURCE WITH EXPONENTIAL DECAY

SPECIES	Cm-245
$T_{1/2}$	8.5×10^3 yr
Release Mode:	
Step	NA
Band Leaching Time	5×10^3 yr
A^o	1.0*
Q	0.1 (m^3/yr)
ν_a	0.75
ν_b	0.25
T_p	5.0 yr

LAYER	L(m)	b (m)	u (m/yr)	Φ
1	50.0	5.0E-03	10.0	0.01
2	75.0	4.0E-03	12.5	0.008
3	100.0	3.0E-03	16.666	0.006
4	150.0	2.0E-03	25.0	0.004
5	∞	1.5E-03	33.333	0.002

Table 2-7. INPUT PARAMETERS FOR CASE 2 PERIODICALLY FLUCTUATING SOURCE WITH EXPONENTIAL DECAY (Continued)

LAYER	ρ (g/cm^3)	D_p (m^2/yr)	K_f (m)	K_r (cm^3/g)
1	2.0	0.01	1.5E-02	1.5
2	2.3	0.02	8.0E-03	1.2
3	2.6	0.06	5.4E-02	1.25
4	2.65	0.05	1.0E-02	0.75
5	2.7	0.03	4.5E-03	2.0

LAYER	a_1^*	a_2^*	α (m^{-1})	b_1^*
1	1.50E-05	-0.50E-05	0.05	1.00E-06
2	2.00E-05	-0.25E-06	0.05	1.75E-06
3	1.75E-05	-0.20E-06	0.05	1.25E-06
4	2.00E-05	-0.15E-06	0.05	1.05E-06
5	1.50E-05	-0.20E-06	0.05	1.05E-06

* (arbitrary units of activity/L^3)

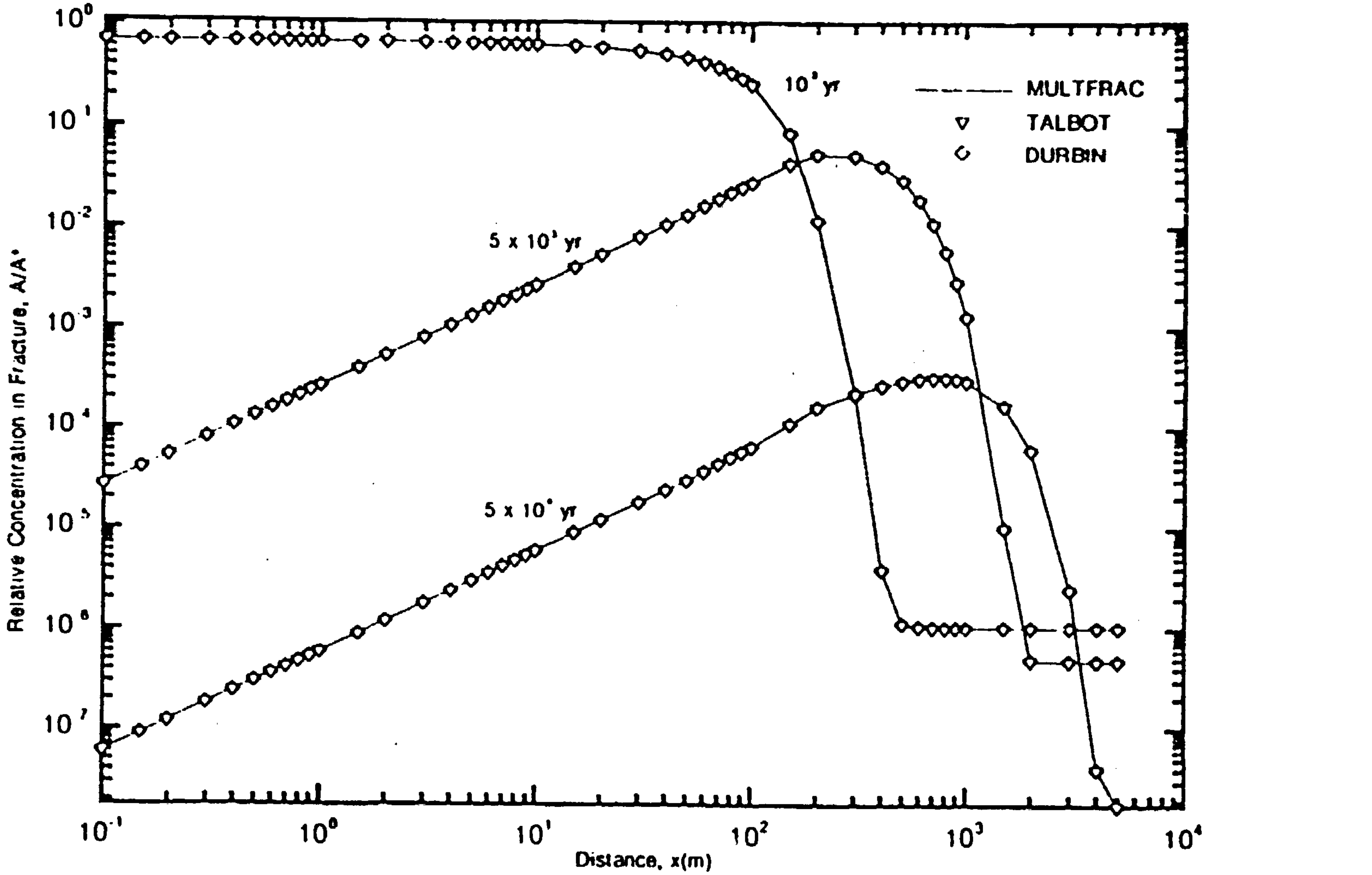

Figure 2-3(a). Relative concentration of Cm-245 vs. distance in the fracture at different times t = 1,000, 5,000, and 50,000 years (Periodically fluctuating source with exponential decay).

Table 2-8(a). CASE 2 RESULTS: CONCENTRATION OF Cm-245 IN THE FRACTURE AT TIME t = 1,000 YEARS (PERIODICALLY FLUCTUATING SOURCE WITH EXPONENTIAL DECAY AND STEP RELEASE MODE)

DISTANCE x(m)	MULTFRAC	TALBOT	DURBIN
1.000E-01	6.908E-01	6.908E-01	6.908E-01
1.500E-01	6.906E-01	6.906E-01	6.906E-01
2.000E-01	6.904E-01	6.904E-01	6.904E-01
3.000E-01	6.900E-01	6.900E-01	6.900E-01
4.000E-01	6.896E-01	6.896E-01	6.896E-01
5.000E-01	6.891E-01	6.891E-01	6.891E-01
6.000E-01	6.887E-01	6.887E-01	6.887E-01
7.000E-01	6.883E-01	6.883E-01	6.883E-01
8.000E-01	6.879E-01	6.879E-01	6.879E-01
9.000E-01	6.874E-01	6.874E-01	6.874E-01
1.000E+00	6.870E-01	6.870E-01	6.870E-01
1.500E+00	6.849E-01	6.849E-01	6.849E-01
2.000E+00	6.827E-01	6.827E-01	6.827E-01
3.000E+00	6.785E-01	6.785E-01	6.785E-01
4.000E+00	6.742E-01	6.742E-01	6.742E-01
5.000E+00	6.700E-01	6.700E-01	6.700E-01
6.000E+00	6.657E-01	6.657E-01	6.657E-01
7.000E+00	6.614E-01	6.614E-01	6.614E-01
8.000E+00	6.572E-01	6.572E-01	6.572E-01
9.000E+00	6.529E-01	6.529E-01	6.529E-01
1.000E+01	6.486E-01	6.486E-01	6.486E-01
1.500E+01	6.273E-01	6.273E-01	6.273E-01
2.000E+01	6.061E-01	6.061E-01	6.061E-01
3.000E+01	5.639E-01	5.639E-01	5.639E-01
4.000E+01	5.223E-01	5.223E-01	5.223E-01
5.000E+01	4.815E-01	4.815E-01	4.815E-01
6.000E+01	4.338E-01	4.338E-01	4.338E-01
7.000E+01	3.881E-01	3.881E-01	3.881E-01
8.000E+01	3.448E-01	3.447E-01	3.447E-01
9.000E+01	3.040E-01	3.040E-01	3.040E-01
1.000E+02	2.661E-01	2.661E-01	2.661E-01
1.500E+02	8.846E-02	8.842E-02	8.842E-02
2.000E+02	1.177E-02	1.176E-02	1.176E-02
3.000E+02	2.178E-04	2.174E-04	2.172E-04
4.000E+02	3.934E-06	3.925E-06	3.953E-06
5.000E+02	1.145E-06	1.145E-06	1.154E-06
6.000E+02	1.066E-06	1.066E-06	1.080E-06
7.000E+02	1.047E-06	1.047E-06	1.061E-06

Table 2-8(a). CASE 2 RESULTS: CONCENTRATION OF Cm-245 IN THE FRACTURE AT TIME t = 1,000 YEARS (PERIODICALLY FLUCTUATING SOURCE WITH EXPONENTIAL DECAY AND STEP RELEASE MODE) (Continued)

DISTANCE x(m)	MULTFRAC	TALBOT	DURBIN
8.000E+02	1.045E-06	1.045E-06	1.058E-06
9.000E+02	1.044E-06	1.044E-06	1.057E-06
1.000E+03	1.044E-06	1.044E-06	1.057E-06
1.500E+03	1.044E-06	1.044E-06	1.057E-06
2.000E+03	1.044E-06	1.044E-06	1.057E-06
3.000E+03	1.044E-06	1.044E-06	1.057E-06
4.000E+03	1.044E-06	1.044E-06	1.057E-06
5.000E+03	1.044E-06	1.044E-06	1.057E-06

Table 2-8(b). CASE 2 RESULTS: CONCENTRATION OF Cm-245 IN THE FRACTURE AT TIME t = 5,000 YEARS (PERIODICALLY FLUCTUATING SOURCE WITH EXPONENTIAL DECAY AND BAND RELEASE MODE)

DISTANCE x(m)	MULTFRAC	TALBOT	DURBIN
1.000E-01	2.675E-05	2.677E-05	2.679E-05
1.500E-01	4.014E-05	4.016E-05	4.018E-05
2.000E-01	5.352E-05	5.355E-05	5.357E-05
3.000E-01	8.030E-05	8.033E-05	8.035E-05
4.000E-01	1.071E-04	1.071E-04	1.071E-04
5.000E-01	1.338E-04	1.339E-04	1.339E-04
6.000E-01	1.606E-04	1.607E-04	1.607E-04
7.000E-01	1.874E-04	1.874E-04	1.875E-04
8.000E-01	2.142E-04	2.142E-04	2.142E-04
9.000E-01	2.410E-04	2.410E-04	2.410E-04
1.000E+00	2.677E-04	2.678E-04	2.678E-04
1.500E+00	4.016E-04	4.017E-04	4.017E-04
2.000E+00	5.355E-04	5.356E-04	5.356E-04
3.000E+00	8.034E-04	8.034E-04	8.034E-04
4.000E+00	1.071E-03	1.071E-03	1.071E-03
5.000E+00	1.339E-03	1.339E-03	1.339E-03
6.000E+00	1.607E-03	1.607E-03	1.607E-03
7.000E+00	1.875E-03	1.875E-03	1.875E-03
8.000E+00	2.143E-03	2.143E-03	2.143E-03
9.000E+00	2.411E-03	2.411E-03	2.411E-03
1.000E+01	2.678E-03	2.679E-03	2.679E-03
1.500E+01	4.017E-03	4.018E-03	4.018E-03

Table 2-8(b). CASE 2 RESULTS: CONCENTRATION OF Cm-245 IN THE FRACTURE AT TIME t = 5,000 YEARS (PERIODICALLY FLUCTUATING SOURCE WITH EXPONENTIAL DECAY AND BAND RELEASE MODE) (Continued)

DISTANCE x(m)	MULTFRAC	TALBOT	DURBIN
2.000E+01	5.355E-03	5.355E-03	5.355E-03
3.000E+01	8.021E-03	8.022E-03	8.022E-03
4.000E+01	1.067E-02	1.067E-02	1.067E-02
5.000E+01	1.330E-02	1.330E-02	1.330E-02
6.000E+01	1.644E-02	1.644E-02	1.644E-02
7.000E+01	1.952E-02	1.952E-02	1.952E-02
8.000E+01	2.253E-02	2.253E-02	2.253E-02
9.000E+01	2.545E-02	2.545E-02	2.545E-02
1.000E+02	2.828E-02	2.828E-02	2.828E-02
1.500E+02	4.409E-02	4.409E-02	4.409E-02
2.000E+02	5.491E-02	5.491E-02	5.491E-02
3.000E+02	5.303E-02	5.303E-02	5.303E-02
4.000E+02	4.201E-02	4.201E-02	4.201E-02
5.000E+02	2.974E-02	2.974E-02	2.974E-02
6.000E+02	1.893E-02	1.893E-02	1.893E-02
7.000E+02	1.097E-02	1.097E-02	1.097E-02
8.000E+02	5.839E-03	5.838E-03	5.838E-03
9.000E+02	2.877E-03	2.876E-03	2.877E-03
1.000E+03	1.319E-03	1.318E-03	1.318E-03
1.500E+03	1.019E-05	1.018E-05	1.019E-05
2.000E+03	4.896E-07	4.896E-07	4.969E-07
3.000E+03	4.762E-07	4.762E-07	4.840E-07
4.000E+03	4.762E-07	4.762E-07	4.840E-07
5.000E+03	4.762E-07	4.762E-07	4.840E-07

Table 2-8(c). CASE 2 RESULTS: CONCENTRATION OF Cm-245 IN THE FRACTURE AT TIME t = 50,000 YEARS (PERIODICALLY FLUCTUATING SOURCE WITH EXPONENTIAL DECAY AND BAND RELEASE MODE)

DISTANCE x(m)	MULTFRAC	TALBOT	DURBIN
1.000E-01	5.953E-08	5.991E-08	5.991E-08
1.500E-01	8.949E-08	8.987E-08	8.987E-08
2.000E-01	1.194E-07	1.198E-07	1.198E-07
3.000E-01	1.794E-07	1.797E-07	1.797E-07
4.000E-01	2.393E-07	2.397E-07	2.397E-07

Table 2-8(c). CASE 2 RESULTS: CONCENTRATION OF Cm-245 IN THE FRACTURE AT TIME t = 50,000 YEARS (PERIODICALLY FLUCTUATING SOURCE WITH EXPONENTIAL DECAY AND BAND RELEASE MODE) (Continued)

DISTANCE x(m)	MULTFRAC	TALBOT	DURBIN
5.000E-01	2.992E-07	2.996E-07	2.996E-07
6.000E-01	3.591E-07	3.595E-07	3.595E-07
7.000E-01	4.190E-07	4.194E-07	4.194E-07
8.000E-01	4.789E-07	4.793E-07	4.793E-07
9.000E-01	5.389E-07	5.392E-07	5.392E-07
1.000E+00	5.988E-07	5.991E-07	5.991E-07
1.500E+00	8.983E-07	8.987E-07	8.987E-07
2.000E+00	1.198E-06	1.198E-06	1.198E-06
3.000E+00	1.797E-06	1.797E-06	1.797E-06
4.000E+00	2.396E-06	2.397E-06	2.397E-06
5.000E+00	2.995E-06	2.996E-06	2.996E-06
6.000E+00	3.595E-06	3.595E-06	3.595E-06
7.000E+00	4.194E-06	4.194E-06	4.194E-06
8.000E+00	4.793E-06	4.793E-06	4.793E-06
9.000E+00	5.392E-06	5.393E-06	5.393E-06
1.000E+01	5.991E-06	5.992E-06	5.992E-06
1.500E+01	8.987E-06	8.987E-06	8.987E-06
2.000E+01	1.198E-05	1.198E-05	1.198E-05
3.000E+01	1.797E-05	1.797E-05	1.797E-05
4.000E+01	2.395E-05	2.395E-05	2.395E-05
5.000E+01	2.993E-05	2.993E-05	2.993E-05
6.000E+01	3.717E-05	3.717E-05	3.717E-05
7.000E+01	4.439E-05	4.439E-05	4.439E-05
8.000E+01	5.158E-05	5.158E-05	5.158E-05
9.000E+01	5.875E-05	5.875E-05	5.876E-05
1.000E+02	6.589E-05	6.589E-05	6.590E-05
1.500E+02	1.118E-04	1.118E-04	1.118E-04
2.000E+02	1.651E-04	1.651E-04	1.650E-04
3.000E+02	2.286E-04	2.286E-04	2.286E-04
4.000E+02	2.701E-04	2.701E-04	2.701E-04
5.000E+02	2.984E-04	2.984E-04	2.984E-04
6.000E+02	3.167E-04	3.167E-04	3.167E-04
7.000E+02	3.250E-04	3.250E-04	3.250E-04
8.000E+02	3.240E-04	3.240E-04	3.240E-04
9.000E+02	3.149E-04	3.149E-04	3.149E-04
1.000E+03	2.988E-04	2.988E-04	2.990E-04
1.500E+03	1.695E-04	1.695E-04	1.696E-04
2.000E+03	6.162E-05	6.162E-05	6.162E-05

Table 2-8(c). CASE 2 RESULTS: CONCENTRATION OF Cm-245 IN THE FRACTURE AT TIME t = 50,000 YEARS (PERIODICALLY FLUCTUATING SOURCE WITH EXPONENTIAL DECAY AND BAND RELEASE MODE) (Continued)

DISTANCE x(m)	MULTFRAC	TALBOT	DURBIN
3.000E+03	2.503E-06	2.503E-06	2.504E-06
4.000E+03	4.072E-08	4.072E-08	4.073E-08
5.000E+03	1.805E-08	1.805E-08	1.805E-08

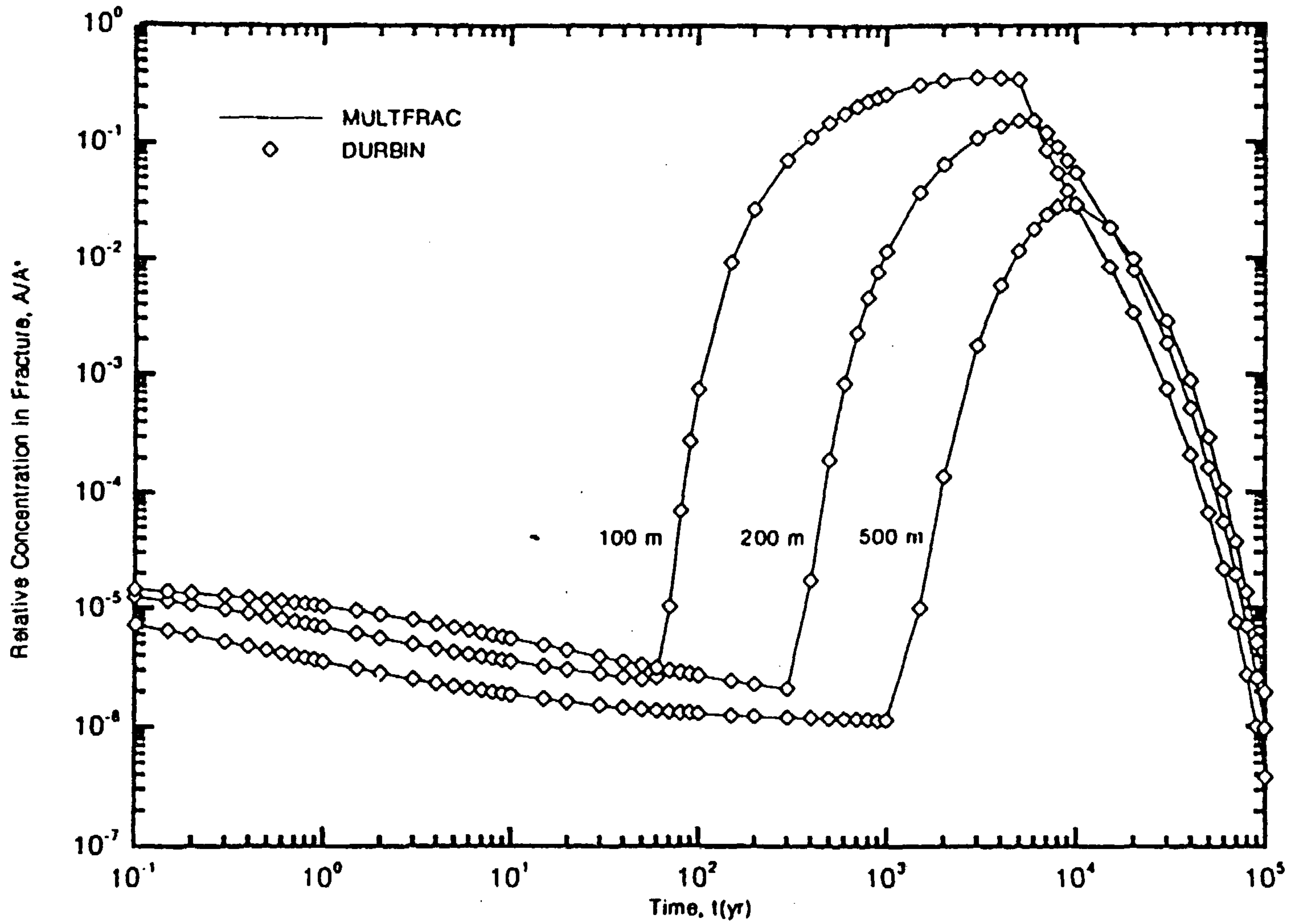

Figure 2-3(b). Relative concentration of Cm-245 in the fracture vs. time at different positions x = 100 meters, 200 meters, and 500 meters (Periodically fluctuating source with exponential decay).

Table 2-9(a). CASE 2 RESULTS: CONCENTRATION OF Cm-245 IN THE FRACTURE IN LAYER 2, AT DISTANCE x = 100 METERS (PERIODICALLY FLUCTUATING SOURCE WITH EXPONENTIAL DECAY AND STEP RELEASE MODE)

TIME (y)	MULTFRAC	TALBOT	DURBIN
1.000E-01	1.250E-05	2.184+188	1.253E-05
1.500E-01	1.151E-05	-4.441+246	1.154E-05
2.000E-01	1.079E-05	-4.572+261	1.081E-05
3.000E-01	9.765E-06	2.005+243	9.791E-06
4.000E-01	9.052E-06	4.431+259	9.076E-06
5.000E-01	8.511E-06	-5.666+260	8.535E-06
6.000E-01	8.082E-06	2.925+222	8.105E-06
7.000E-01	7.728E-06	4.361+238	7.751E-06
8.000E-01	7.431E-06	-2.506+272	7.453E-06
9.000E-01	7.175E-06	2.301+238	7.196E-06
1.000E+00	6.951E-06	-1.678+213	6.973E-06
1.500E+00	6.147E-06	-1.604+242	6.167E-06
2.000E+00	5.632E-06	-1.656+242	5.650E-06
3.000E+00	4.986E-06	2.438+224	5.002E-06
4.000E+00	4.583E-06	-2.694+160	4.598E-06
5.000E+00	4.301E-06	1.553+200	4.316E-06
6.000E+00	4.090E-06	8.813+159	4.103E-06
7.000E+00	3.923E-06	1.114+131	3.936E-06
8.000E+00	3.788E-06	2.442+109	3.800E-06
9.000E+00	3.675E-06	-2.759E+92	3.686E-06
1.000E+01	3.578E-06	6.475+172	3.590E-06
1.500E+01	3.248E-06	5.749E+87	3.259E-06
2.000E+01	3.049E-06	-1.702E+45	3.058E-06
3.000E+01	2.810E-06	-5.177E+02	2.837E-06
4.000E+01	2.667E-06	2.680E-06	2.673E-06
5.000E+01	2.570E-06	2.568E-06	2.544E-06
6.000E+01	2.703E-06	2.708E-06	2.669E-06
7.000E+01	1.027E-05	1.050E-05	1.054E-05
8.000E+01	6.893E-05	7.056E-05	7.053E-05
9.000E+01	2.757E-04	2.814E-04	2.813E-04
1.000E+02	7.497E-04	7.634E-04	7.635E-04
1.500E+02	9.519E-03	9.442E-03	9.442E-03
2.000E+02	2.718E-02	2.723E-02	2.723E-02
3.000E+02	7.209E-02	7.214E-02	7.215E-02
4.000E+02	1.152E-01	1.152E-01	1.152E-01
5.000E+02	1.522E-01	1.522E-01	1.522E-01
6.000E+02	1.834E-01	1.833E-01	1.833E-01
7.000E+02	2.095E-01	2.094E-01	2.094E-01

Table 2-9(a). CASE 2 RESULTS: CONCENTRATION OF Cm-245 IN THE FRACTURE IN LAYER 2, AT DISTANCE x = 100 METERS (PERIODICALLY FLUCTUATING SOURCE WITH EXPONENTIAL DECAY AND STEP RELEASE MODE) (Continued)

TIME (y)	MULTFRAC	TALBOT	DURBIN
8.000E+02	2.315E-01	2.314E-01	2.314E-01
9.000E+02	2.502E-01	2.501E-01	2.501E-01
1.000E+03	2.661E-01	2.661E-01	2.661E-01
1.500E+03	3.189E-01	3.189E-01	3.189E-01
2.000E+03	3.456E-01	3.455E-01	3.455E-01
3.000E+03	3.640E-01	3.640E-01	3.640E-01
4.000E+03	3.615E-01	3.615E-01	3.615E-01
5.000E+03	3.499E-01	3.499E-01	3.499E-01
6.000E+03	1.570E-01	1.570E-01	1.570E-01
7.000E+03	8.635E-02	8.636E-02	8.636E-02
8.000E+03	5.556E-02	5.556E-02	5.556E-02
9.000E+03	3.869E-02	3.869E-02	3.869E-02
1.000E+04	2.828E-02	2.828E-02	2.828E-02
1.500E+04	8.507E-03	8.508E-03	8.508E-03
2.000E+04	3.400E-03	3.400E-03	3.400E-03
3.000E+04	7.630E-04	7.630E-04	7.629E-04
4.000E+04	2.121E-04	2.121E-04	2.121E-04
5.000E+04	6.589E-05	6.589E-05	6.590E-05
6.000E+04	2.190E-05	2.190E-05	2.190E-05
7.000E+04	7.622E-06	7.622E-06	7.622E-06
8.000E+04	2.742E-06	2.742E-06	2.742E-06
9.000E+04	1.012E-06	1.012E-06	1.012E-06
1.000E+05	3.806E-07	3.806E-07	3.806E-07
1.500E+05	3.471E-09	3.471E-09	3.471E-09
2.000E+05	3.800E-11	3.800E-11	3.800E-11
3.000E+05	5.910E-15	5.982E-15	5.896E-15
4.000E+05	1.100E-18	4.007E-16	1.408E-17
5.000E+05	2.258E-22	5.580E-16	-7.545E-18
6.000E+05	4.932E-26	6.163E-16	1.497E-17
7.000E+05	1.124E-29	3.204E-16	5.328E-18
8.000E+05	2.642E-33	2.729E-16	2.488E-17
9.000E+05	6.361E-37	2.835E-17	-5.385E-18
1.000E+06	1.560E-40	7.371E-17	-8.938E-19

Table 2-9(b). CASE 2 RESULTS: CONCENTRATION OF Cm-245 IN THE FRACTURE IN LAYER 3, AT DISTANCE x = 200 METERS (PERIODICALLY FLUCTUATING SOURCE WITH EXPONENTIAL DECAY AND BAND RELEASE MODE)

TIME (y)	MULTFRAC	TALBOT	DURBIN
1.000E-01	1.453E-05	5.273+234	1.456E-05
1.500E-01	1.399E-05	1.474+113	1.401E-05
2.000E-01	1.355E-05	-3.527E+69	1.358E-05
3.000E-01	1.288E-05	1.812+209	1.290E-05
4.000E-01	1.235E-05	4.523+256	1.238E-05
5.000E-01	1.193E-05	1.438+236	1.195E-05
6.000E-01	1.156E-05	-4.659+264	1.159E-05
7.000E-01	1.124E-05	-2.491+267	1.127E-05
8.000E-01	1.096E-05	-1.440+249	1.099E-05
9.000E-01	1.071E-05	-4.417+247	1.073E-05
1.000E+00	1.048E-05	-2.991+269	1.051E-05
1.500E+00	9.584E-06	1.216+268	9.608E-06
2.000E+00	8.938E-06	1.989+261	8.961E-06
3.000E+00	8.032E-06	9.815+270	8.054E-06
4.000E+00	7.405E-06	1.001+263	7.426E-06
5.000E+00	6.933E-06	-2.075+225	6.954E-06
6.000E+00	6.560E-06	-8.843+254	6.580E-06
7.000E+00	6.255E-06	-1.437+214	6.274E-06
8.000E+00	5.998E-06	-1.726+228	6.017E-06
9.000E+00	5.778E-06	-3.403+236	5.796E-06
1.000E+01	5.586E-06	-3.213+209	5.604E-06
1.500E+01	4.900E-06	-3.235+211	4.917E-06
2.000E+01	4.464E-06	-5.380+189	4.479E-06
3.000E+01	3.919E-06	-6.937+186	3.933E-06
4.000E+01	3.581E-06	-7.301+162	3.593E-06
5.000E+01	3.344E-06	2.565+113	3.356E-06
6.000E+01	3.167E-06	-2.135E+80	3.178E-06
7.000E+01	3.027E-06	-2.093E+57	3.037E-06
8.000E+01	2.913E-06	9.066E+39	2.923E-06
9.000E+01	2.818E-06	1.164E+26	2.827E-06
1.000E+02	2.737E-06	-2.442E+15	2.746E-06
1.500E+02	2.457E-06	2.460E-06	2.482E-06
2.000E+02	2.284E-06	2.284E-06	2.312E-06
3.000E+02	2.133E-06	2.135E-06	2.127E-06
4.000E+02	1.718E-05	1.740E-05	1.756E-05
5.000E+02	1.94[illegible]-04	1.966E-04	1.963E-04
6.000E+02	8.[illegible]-04	8.640E-04	8.643E-04
7.000E+02	2.[illegible]E-03	2.305E-03	2.305E-03

Table 2-9(b). CASE 2 RESULTS: CONCENTRATION OF Cm-245 IN THE FRACTURE IN LAYER 3, AT DISTANCE x = 200 METERS (PERIODICALLY FLUCTUATING SOURCE WITH EXPONENTIAL DECAY AND BAND RELEASE MODE) (Continued)

TIME (y)	MULTFRAC	TALBOT	DURBIN
8.000E+02	4.644E-03	4.636E-03	4.636E-03
9.000E+02	7.835E-03	7.826E-03	7.826E-03
1.000E+03	1.177E-02	1.176E-02	1.176E-02
1.500E+03	3.776E-02	3.775E-02	3.775E-02
2.000E+03	6.558E-02	6.557E-02	6.557E-02
3.000E+03	1.103E-01	1.103E-01	1.103E-01
4.000E+03	1.389E-01	1.388E-01	1.388E-01
5.000E+03	1.555E-01	1.555E-01	1.555E-01
6.000E+03	1.562E-01	1.562E-01	1.562E-01
7.000E+03	1.235E-01	1.235E-01	1.235E-01
8.000E+03	9.306E-02	9.307E-02	9.307E-02
9.000E+03	7.086E-02	7.087E-02	7.087E-02
1.000E+04	5.491E-02	5.491E-02	5.491E-02
1.500E+04	1.882E-02	1.882E-02	1.882E-02
2.000E+04	7.907E-03	7.907E-03	7.907E-03
3.000E+04	1.853E-03	1.853E-03	1.853E-03
4.000E+04	5.256E-04	5.256E-04	5.256E-04
5.000E+04	1.651E-04	1.651E-04	1.650E-04
6.000E+04	5.529E-05	5.529E-05	5.529E-05
7.000E+04	1.934E-05	1.934E-05	1.934E-05
8.000E+04	6.985E-06	6.985E-06	6.985E-06
9.000E+04	2.585E-06	2.585E-06	2.585E-06
1.000E+05	9.747E-07	9.747E-07	9.747E-07
1.500E+05	8.950E-09	8.951E-09	8.951E-09
2.000E+05	9.832E-11	9.832E-11	9.832E-11
3.000E+05	1.534E-14	1.540E-14	-5.189E-07
4.000E+05	2.861E-18	7.985E-17	-7.419E-08
5.000E+05	5.879E-22	1.400E-16	-4.753E-07
6.000E+05	1.285E-25	2.871E-16	-3.961E-07
7.000E+05	2.929E-29	3.949E-16	-6.632E-08
8.000E+05	6.889E-33	1.189E-16	2.972E-07
9.000E+05	1.659E-36	2.184E-16	2.641E-07
1.000E+06	4.071E-40	2.190E-17	2.377E-07

Table 2-9(c). CASE 2 RESULTS: CONCENTRATION OF Cm-245 IN THE FRACTURE IN LAYER 5, AT DISTANCE x = 500 METERS (PERIODICALLY FLUCTUATING SOURCE WITH EXPONENTIAL DECAY AND BAND RELEASE MODE)

TIME (y)	MULTFRAC	TALBOT	DURBIN
1.000E-01	7.219E-06	8.689+218	7.238E-06
1.500E-01	6.453E-06	-4.152+271	6.471E-06
2.000E-01	5.929E-06	-2.893+190	5.946E-06
3.000E-01	5.232E-06	4.875+250	5.249E-06
4.000E-01	4.774E-06	7.382+227	4.790E-06
5.000E-01	4.442E-06	1.802+261	4.457E-06
6.000E-01	4.187E-06	3.548+242	4.201E-06
7.000E-01	3.982E-06	-1.281+242	3.996E-06
8.000E-01	3.813E-06	2.024+261	3.826E-06
9.000E-01	3.671E-06	-1.002+273	3.684E-06
1.000E+00	3.549E-06	-2.800+235	3.561E-06
1.500E+00	3.121E-06	3.914+264	3.132E-06
2.000E+00	2.858E-06	-8.926+248	2.868E-06
3.000E+00	2.539E-06	4.032+250	2.565E-06
4.000E+00	2.344E-06	-9.699+245	2.369E-06
5.000E+00	2.211E-06	-2.552+260	2.233E-06
6.000E+00	2.111E-06	-4.125+265	2.133E-06
7.000E+00	2.033E-06	-1.167+245	2.054E-06
8.000E+00	1.971E-06	2.827+265	1.991E-06
9.000E+00	1.918E-06	1.118+232	1.938E-06
1.000E+01	1.874E-06	3.661+256	1.893E-06
1.500E+01	1.723E-06	-3.137+241	1.741E-06
2.000E+01	1.633E-06	3.227+198	1.649E-06
3.000E+01	1.525E-06	-1.671+205	1.540E-06
4.000E+01	1.460E-06	-1.511+142	1.475E-06
5.000E+01	1.415E-06	-1.568+172	1.430E-06
6.000E+01	1.382E-06	-3.968+181	1.396E-06
7.000E+01	1.356E-06	1.606+143	1.370E-06
8.000E+01	1.335E-06	-1.064+116	1.349E-06
9.000E+01	1.317E-06	-4.803E+93	1.331E-06
1.000E+02	1.302E-06	-3.967E+75	1.316E-06
1.500E+02	1.255E-06	-4.242E+22	1.269E-06
2.000E+02	1.231E-06	-2.924E-05	1.245E-06
3.000E+02	1.207E-06	1.207E-06	1.220E-06
4.000E+02	1.191E-06	1.192E-06	1.205E-06
5.000E+02	1.177E-06	1.178E-06	1.192E-06
6.000E+02	1.164E-06	1.165E-06	1.181E-06
7.000E+02	1.152E-06	1.154E-06	1.174E-06

Table 2-9(c). CASE 2 RESULTS: CONCENTRATION OF Cm-245 IN THE FRACTURE IN LAYER 5, AT DISTANCE x = 500 METERS (PERIODICALLY FLUCTUATING SOURCE WITH EXPONENTIAL DECAY AND BAND RELEASE MODE) (Continued)

TIME (y)	MULTFRAC	TALBOT	DURBIN
8.000E+02	1.144E-06	1.144E-06	1.164E-06
9.000E+02	1.136E-06	1.137E-06	1.145E-06
1.000E+03	1.145E-06	1.145E-06	1.154E-06
1.500E+03	1.001E-05	9.994E-06	1.008E-05
2.000E+03	1.396E-04	1.394E-04	1.392E-04
3.000E+03	1.784E-03	1.783E-03	1.783E-03
4.000E+03	5.934E-03	5.932E-03	5.932E-03
5.000E+03	1.178E-02	1.178E-02	1.178E-02
6.000E+03	1.817E-02	1.816E-02	1.816E-02
7.000E+03	2.417E-02	2.417E-02	2.417E-02
8.000E+03	2.844E-02	2.844E-02	2.844E-02
9.000E+03	3.013E-02	3.013E-02	3.013E-02
1.000E+04	2.974E-02	2.974E-02	2.974E-02
1.500E+04	1.860E-02	1.860E-02	1.860E-02
2.000E+04	9.942E-03	9.942E-03	9.942E-03
3.000E+04	2.878E-03	2.878E-03	2.878E-03
4.000E+04	8.989E-04	8.989E-04	8.989E-04
5.000E+04	2.984E-04	2.984E-04	2.984E-04
6.000E+04	1.036E-04	1.036E-04	1.035E-04
7.000E+04	3.716E-05	3.716E-05	3.711E-05
8.000E+04	1.367E-05	1.367E-05	1.367E-05
9.000E+04	5.133E-06	5.133E-06	5.133E-06
1.000E+05	1.958E-06	1.958E-06	1.956E-06
1.500E+05	1.860E-08	1.860E-08	1.860E-08
2.000E+05	2.077E-10	2.077E-10	2.077E-10
3.000E+05	3.296E-14	3.322E-14	1.447E-07
4.000E+05	6.195E-18	6.849E-17	5.450E-07
5.000E+05	1.279E-21	1.129E-16	-4.404E-07
6.000E+05	2.805E-25	7.443E-17	-3.660E-07
7.000E+05	6.410E-29	5.215E-17	-5.327E-07
8.000E+05	1.510E-32	-2.602E-17	4.667E-07
9.000E+05	3.642E-36	-1.457E-17	-8.083E-08
1.000E+06	8.945E-40	-2.802E-17	7.299E-08

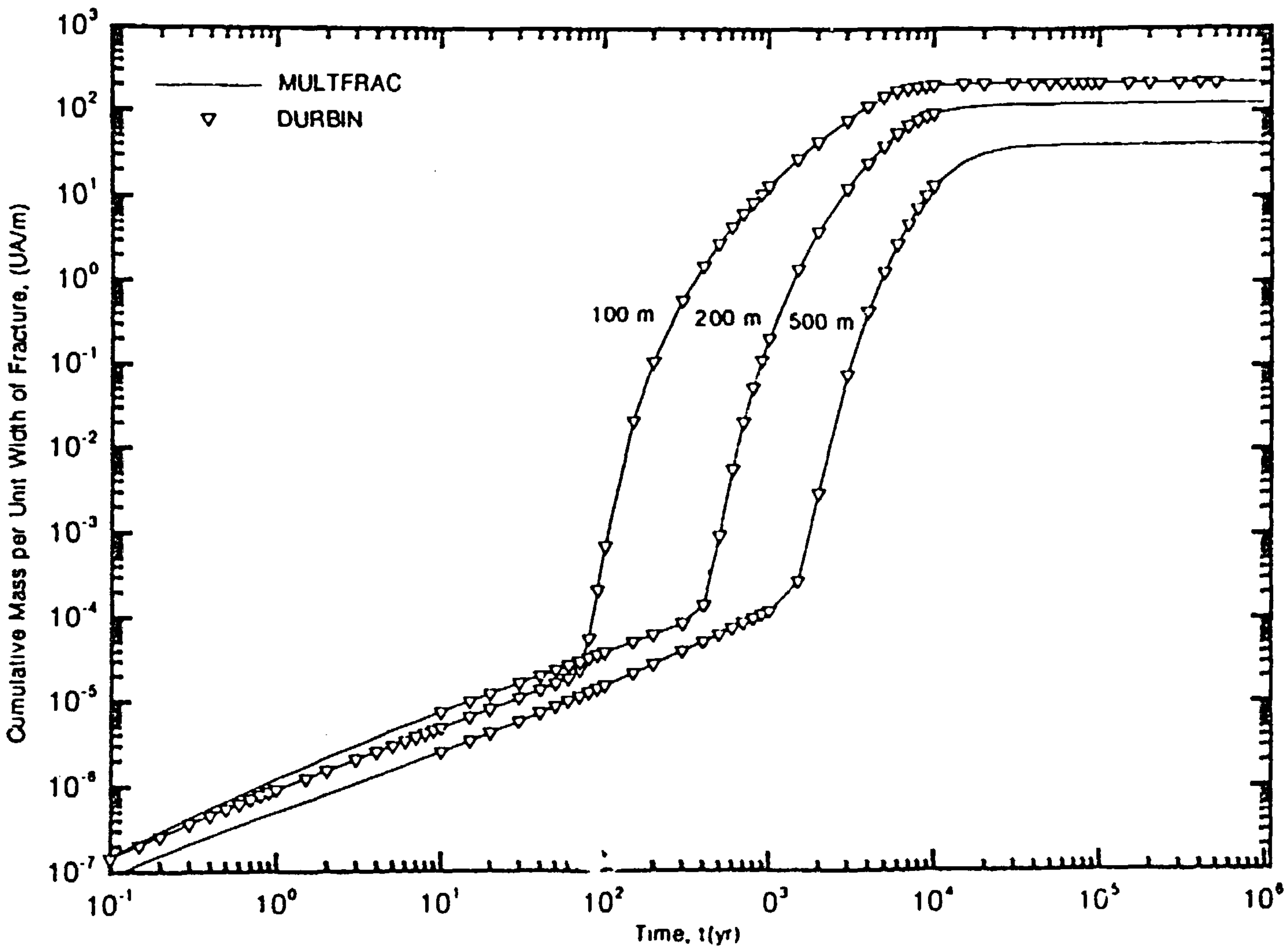

Figure 2-3(c). Cumulative mass of Cm-245 per unit in the fracture vs. time at different positions x = 100, 200, and 500 meters (Periodically fluctuating source with exponential decay).

Table 2-10(a). CASE 2 RESULTS: CUMULATIVE MASS OF Cm-245 IN THE FRACTURE AT DISTANCE x = 100 METERS (PERIODICALLY FLUCTUATING SOURCE WITH EXPONENTIAL DECAY AND BAND RELEASE MODE)

TIME (yr)	MULTFRAC	DURBIN
1.000E-01	1.448E-07	1.451E-07
1.500E-01	2.047E-07	2.051E-07
2.000E-01	2.603E-07	2.609E-07
3.000E-01	3.627E-07	3.636E-07
4.000E-01	4.566E-07	4.577E-07
5.000E-01	5.443E-07	5.457E-07
6.000E-01	6.272E-07	6.288E-07
7.000E-01	7.062E-07	7.080E-07
8.000E-01	7.820E-07	7.840E-07
9.000E-01	8.550E-07	8.572E-07
1.000E+00	9.256E-07	9.280E-07
1.500E+00	1.251E-06	1.255E-06
2.000E+00	1.545E-06	1.549E-06
3.000E+00	2.073E-06	2.079E-06
4.000E+00	2.550E-06	2.558E-06
5.000E+00	2.993E-06	3.003E-06
6.000E+00	3.413E-06	3.423E-06
7.000E+00	3.813E-06	3.825E-06
8.000E+00	4.198E-06	4.211E-06
9.000E+00	4.571E-06	4.585E-06
1.000E+01	4.934E-06	4.949E-06
1.500E+01	6.632E-06	6.652E-06
2.000E+01	8.203E-06	8.229E-06
3.000E+01	1.112E-05	1.117E-05
4.000E+01	1.385E-05	1.392E-05
5.000E+01	1.647E-05	1.653E-05
6.000E+01	1.904E-05	1.910E-05
7.000E+01	2.456E-05	2.402E-05
8.000E+01	6.008E-05	5.680E-05
9.000E+01	2.289E-04	2.151E-04
1.000E+02	7.479E-04	7.101E-04
1.500E+02	2.207E-02	2.164E-02
2.000E+02	1.119E-01	1.106E-01
3.000E+02	6.078E-01	6.043E-01
4.000E+02	1.551E+00	1.546E+00
5.000E+02	2.895E+00	2.888E+00
6.000E+02	4.579E+00	4.570E+00
7.000E+02	6.548E+00	6.537E+00

Table 2-10(a). CASE 2 RESULTS: CUMULATIVE MASS OF Cm-245 IN THE FRACTURE AT DISTANCE x = 100 METERS (PERIODICALLY FLUCTUATING DECAYING SOURCE AND BAND RELEASE MODE) (Continued)

TIME (yr)	MULTFRAC	DURBIN
8.000E+02	8.756E+00	8.744E+00
9.000E+02	1.117E+01	1.115E+01
1.000E+03	1.375E+01	1.374E+01
1.500E+03	2.853E+01	2.852E+01
2.000E+03	4.522E+01	4.520E+01
3.000E+03	8.096E+01	8.094E+01
4.000E+03	1.173E+02	1.173E+02
5.000E+03	1.530E+02	1.529E+02
6.000E+03	1.780E+02	1.780E+02
7.000E+03	1.896E+02	1.896E+02
8.000E+03	1.965E+02	1.965E+02
9.000E+03	2.012E+02	2.012E+02
1.000E+04	2.045E+02	2.045E+02
1.500E+04	2.124E+02	2.124E+02
2.000E+04	2.152E+02	2.152E+02
3.000E+04	2.169E+02	2.169E+02
4.000E+04	2.173E+02	2.174E+02
5.000E+04	2.174E+02	2.175E+02
6.000E+04	2.175E+02	2.175E+02
7.000E+04	2.175E+02	2.174E+02
8.000E+04	2.175E+02	2.174E+02
9.000E+04	2.175E+02	2.173E+02
1.000E+05	2.175E+02	2.173E+02
1.500E+05	2.175E+02	2.172E+02
2.000E+05	2.175E+02	2.172E+02
3.000E+05	2.175E+02	2.174E+02
4.000E+05	2.175E+02	2.179E+02
5.000E+05	2.175E+02	2.184E+02
6.000E+05	2.175E+02	NA
7.000E+05	2.175E+02	NA
8.000E+05	2.175E+02	NA
9.000E+05	2.175E+02	NA
1.000E+06	2.175E+02	NA

Table 2-10(b). CASE 2 RESULTS: CUMULATIVE MASS OF Cm-245 IN THE FRACTURE AT DISTANCE x = 200 METERS (PERIODICALLY FLUCTUATING SOURCE WITH EXPONENTIAL DECAY AND BAND RELEASE MODE)

TIME (yr)	MULTFRAC	DURBIN
1.000E-01	1.544E-07	NA
1.500E-01	2.257E-07	NA
2.000E-01	2.945E-07	NA
3.000E-01	4.264E-07	NA
4.000E-01	5.525E-07	NA
5.000E-01	6.738E-07	NA
6.000E-01	7.912E-07	NA
7.000E-01	9.052E-07	NA
8.000E-01	1.016E-06	NA
9.000E-01	1.125E-06	NA
1.000E+00	1.230E-06	NA
1.500E+00	1.731E-06	NA
2.000E+00	2.193E-06	NA
3.000E+00	3.038E-06	NA
4.000E+00	3.809E-06	NA
5.000E+00	4.524E-06	NA
6.000E+00	5.198E-06	NA
7.000E+00	5.839E-06	NA
8.000E+00	6.451E-06	NA
9.000E+00	7.040E-06	NA
1.000E+01	7.608E-06	7.628E-06
1.500E+01	1.021E-05	1.024E-05
2.000E+01	1.255E-05	1.259E-05
3.000E+01	1.671E-05	1.677E-05
4.000E+01	2.045E-05	2.052E-05
5.000E+01	2.391E-05	2.399E-05
6.000E+01	2.716E-05	2.725E-05
7.000E+01	3.026E-05	3.035E-05
8.000E+01	3.322E-05	3.333E-05
9.000E+01	3.609E-05	3.620E-05
1.000E+02	3.886E-05	3.899E-05
1.500E+02	5.178E-05	5.202E-05
2.000E+02	6.360E-05	6.397E-05
3.000E+02	8.532E-05	8.581E-05
4.000E+02	1.439E-04	1.435E-04
5.000E+02	9.618E-04	9.541E-04
6.000E+02	5.744E-03	5.708E-03
7.000E+02	2.093E-02	2.084E-02

Table 2-10(b). CASE 2 RESULTS: CUMULATIVE MASS OF Cm-245 IN THE FRACTURE AT DISTANCE x = 200 METERS (PERIODICALLY FLUCTUATING SOURCE WITH EXPONENTIAL DECAY AND BAND RELEASE MODE) (Continued)

TIME (yr)	MULTFRAC	DURBIN
8.000E+02	5.497E-02	5.480E-02
9.000E+02	1.167E-01	1.164E-01
1.000E+03	2.142E-01	2.138E-01
1.500E+03	1.424E+00	1.423E+00
2.000E+03	4.016E+00	4.014E+00
3.000E+03	1.295E+01	1.295E+01
4.000E+03	2.553E+01	2.552E+01
5.000E+03	4.033E+01	4.032E+01
6.000E+03	5.622E+01	5.621E+01
7.000E+03	7.028E+01	7.028E+01
8.000E+03	8.104E+01	8.103E+01
9.000E+03	8.917E+01	8.917E+01
1.000E+04	9.542E+01	9.542E+01
1.500E+04	1.119E+02	NA
2.000E+04	1.181E+02	NA
3.000E+04	1.222E+02	NA
4.000E+04	1.232E+02	NA
5.000E+04	1.235E+02	NA
6.000E+04	1.236E+02	NA
7.000E+04	1.237E+02	NA
8.000E+04	1.237E+02	NA
9.000E+04	1.237E+02	NA
1.000E+05	1.237E+02	NA
1.500E+05	1.237E+02	NA
2.000E+05	1.237E+02	NA
3.000E+05	1.237E+02	NA
4.000E+05	1.237E+02	NA
5.000E+05	1.237E+02	NA
6.000E+05	1.237E+02	NA
7.000E+05	1.237E+02	NA
8.000E+05	1.237E+02	NA
9.000E+05	1.237E+02	NA
1.000E+06	1.237E+02	NA

TABLE 2-10(c). CASE 2 RESULTS: CUMULATIVE MASS OF Cm-245 IN THE FRACTURE AT DISTANCE x = 500 METERS (PERIODICALLY FLUCTUATING SOURCE WITH EXPONENTIAL DECAY AND BAND RELEASE MODE)

TIME (yr)	MULTFRAC	DURBIN
1.000E-01	8.996E-08	NA
1.500E-01	1.240E-07	NA
2.000E-01	1.549E-07	NA
3.000E-01	2.104E-07	NA
4.000E-01	2.603E-07	NA
5.000E-01	3.063E-07	NA
6.000E-01	3.494E-07	NA
7.000E-01	3.902E-07	NA
8.000E-01	4.292E-07	NA
9.000E-01	4.666E-07	NA
1.000E+00	5.027E-07	NA
1.500E+00	6.684E-07	NA
2.000E+00	8.174E-07	NA
3.000E+00	1.086E-06	NA
4.000E+00	1.329E-06	NA
5.000E+00	1.557E-06	NA
6.000E+00	1.772E-06	NA
7.000E+00	1.980E-06	NA
8.000E+00	2.180E-06	NA
9.000E+00	2.374E-06	NA
1.000E+01	2.564E-06	2.582E-06
1.500E+01	3.459E-06	3.486E-06
2.000E+01	4.297E-06	4.331E-06
3.000E+01	5.870E-06	5.920E-06
4.000E+01	7.360E-06	7.423E-06
5.000E+01	8.796E-06	8.873E-06
6.000E+01	1.019E-05	1.028E-05
7.000E+01	1.156E-05	1.167E-05
8.000E+01	1.291E-05	1.302E-05
9.000E+01	1.423E-05	1.436E-05
1.000E+02	1.554E-05	1.568E-05
1.500E+02	2.192E-05	2.212E-05
2.000E+02	2.813E-05	2.839E-05
3.000E+02	4.032E-05	4.069E-05
4.000E+02	5.231E-05	5.280E-05
5.000E+02	6.415E-05	6.477E-05
6.000E+02	7.587E-05	7.662E-05
7.000E+02	8.746E-05	8.838E-05

TABLE 2-10(c). CASE 2 RESULTS: CUMULATIVE MASS OF Cm-245 IN THE FRACTURE AT DISTANCE x = 500 METERS (PERIODICALLY FLUCTUATING SOURCE WITH EXPONENTIAL DECAY AND BAND RELEASE MODE) (Continued)

TIME (yr)	MULTFRAC	DURBIN
8.000E+02	9.896E-05	1.001E-04
9.000E+02	1.104E-04	1.116E-04
1.000E+03	1.217E-04	1.230E-04
1.500E+03	2.765E-04	2.782E-04
2.000E+03	3.020E-03	3.014E-03
3.000E+03	7.903E-02	7.893E-02
4.000E+03	4.459E-01	4.455E-01
5.000E+03	1.323E+00	1.322E+00
6.000E+03	2.820E+00	2.819E+00
7.000E+03	4.945E+00	4.943E+00
8.000E+03	7.596E+00	7.595E+00
9.000E+03	1.055E+01	1.054E+01
1.000E+04	1.355E+01	1.355E+01
1.500E+04	2.580E+01	NA
2.000E+04	3.273E+01	NA
3.000E+04	3.840E+01	NA
4.000E+04	4.009E+01	NA
5.000E+04	4.063E+01	NA
6.000E+04	4.082E+01	NA
7.000E+04	4.088E+01	NA
8.000E+04	4.090E+01	NA
9.000E+04	4.091E+01	NA
1.000E+05	4.092E+01	NA
1.500E+05	4.092E+01	NA
2.000E+05	4.092E+01	NA
3.000E+05	4.092E+01	NA
4.000E+05	4.092E+01	NA
5.000E+05	4.092E+01	NA
6.000E+05	4.092E+01	NA
7.000E+05	4.092E+01	NA
8.000E+05	4.092E+01	NA
9.000E+05	4.092E+01	NA
1.000E+06	4.092E+01	NA

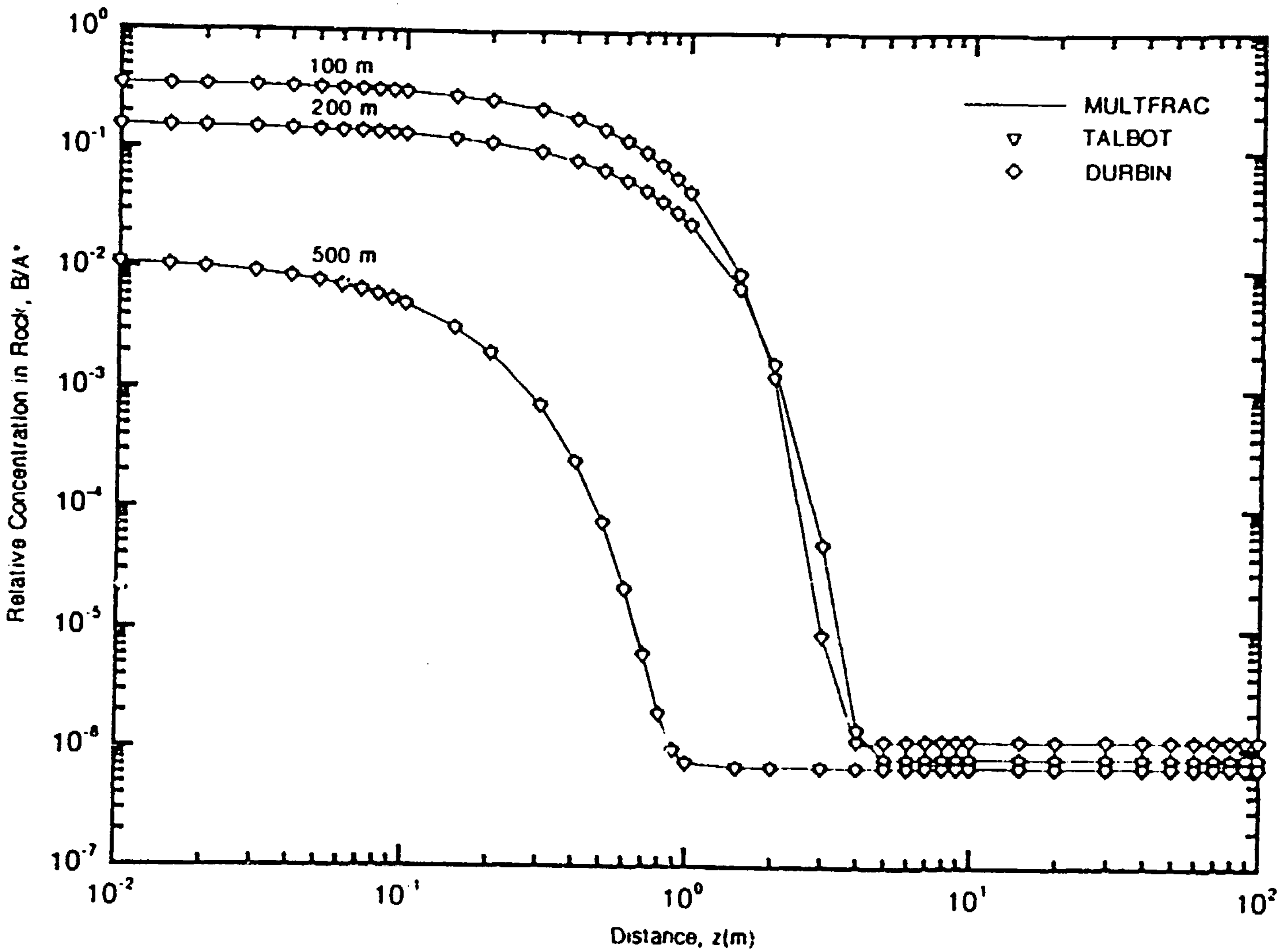

Figure 2-3(d). Relative concentration of Cm-245 in rock vs. distance z at time t = 5,000 years and distances from the source x = 100, 200, and 500 meters (Periodically fluctuating source with exponential decay).

Table 2-11(a). CASE 2 Results: CONCENTRATION OF Cm-245 IN THE ROCK MATRIX LAYER 2, AT DISTANCE x = 100 METERS AND TIME t = 5,000 YEARS (PERIODICALLY FLUCTUATING SOURCE WITH EXPONENTIAL DECAY AND STEP RELEASE MODE)

DISTANCE z(m)	MULTFRAC	TALBOT	DURBIN
1.500E-02	3.446E-01	3.446E-01	3.446E-01
2.000E-02	3.421E-01	3.421E-01	3.421E-01
3.000E-02	3.373E-01	3.373E-01	3.373E-01
4.000E-02	3.326E-01	3.326E-01	3.326E-01
5.000E-02	3.278E-01	3.278E-01	3.278E-01
6.000E-02	3.231E-01	3.231E-01	3.231E-01
7.000E-02	3.184E-01	3.184E-01	3.184E-01
8.000E-02	3.137E-01	3.137E-01	3.137E-01
9.000E-02	3.091E-01	3.091E-01	3.091E-01
1.000E-01	3.045E-01	3.045E-01	3.045E-01
1.500E-01	2.819E-01	2.819E-01	2.819E-01
2.000E-01	2.602E-01	2.601E-01	2.601E-01
3.000E-01	2.194E-01	2.194E-01	2.194E-01
4.000E-01	1.826E-01	1.826E-01	1.826E-01
5.000E-01	1.499E-01	1.499E-01	1.499E-01
6.000E-01	1.214E-01	1.214E-01	1.214E-01
7.000E-01	9.689E-02	9.689E-02	9.689E-02
8.000E-01	7.624E-02	7.624E-02	7.624E-02
9.000E-01	5.913E-02	5.912E-02	5.912E-02
1.000E+00	4.518E-02	4.517E-02	4.517E-02
1.500E+00	9.377E-03	9.376E-03	9.376E-03
2.000E+00	1.319E-03	1.318E-03	1.318E-03
3.000E+00	8.914E-06	8.910E-06	9.171E-06
4.000E+00	1.076E-06	1.173E-06	1.189E-06
5.000E+00	1.164E-06	1.164E-06	1.184E-06
6.000E+00	1.164E-06	1.164E-06	1.184E-06
7.000E+00	1.164E-06	1.164E-06	1.184E-06
8.000E+00	1.164E-06	1.164E-06	1.184E-06
9.000E+00	1.164E-06	1.164E-06	1.184E-06
1.000E+01	1.164E-06	1.164E-06	1.184E-06
1.500E+01	1.164E-06	1.164E-06	1.184E-06
2.000E+01	1.164E-06	1.164E-06	1.184E-06
3.000E+01	1.164E-06	1.164E-06	1.184E-06
4.000E+01	1.164E-06	1.164E-06	1.184E-06
5.000E+01	1.164E-06	1.164E-06	1.184E-06
6.000E+01	1.164E-06	1.164E-06	1.184E-06
7.000E+01	1.164E-06	1.164E-06	1.184E-06

Table 2-11(a). CASE 2 RESULTS: CONCENTRATION OF Cm-245 IN THE ROCK MATRIX LAYER 2, AT DISTANCE x = 100 METERS AND TIME t = 5,000 YEARS (PERIODICALLY FLUCTUATING SOURCE WITH EXPONENTIAL DECAY AND STEP RELEASE MODE) (Continued)

DISTANCE z(m)	MULTFRAC	TALBOT	DURBIN
8.000E+01	1.164E-06	1.164E-06	1.184E-06
9.000E+01	1.164E-06	1.164E-06	1.184E-06
1.000E+02	1.164E-06	1.164E-06	1.184E-06

Table 2-11(b). CASE 2 RESULTS: CONCENTRATION OF Cm-245 IN THE ROCK MATRIX LAYER 3, AT DISTANCE x = 200 METERS AND TIME t = 5,000 YEARS (PERIODICALLY FLUCTUATING SOURCE WITH EXPONENTIAL DECAY AND STEP RELEASE MODE)

DISTANCE z(m)	MULTFRAC	TALBOT	DURBIN
1.000E-02	1.539E-01	1.539E-01	1.539E-01
1.500E-02	1.528E-01	1.528E-01	1.528E-01
2.000E-02	1.516E-01	1.516E-01	1.516E-01
3.000E-02	1.494E-01	1.494E-01	1.494E-01
4.000E-02	1.472E-01	1.472E-01	1.472E-01
5.000E-02	1.450E-01	1.450E-01	1.450E-01
6.000E-02	1.428E-01	1.428E-01	1.428E-01
7.000E-02	1.407E-01	1.407E-01	1.407E-01
8.000E-02	1.385E-01	1.385E-01	1.385E-01
9.000E-02	1.364E-01	1.364E-01	1.364E-01
1.000E-01	1.343E-01	1.343E-01	1.343E-01
1.500E-01	1.242E-01	1.242E-01	1.242E-01
2.000E-01	1.147E-01	1.147E-01	1.147E-01
3.000E-01	9.714E-02	9.713E-02	9.713E-02
4.000E-01	8.166E-02	8.165E-02	8.165E-02
5.000E-01	6.812E-02	6.811E-02	6.811E-02
6.000E-01	5.638E-02	5.637E-02	5.637E-02
7.000E-01	4.630E-02	4.629E-02	4.629E-02
8.000E-01	3.771E-02	3.771E-02	3.771E-02
9.000E-01	3.048E-02	3.047E-02	3.047E-02
1.000E+00	2.443E-02	2.443E-02	2.443E-02
1.500E+00	7.149E-03	7.148E-03	7.149E-03
2.000E+00	1.692E-03	1.697E-03	1.697E-03
3.000E+00	5.103E-05	5.102E-05	5.093E-05
4.000E+00	1.450E-06	1.450E-06	1.462E-06
5.000E+00	8.346E-07	8.346E-07	8.221E-07

Table 2-11(b). CASE 2 RESULTS: CONCENTRATION OF Cm-245 IN THE ROCK MATRIX LAYER 3, AT DISTANCE x = 200 METERS AND TIME t = 5,000 YEARS (PERIODICALLY FLUCTUATING SOURCE WITH EXPONENTIAL DECAY AND STEP RELEASE MODE) (Continued)

DISTANCE z(m)	MULTFRAC	TALBOT	DURBIN
6.000E+00	8.315E-07	8.315E-07	8.258E-07
7.000E+00	8.314E-07	8.314E-07	8.257E-07
8.000E+00	8.314E-07	8.314E-07	8.257E-07
9.000E+00	8.314E-07	8.314E-07	8.257E-07
1.000E+01	8.314E-07	8.314E-07	8.257E-07
1.500E+01	8.314E-07	8.314E-07	8.257E-07
2.000E+01	8.314E-07	8.314E-07	8.257E-07
3.000E+01	8.314E-07	8.314E-07	8.257E-07
4.000E+01	8.314E-07	8.314E-07	8.257E-07
5.000E+01	8.314E-07	8.314E-07	8.257E-07
6.000E+01	8.314E-07	8.314E-07	8.257E-07
7.000E+01	8.314E-07	8.314E-07	8.257E-07
8.000E+01	8.314E-07	8.314E-07	8.257E-07
9.000E+01	8.314E-07	8.314E-07	8.257E-07
1.000E+02	8.314E-07	8.314E-07	8.257E-07

Table 2-11(c). CASE 2 RESULTS: CONCENTRATION OF Cm-245 IN THE ROCK MATRIX LAYER 5, AT DISTANCE x = 500 METERS AND TIME t = 5,000 YEARS (PERIODICALLY FLUCTUATING SOURCE WITH EXPONENTIAL DECAY AND STEP RELEASE MODE)

DISTANCE z(m)	MULTFRAC	TALBOT	DURBIN
1.000E-02	1.101E-02	1.100E-02	1.100E-02
1.500E-02	1.057E-02	1.057E-02	1.057E-02
2.000E-02	1.015E-02	1.015E-02	1.015E-02
3.000E-02	9.353E-03	9.352E-03	9.352E-03
4.000E-02	8.611E-03	8.610E-03	8.610E-03
5.000E-02	7.921E-03	7.920E-03	7.920E-03
6.000E-02	7.281E-03	7.279E-03	7.280E-03
7.000E-02	6.686E-03	6.685E-03	6.685E-03
8.000E-02	6.135E-03	6.134E-03	6.134E-03
9.000E-02	5.624E-03	5.623E-03	5.624E-03
1.000E-01	5.152E-03	5.151E-03	5.151E-03
1.500E-01	3.280E-03	3.279E-03	3.279E-03
2.000E-01	2.043E-03	2.043E-03	2.043E-03
3.000E-01	7.436E-04	7.434E-04	7.434E-04

Table 2-11(c). CASE 2 RESULTS: CONCENTRATION OF Cm-245 IN THE ROCK MATRIX LAYER 5, AT DISTANCE x = 500 METERS AND TIME t = 5,000 YEARS (PERIODICALLY FLUCTUATING SOURCE WITH EXPONENTIAL DECAY AND STEP RELEASE MODE) (Continued)

DISTANCE z(m)	MULTFRAC	TALBOT	DURBIN
4.000E-01	2.482E-04	2.481E-04	2.474E-04
5.000E-01	7.621E-05	7.618E-05	7.615E-05
6.000E-01	2.178E-05	2.177E-05	2.176E-05
7.000E-01	6.080E-06	6.077E-06	6.301E-06
8.000E-01	1.954E-06	1.954E-06	1.971E-06
9.000E-01	9.661E-07	9.665E-07	9.755E-07
1.000E+00	7.506E-07	7.508E-07	7.587E-07
1.500E+00	6.984E-07	6.984E-07	6.845E-07
2.000E+00	6.984E-07	6.984E-07	6.852E-07
3.000E+00	6.984E-07	6.984E-07	6.852E-07
4.000E+00	6.984E-07	6.984E-07	6.852E-07
5.000E+00	6.984E-07	6.984E-07	6.852E-07
6.000E+00	6.984E-07	6.984E-07	6.852E-07
7.000E+00	6.984E-07	6.984E-07	6.852E-07
8.000E+00	6.984E-07	6.984E-07	6.852E-07
9.000E+00	6.984E-07	6.984E-07	6.852E-07
1.000E+01	6.984E-07	6.984E-07	6.852E-07
1.500E+01	6.984E-07	6.984E-07	6.852E-07
2.000E+01	6.984E-07	6.984E-07	6.852E-07
3.000E+01	6.984E-07	6.984E-07	6.852E-07
4.000E+01	6.984E-07	6.984E-07	6.852E-07
5.000E+01	6.984E-07	6.984E-07	6.852E-07
6.000E+01	6.984E-07	6.984E-07	6.852E-07
7.000E+01	6.984E-07	6.984E-07	6.852E-07
8.000E+01	6.984E-07	6.984E-07	6.852E-07
9.000E+01	6.984E-07	6.984E-07	6.852E-07
1.000E+02	6.984E-07	6.984E-07	6.852E-07

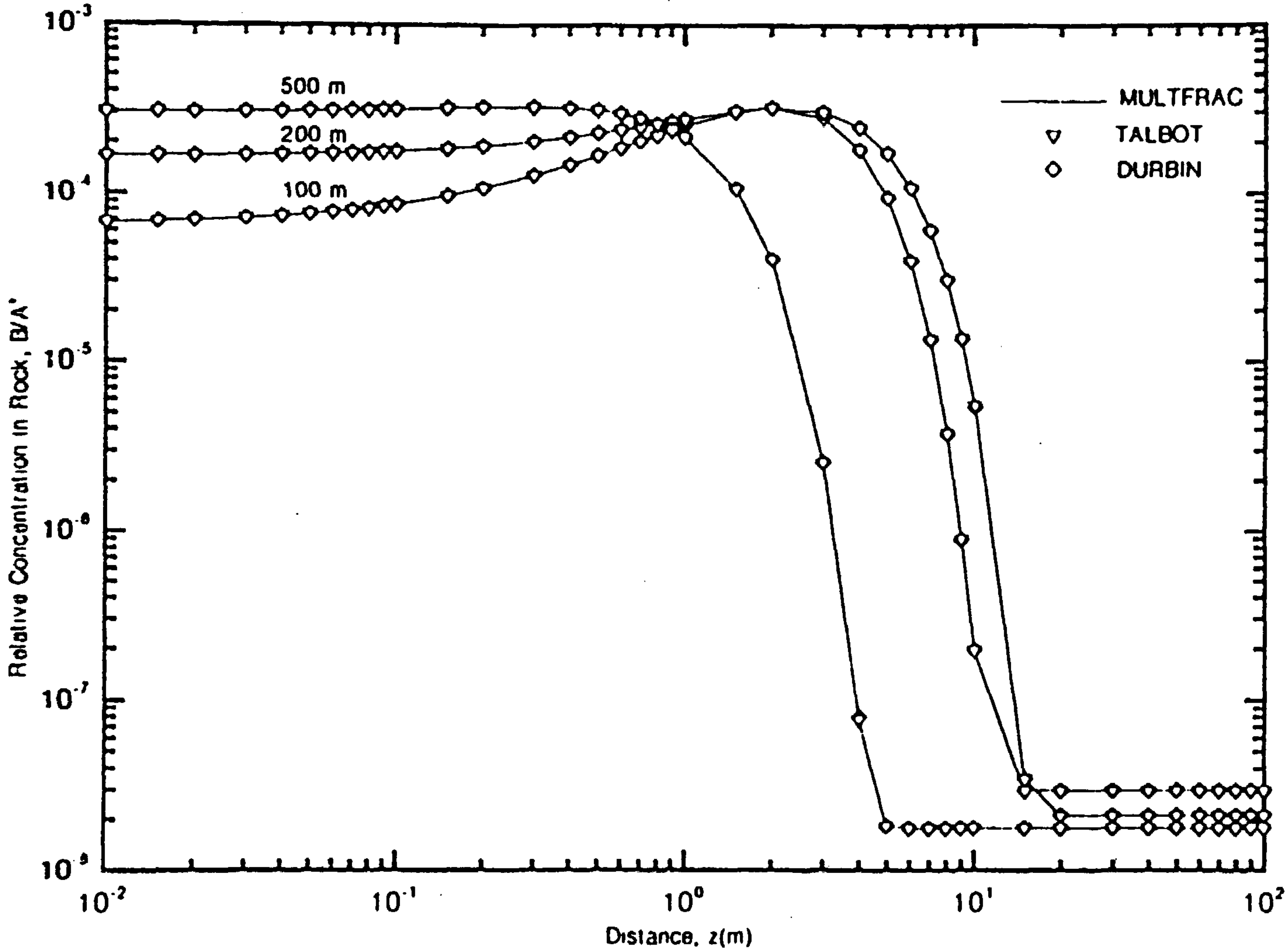

Figure 2-3(e). Relative concentration of Cm-245 in rock vs. distance at t = 50,000 years (Periodically fluctuating source with exponential decay).

Table 2-12(a). CASE 2 RESULTS: CONCENTRATION OF Cm-245 IN THE ROCK MATRIX LAYER 2, AT DISTANCE x = 100 METERS AND TIME t = 50,000 YEARS (PERIODICALLY FLUCTUATING SOURCE WITH EXPONENTIAL DECAY AND BAND RELEASE MODE)

DISTANCE z(m)	MULTFRAC	TALBOT	DURBIN
1.000E-02	6.722E-05	6.722E-05	6.723E-05
1.500E-02	6.833E-05	6.833E-05	6.834E-05
2.000E-02	6.944E-05	6.944E-05	6.944E-05
3.000E-02	7.166E-05	7.166E-05	7.165E-05
4.000E-02	7.387E-05	7.387E-05	7.387E-05
5.000E-02	7.608E-05	7.608E-05	7.607E-05
6.000E-02	7.828E-05	7.828E-05	7.828E-05
7.000E-02	8.048E-05	8.048E-05	8.048E-05
8.000E-02	8.267E-05	8.268E-05	8.267E-05
9.000E-02	8.486E-05	8.487E-05	8.486E-05
1.000E-01	8.705E-05	8.705E-05	8.705E-05
1.500E-01	9.791E-05	9.791E-05	9.791E-05
2.000E-01	1.086E-04	1.086E-04	1.086E-04
3.000E-01	1.296E-04	1.296E-04	1.296E-04
4.000E-01	1.500E-04	1.500E-04	1.500E-04
5.000E-01	1.695E-04	1.695E-04	1.694E-04
6.000E-01	1.881E-04	1.881E-04	1.880E-04
7.000E-01	2.058E-04	2.058E-04	2.058E-04
8.000E-01	2.224E-04	2.224E-04	2.224E-04
9.000E-01	2.379E-04	2.379E-04	2.379E-04
1.000E+00	2.522E-04	2.522E-04	2.522E-04
1.500E+00	3.046E-04	3.046E-04	3.046E-04
2.000E+00	3.241E-04	3.241E-04	3.241E-04
3.000E+00	2.811E-04	2.811E-04	2.811E-04
4.000E+00	1.847E-04	1.847E-04	1.847E-04
5.000E+00	9.587E-05	9.587E-05	9.583E-05
6.000E+00	4.008E-05	4.008E-05	4.002E-05
7.000E+00	1.366E-05	1.366E-05	1.360E-05
8.000E+00	3.838E-06	3.838E-06	3.823E-06
9.000E+00	9.069E-07	9.069E-07	8.981E-07
1.000E+01	1.969E-07	1.969E-07	1.995E-07
1.500E+01	2.967E-08	2.967E-08	2.967E-08
2.000E+01	2.967E-08	2.967E-08	2.967E-08
3.000E+01	2.967E-08	2.967E-08	2.967E-08
4.000E+01	2.967E-08	2.967E-08	2.967E-08
5.000E+01	2.967E-08	2.967E-08	2.967E-08
6.000E+01	2.967E-08	2.967E-08	2.967E-08

Table 2-12(a). CASE 2 RESULTS: CONCENTRATION OF Cm-245 IN THE ROCK MATRIX LAYER 2, AT DISTANCE x = 100 METERS AND TIME t = 50,000 YEARS (PERIODICALLY FLUCTUATING SOURCE WITH EXPONENTIAL DECAY AND BAND RELEASE MODE) (Continued)

DISTANCE z(m)	MULTFRAC	TALBOT	DURBIN
7.000E+01	2.967E-08	2.967E-08	2.967E-08
8.000E+01	2.967E-08	2.967E-08	2.967E-08
9.000E+01	2.967E-08	2.967E-08	2.967E-08
1.000E+02	2.967E-08	2.967E-08	2.967E-08

Table 2-12(b). CASE 2 RESULTS: CONCENTRATION OF Cm-245 IN THE ROCK MATRIX LAYER 3, AT DISTANCE X = 200 METERS AND TIME t = 50,000 YEARS (PERIODICALLY FLUCTUATING SOURCE WITH EXPONENTIAL DECAY AND BAND RELEASE MODE)

DISTANCE z(m)	MULTFRAC	TALBOT	DURBIN
1.000E-02	1.661E-04	1.661E-04	1.660E-04
1.500E-02	1.668E-04	1.668E-04	1.667E-04
2.000E-02	1.675E-04	1.675E-04	1.674E-04
3.000E-02	1.689E-04	1.689E-04	1.688E-04
4.000E-02	1.703E-04	1.703E-04	1.702E-04
5.000E-02	1.716E-04	1.716E-04	1.716E-04
6.000E-02	1.730E-04	1.730E-04	1.729E-04
7.000E-02	1.744E-04	1.744E-04	1.743E-04
8.000E-02	1.758E-04	1.758E-04	1.757E-04
9.000E-02	1.771E-04	1.771E-04	1.770E-04
1.000E-01	1.785E-04	1.785E-04	1.784E-04
1.500E-01	1.852E-04	1.852E-04	1.851E-04
2.000E-01	1.918E-04	1.918E-04	1.917E-04
3.000E-01	2.046E-04	2.046E-04	2.046E-04
4.000E-01	2.168E-04	2.168E-04	2.168E-04
5.000E-01	2.285E-04	2.285E-04	2.285E-04
6.000E-01	2.395E-04	2.395E-04	2.395E-04
7.000E-01	2.500E-04	2.500E-04	2.500E-04
8.000E-01	2.598E-04	2.598E-04	2.598E-04
9.000E-01	2.689E-04	2.689E-04	2.689E-04
1.000E+00	2.774E-04	2.774E-04	2.774E-04
1.500E+00	3.092E-04	3.092E-04	3.092E-04
2.000E+00	3.238E-04	3.238E-04	3.237E-04
3.000E+00	3.068E-04	3.068E-04	3.068E-04
4.000E+00	2.482E-04	2.482E-04	2.482E-04

Table 2-12(b). CASE 2 RESULTS: CONCENTRATION OF Cm-245 IN THE ROCK MATRIX LAYER 3, AT DISTANCE X = 200 METERS AND TIME t = 50,000 YEARS (PERIODICALLY FLUCTUATING SOURCE WITH EXPONENTIAL DECAY AND BAND RELEASE MODE) (Continued)

DISTANCE z(m)	MULTFRAC	TALBOT	DURBIN
5.000E+00	1.755E-04	1.755E-04	1.755E-04
6.000E+00	1.098E-04	1.098E-04	1.099E-04
7.000E+00	6.129E-05	6.129E-05	6.131E-05
8.000E+00	3.065E-05	3.065E-05	3.075E-05
9.000E+00	1.378E-05	1.378E-05	1.371E-05
1.000E+01	5.596E-06	5.596E-06	5.457E-06
1.500E+01	3.477E-08	3.477E-08	3.477E-08
2.000E+01	2.119E-08	2.119E-08	2.119E-08
3.000E+01	2.119E-08	2.119E-08	2.119E-08
4.000E+01	2.119E-08	2.119E-08	2.119E-08
5.000E+01	2.119E-08	2.119E-08	2.119E-08
6.000E+01	2.119E-08	2.119E-08	2.119E-08
7.000E+01	2.119E-08	2.119E-08	2.119E-08
8.000E+01	2.119E-08	2.119E-08	2.119E-08
9.000E+01	2.119E-08	2.119E-08	2.119E-08
1.000E+02	2.119E-08	2.119E-08	2.119E-08

Table 2-12(c). CASE 2 RESULTS: CONCENTRATION OF Cm-245 IN THE ROCK MATRIX LAYER 5, AT DISTANCE x = 500 METERS AND TIME t = 50,000 YEARS (PERIODICALLY FLUCTUATING SOURCE WITH EXPONENTIAL DECAY AND BAND RELEASE MODE)

DISTANCE z(m)	MULTFRAC	TALBOT	DURBIN
1.000E-02	3.001E-04	3.001E-04	3.001E-04
1.500E-02	3.010E-04	3.010E-04	3.010E-04
2.000E-02	3.019E-04	3.019E-04	3.019E-04
3.000E-02	3.037E-04	3.037E-04	3.037E-04
4.000E-02	3.054E-04	3.054E-04	3.054E-04
5.000E-02	3.070E-04	3.070E-04	3.070E-04
6.000E-02	3.086E-04	3.086E-04	3.085E-04
7.000E-02	3.100E-04	3.100E-04	3.100E-04
8.000E-02	3.115E-04	3.115E-04	3.115E-04
9.000E-02	3.128E-04	3.128E-04	3.128E-04
1.000E-01	3.141E-04	3.141E-04	3.141E-04
1.500E-01	3.194E-04	3.194E-04	3.194E-04
2.000E-01	3.231E-04	3.231E-04	3.231E-04

Table 2-12(c). CASE 2 RESULTS: CONCENTRATION OF Cm-245 IN THE ROCK MATRIX LAYER 5, AT DISTANCE x = 500 METERS AND TIME t = 50,000 YEARS (PERIODICALLY FLUCTUATING SOURCE WITH EXPONENTIAL DECAY AND BAND RELEASE MODE) (Continued)

DISTANCE z(m)	MULTFRAC	TALBOT	DURBIN
3.000E-01	3.254E-04	3.254E-04	3.253E-04
4.000E-01	3.217E-04	3.217E-04	3.216E-04
5.000E-01	3.125E-04	3.125E-04	3.126E-04
6.000E-01	2.988E-04	2.988E-04	2.990E-04
7.000E-01	2.814E-04	2.814E-04	2.814E-04
8.000E-01	2.613E-04	2.613E-04	2.613E-04
9.000E-01	2.393E-04	2.393E-04	2.392E-04
1.000E+00	2.162E-04	2.162E-04	2.162E-04
1.500E+00	1.083E-04	1.083E-04	1.083E-04
2.000E+00	4.066E-05	4.066E-05	4.078E-05
3.000E+00	2.598E-06	2.598E-06	2.599E-06
4.000E+00	7.751E-08	7.751E-08	8.064E-08
5.000E+00	1.832E-08	1.832E-08	1.833E-08
6.000E+00	1.780E-08	1.780E-08	1.780E-08
7.000E+00	1.780E-08	1.780E-08	1.780E-08
8.000E+00	1.780E-08	1.780E-08	1.780E-08
9.000E+00	1.780E-08	1.780E-08	1.780E-08
1.000E+01	1.780E-08	1.780E-08	1.780E-08
1.500E+01	1.780E-08	1.780E-08	1.780E-08
2.000E+01	1.780E-08	1.780E-08	1.780E-08
3.000E+01	1.780E-08	1.780E-08	1.780E-08
4.000E+01	1.780E-08	1.780E-08	1.780E-08
5.000E+01	1.780E-08	1.780E-08	1.780E-08
6.000E+01	1.780E-08	1.780E-08	1.780E-08
7.000E+01	1.780E-08	1.780E-08	1.780E-08
8.000E+01	1.780E-08	1.780E-08	1.780E-08
9.000E+01	1.780E-08	1.780E-08	1.780E-08
1.000E+02	1.780E-08	1.780E-08	1.780E-08

3. ANALYTICALLY DERIVED SENSITIVITIES IN THE FRACTURE

3.1. LOCAL SENSITIVITIES

Local sensitivities or first-order derivatives of the concentration and cumulative mass in the fracture, with respect to a typical parameter α (i.e., $\partial \Lambda_i / \partial \alpha$, and $\partial M_i / \partial \alpha_i$), are required in parameter estimation or sampling design studies (sensitivity of concentration), and in predicting the sensitivity and uncertainty of the performance of a system (sensitivity of cumulative mass). There are two classical methods for evaluating the local sensitivities. The first (and the most accurate) is the analytically derived solution, which is estimated after a direct differentiation of the closed form solution with respect to the parameters of interest. The second uses numerical derivatives obtained from finite-difference approximations. In the following, we report the analytically derived sensitivities related to the concentration in the fracture, where the initial concentration in both fracture and rock matrix are assumed to correspond to some constant values. In addition, we provide the verification, performed through a comparison of the results with those derived through finite-difference approximations (i.e., forward-difference and central-difference) currently available as options in the associated mathematical model.

3.2. ANALYTICAL DERIVATIVES

This section presents the analytically derived local sensitivities of the concentrations and cumulative mass flux in the fracture with respect to the entire range of parameters governing the non-dispersive transport process in the fractured rock system of interest described by the equations reported in the previous chapter of this report.

3.2.1. Total Differentials

In order to evaluate the first order derivatives of the concentration and cumulative mass in the fracture reported in the preceding sections, the total differentials of R_i, R'_i, c_{fi}, p_i, θ_{mn}, γ_{mn}, q_i, and β_{ji}, given by Equations (2-5), (2-6), (2-29), (2-35b), (2-39), (2-40), (2-47) and (2-48) (see also Appendix F) have to be defined. Applying the chain rule of differentiation, these may be written as

$$dR_i = \frac{\partial R_i}{\partial K_{fi}} dK_{fi} + \frac{\partial R_i}{\partial b_i} db_i \tag{3-1}$$

$$dR'_i = \frac{\partial R'_i}{\partial \phi_i} d\phi_i + \frac{\partial R'_i}{\partial \rho_n} d\rho_n + \frac{\partial R'_i}{\partial K_n} dK_n \tag{3-2}$$

$$dc_{fi} = \frac{\partial c_{fi}}{\partial \phi_i} d\phi_i + \frac{\partial c_{fi}}{\partial b_i} db_i + \frac{\partial c_{fi}}{\partial R'_i} dR'_i + \frac{\partial c_{fi}}{\partial D_{p_i}} dD_{p_i} \tag{3-3}$$

$$dp_i = \frac{\partial p_i}{\partial u_i} du_i + \frac{\partial p_i}{\partial \alpha_i} d\alpha_i \tag{3-4}$$

$$d\theta_{mn} = \frac{\partial \theta_{mn}}{\partial c_{fi}} dc_{fi} + \frac{\partial \theta_{mn}}{\partial \Gamma_i} d\Gamma_i \tag{3-5}$$

$$d\gamma_{mn} = \frac{\partial \gamma_{mn}}{\partial R_i} dR_i + \frac{\partial \gamma_{mn}}{\partial \Gamma_i} d\Gamma_i \tag{3-6}$$

$$dq_i = \frac{\partial q_i}{\partial c_{fi}} dc_{fi} + \frac{\partial q_i}{\partial R_i} dR_i + \frac{\partial q_i}{\partial p_i} dp_i \tag{3-7}$$

$$d\beta_{fi} = \frac{\partial \beta_{fi}}{\partial c_{fi}} dc_{fi} + \frac{\partial \beta_{fi}}{\partial R_i} dR_i + \frac{\partial \beta_{fi}}{\partial p_i} dp_i \tag{3-8}$$

$$d\Gamma_i = \frac{\partial \Gamma_i}{\partial L_i} dL_i + \frac{\partial \Gamma_i}{\partial u_i} du_i \tag{3-9}$$

$$\Gamma_i = \bar{\eta}_i \, , \; i < n \tag{3-10a}$$

$$\Gamma_i = \eta_i \, , \; i = n \tag{3-10b}$$

substitution of Equations (3-3) and (3-9) in Equation (3-5) gives

$$d\theta_{mn} = \frac{\partial\theta_{mn}}{\partial c_{fi}}\left[\frac{\partial c_{fi}}{\partial\Phi_i}d\Phi_i + \frac{\partial c_{fi}}{\partial b_i}db_i + \frac{\partial c_{fi}}{\partial R_i'}dR_i' + \frac{\partial c_{fi}}{\partial D_{pi}}dD_{pi}\right]$$

$$+ \frac{\partial\theta_m}{\partial\Gamma_i}\left[\frac{\partial\Gamma_i}{\partial L_i}dL_i + \frac{\partial\Gamma_i}{\partial u_i}du_i\right] \qquad (3\text{-}11)$$

Similarly, substituting Equations (3-1) and (3-9) in Equation (3-6) yields

$$d\gamma_{mn} = \frac{\partial\gamma_{mn}}{\partial R_i}dR_i + \frac{\partial\gamma_{mn}}{\partial\Gamma_i}\left[\frac{\partial\Gamma_i}{\partial L_i}dL_i + \frac{\partial\Gamma_i}{\partial u_i}du_i\right] \qquad (3\text{-}12)$$

where

$$du_i = \frac{\partial u_i}{\partial b_i}db_i \qquad (3\text{-}13)$$

Note that the total differentials of dR_i and dR'_i as given by Equations (3-1) and (3-2) are used whenever appropriate (i.e., if either R_i or R'_i are expressed in terms of their respective components).

Using the following partial derivatives

$$\frac{\partial\Gamma_i}{\partial\bar{L}_i} = \frac{1}{u_i} \qquad (3\text{-}14a)$$

$$\bar{L}_i = \begin{cases} L_i, & i < n \\ x - x_{i-1}, & i = n \end{cases} \qquad (3\text{-}14b)$$

$$\frac{\partial\Gamma_i}{\partial u_i} = -\frac{\bar{L}_i}{u_i^2} \qquad (3\text{-}14c)$$

$$\frac{\partial\theta_m}{\partial c_{fi}} = \Gamma_i \qquad (3.15a)$$

$$\frac{\partial \theta_m}{\partial \Gamma_l} = c_{jl} \tag{3-15b}$$

$$\frac{\partial \gamma_{mn}}{\partial R_l} = \Gamma_l \tag{3-16b}$$

$$\frac{\partial q_l}{\partial c_{jl}} = \frac{c_{jl}}{q_l R_l^2} \tag{3-17a}$$

$$\frac{\partial q_l}{\partial R_l} = -\frac{2}{q_l}\left[\frac{c_{jl}^2}{2R_l^3} + \frac{p_l}{R_l^2}\right] \tag{3-17b}$$

$$\frac{\partial q_l}{\partial p_l} = \frac{2}{q_l R_l} \tag{3-17c}$$

$$\frac{\partial \beta_{jl}}{\partial c_{jl}} = \frac{1}{2R_l} + (-1)^j \frac{c_{jl}}{2q_l R_l^2}, \quad j = 1,2 \tag{3-18a}$$

$$\frac{\partial \beta_{jl}}{\partial R_l} = -\frac{c_{jl}}{2R_l^2} - (-1)^j \frac{1}{R_l^2}\left[\frac{c_{jl}^2}{2R_l} + p_l\right], \quad j = 1,2 \tag{3-18b}$$

$$\frac{\partial \beta_{jl}}{\partial q_l} = (-1)^j \frac{1}{2}, \quad j = 1,2 \tag{3-18c}$$

$$\frac{\partial \beta_{jl}}{\partial p_l} = \frac{\partial \beta_{jl}}{\partial q_l}\frac{\partial q_l}{\partial p_l} = (-1)^j \frac{1}{q_l R_l} \tag{3-18d}$$

$$\frac{\partial p_l}{\partial u_l} = \alpha_l \tag{3-19a}$$

$$\frac{\partial p_l}{\partial \alpha_l} = u_l \tag{3-19b}$$

$$\frac{\partial u_l}{\partial b_l} = -\frac{Q}{2b_l^2} \tag{3-20}$$

the first order derivatives of θ_{mn}, γ_{mn}, c_{fi}, R_i and R'_i with respect to a typical parameter α_i are reported in Tables 3-1 through 3-5, respectively. Whereas the one corresponding to β_{ji} given by Equation (3-8) may be evaluated based on the latter tables and the various derivatives given in Equations (3-14) through (3-20). Note that Q in Equation (3-20) corresponds to the steady flow rate of water ($Q = 2\ u_i\ b_i$) through the fracture.

3.2.2. First Order Derivatives of the Concentrations

Using the notations reported in Appendix D, the various components of Equation (2-42) may now be written as

$$F_{o_{1n}}(x,t) = A^0 e^{-\lambda t}\, {}^1P_{1n}\ U(t - \gamma_{1n}) \tag{3-21a}$$

for a continuously decaying source

$$_1H_{lmn}(x,t) = e^{-\lambda t}\left[b_{1l}\, {}^1P_{mn} + (a_{1l} - b_{1l})\, {}^3P_{lmn}\, {}^4P_{lmn}\, {}^2P_{mn}\right]U(t - \gamma_{mn}) \tag{3-21b}$$

$$_2H_{lmn}(x,t) = e^{-\lambda t}\, a_{2l} \sum_{j=1}^{2} (-1)^j\, {}^9P_{jl}\, {}^8P_{jlmn}\, {}^7P_{jlmn}\, U(t-\gamma_{mn}) \tag{3-21c}$$

$$F_n(x,t) = e^{-\lambda t} a_{2n} \sum_{l=1}^{2} (-1)^l\, {}^9P_{ln}\, {}^{10}P_{ln}\, {}^{11}P_{ln}] + e^{-\lambda t}\left[b_{1n} + (a_{1n} - b_{1n})\, {}^5P_n\, {}^6P_n\right] \tag{3-21d}$$

Table 3-1. FIRST ORDER PARTIAL DERIVATIVES OF θ_{mn} WITH RESPECT TO INPUT PARAMETERS α_i (i.e., L_i, u_i, ϕ_i, ρ_i, D_{pi}, R_i, K_{fi}, R'_i, and K_{ri})

α_i	$\theta_{mn,\alpha i}$	α_i	$\theta_{mn,\alpha i}$
L_i	$\frac{c_{fl}}{u_i}$, $i<n,\ n>1$	D_{pi}	$\frac{c_{fl}}{2D_{pi}}\Gamma_i$
u_i	$-\frac{c_{fl}}{u_i}\Gamma_i$	R_i	NA
b_i	$-\frac{c_{fl}}{b_i}\Gamma_i + \frac{2c_{fl}\hat{L}_i}{Q}$	K_{fi}	NA
ϕ_i	$IDIST(2)=0$: $\frac{c_{fl}}{\phi_i}\Gamma_i$ $IDIST(2)=1$: $\frac{c_{fl}}{\phi_i}\left[1-\frac{\rho_{ri}K_{ri}}{2\phi R'_i}\right]\Gamma_i$	R'_i ‡	$\frac{c_{fl}}{2R'_i}\Gamma_i$
ρ_i †	$\frac{c_{fl}}{2R'_i}\left(\frac{1-\phi_i}{\phi_i}\right)K_{ri}\Gamma_i$	K_{ri} †	$\frac{c_{fl}}{2R'_i}\left(\frac{1-\phi_i}{\phi_i}\right)\rho_{ri}\Gamma_i$

$\Gamma_i = \bar{\eta}_{i},\ i<n;\quad \Gamma_i = \eta_{i},\ i=n$

NA = Not Applicable
† Applicable if IDIST(2) = 1
‡ Applicable if IDIST(2) = 0

Table 3-2. FIRST ORDER PARTIAL DERIVATIVES OF γ_{ma} WITH RESPECT TO INPUT PARAMETERS α_i (i.e., L_i, u_i, b_i, R_i, and K_{fl})

α_i	$\gamma_{ma,\alpha}$
L_i	$\frac{R_i}{u_i}$, $i<n$, $n>1$
u_i	$-\frac{R_i \Gamma_i}{u_i}$
b_i†	$IDIST(1) = 0$: $\frac{2 R_i \bar{L}_i}{Q}$ $IDIST(1) = 1$: $-\frac{K_{fl} \Gamma_i}{b_i^2} + \frac{2 R_i \bar{L}_i}{Q}$
R_i‡	Γ_i
K_{fl}†	$\frac{\Gamma_i}{b_i}$

$\Gamma_i = \bar{\eta}_i$, $i<n$; $\Gamma_i = \eta_i$, $i=n$

† Applicable only if IDIST(1) = 1
‡ Applicable only if IDIST(1) = 0

Table 3-3. FIRST ORDER PARTIAL DERIVATIVES OF c_{fl} WITH RESPECT TO INPUT PARAMETERS α_i (i.e., L_i, u_i, ϕ_i, ρ_i, D_{pl}, R_i, K_{fl}, R'_i, AND K_{rl})

α_i	$C_{fl,\alpha i}$	α_i	$C_{fl,\alpha i}$
L_i	NA	D_{pi}	$\frac{c_{fl}}{2D_{pi}}$
u_i	NA	R_i	NA
b_i	$-\frac{c_{fl}}{b_i}$	K_{fl}	NA
ϕ_i	*IDIST*(2) = 0: $\frac{c_{fl}}{\phi_i}$ *IDIST*(2) = 1: $\frac{c_{fl}}{\phi_i}\left[1 - \frac{\rho_n K_n}{2\phi R'_i}\right]$	R'_i ‡	$\frac{c_{fl}}{2R'_i}$
ρ_i †	$\frac{c_{fl}}{2R'_i}\left(\frac{1-\phi_i}{\phi_i}\right)K'_{rl}$	K_n †	$\frac{c_{fl}}{2R'_i}\left(\frac{1-\phi_i}{\phi_i}\right)\rho_n$

NA = Not Applicable

† Applicable only if IDIST(2) = 1

‡ Applicable only if IDIST(2) = 0

Table 3-4. FIRST ORDER PARTIAL DERIVATIVES OF R_i WITH RESPECT TO INPUT PARAMETERS α_i (i.e., b_i, R_i, and K_β)

α_i	$R_{i,\alpha d}$	α_i	$R_{i,\alpha}$	α_i	$R_{i,\alpha t}$
b_i †	$\frac{K_\beta}{b_i^2}$	R_i ‡	1.0	K_β †	$\frac{1}{b_i}$

† Applicable only if IDIST(1) = 1
‡ Applicable only if IDIST(1) = 0

Table 3-5. FIRST ORDER PARTIAL DERIVATIVES OF R'_i WITH RESPECT TO INPUT PARAMETERS α_i (i.e., Φ_i, ρ_i, K_d AND R'_i)

α_i	$R'_{i,\alpha d}$	α_i	$R'_{i,\alpha}$	α_i	$R'_{i,\alpha t}$	α_i	$R'_{i,\alpha}$
Φ_i †	$\frac{1}{\Phi_i^2}$	ρ_i †	$\frac{(1-\Phi_i)}{\Phi_i} K_d$	K_d †	$\frac{(1-\Phi_i)}{\Phi_i} \rho_d$	R_i ‡	1.0

† Applicable only if IDIST(1) = 1
‡ Applicable only if IDIST(1) = 0

The partial derivatives of the above equations with respect to a typical parameter α at the exclusion of A^0, a_{1i}, $a_{\beta i}$, b_{1i} and λ may now be written as

$$F_{0_{1n_\alpha}}(x,t) = A^0 e^{-\lambda t}\, {}^1P_{1n_{,\alpha}}\, U(t - \gamma_{1n}) \qquad (3\text{-}22a)$$

$$\begin{aligned} {}_1H_{lmn_{,\alpha}}(x,t) = e^{-\lambda t}\Big\{ b_{1i}\, {}^1P_{mn_{,\alpha}} + (a_{1i} - b_{1i})\Big[\, {}^1P_{lmn_{,\alpha}}\, {}^4P_{lmn}\, {}^2P_{mn} \\ + {}^3P_{lmn}\Big({}^4P_{lmn_{,\alpha}}\, {}^2P_{mn} + {}^4P_{lmn}\, {}^2P_{mn_{,\alpha}}\Big)\Big]\Big\} U(t - \gamma_{mn}) \end{aligned} \qquad (3\text{-}22b)$$

$$ {}_2H_{lmn_{,a}}(x,t) = e^{-\lambda t} a_{2l} \Bigg[\sum_{j=1}^{2} (-1)^j \; {}^9P_{jl_{,a}} \, {}^8P_{jlmn} \, {}^7P_{jlmn} + {}^9P_{jl} \left({}^8P_{jlmn_{,a}} \, {}^7P_{jlmn} + {}^8P_{jlmn} \, {}^7P_{jlmn_{,a}} \right) \Bigg] U(t - \gamma_{mn}) \tag{3-22c} $$

$$ F_{n_{,a}}(x,t) = e^{-\lambda t} a_{2n} \sum_{j=1}^{2} (-1)^j \left[{}^9P_{jn} \left({}^{10}P_{jn_{,a}} \, {}^{11}P_{jn} + {}^{10}P_{jn} \, {}^{11}P_{jn_{,a}} \right) + {}^9P_{jn_{,a}} \, {}^{10}P_{jn} \, {}^{11}P_{jn} \right] + e^{-\lambda t} \left[b_{1n} + (a_{1n} - b_{1n}) \left({}^5P_{n_{,a}} \, {}^6P_{n} + {}^5P_{n} \, {}^6P_{n_{,a}} \right) \right] \tag{3-22d} $$

the first order partial derivatives of the functions given by Equations (3-21) with respect to A^0, a_{1i}, a_{2i}, and b_{1i} may now be written as

$$ F_{o_{1n_{,A^o}}}(x,t) = e^{-\lambda t} \, {}^1P_{1n} U(t - \gamma_{1n}) \tag{3-23a} $$

$$ F_{o_{1n_{,\lambda}}}(x,t) = -t \; F_{o_{1n}}(x,t) \; U(t - \gamma_{1n}) \tag{3-23b} $$

$$ {}_1H_{lmn_{,a_{1l}}}(x,t) = e^{-\lambda t} \left[{}^3P_{lmn} \, {}^4P_{lmn} \, {}^2P_{mn} \right] U(t - \gamma_{mn}) \tag{3-24a} $$

$$ {}_1H_{lmn_{,\lambda}}(x,t) = -t \; {}_1H_{lmn}(x,t) \; U(t - \gamma_{mn}) \tag{3-24b} $$

$$ {}_1H_{lmn_{,b_{1l}}}(x,t) = e^{-\lambda t} \left[{}^1P_{mn} - {}^3P_{lmn} \, {}^4P_{lmn} \, {}^2P_{mn} \right] U(t - \gamma_{mn}) \tag{3-24c} $$

$$ {}_2H_{lmn_{,a_{2l}}}(x,t) = \frac{1}{a_{2l}} \; {}_2H_{lmn}(x,t) \; U(t - \gamma_{mn}) \tag{3-25a} $$

$$ {}_2H_{lmn_{,\lambda}}(x,t) = -t \; {}_2H_{lmn}(x,t) \; U(t - \gamma_{mn}) \tag{3-25b} $$

$$F_{n_{a_{1n}}}(x,t) = e^{-\lambda t}\ {}^5P_n\,{}^6P_n \tag{3-26a}$$

$$F_{n,a_{2n}} = e^{-\lambda t}\left[\sum_{i=1}^{2}(-1)^i\ {}^{10}P_{in}\ {}^{11}P_{in}\right] \tag{3-26b}$$

$$F_{n_{b_{1n}}}(x,t) = 1 - e^{-\lambda t}\left[{}^5P_n\,{}^6P_n\right] \tag{3-26c}$$

$$F_{n,\lambda}(x,t) = -t\,F_n(x,t) \tag{3-26d}$$

3.2.3. First Order Derivatives of the Cumulative Mass

Using the notations reported in Appendix E, the various components of Equation (2-62) may now be written as

$$Q_{0_{1n}}(x,t) = A^0\left\{-{}^0G\,{}^1G_{1n} + \left[{}^3G_{1n}^+\,{}^2G_{1n}^+ + {}^3G_{1n}^-\,{}^2G_{1n}^-\right]\right\}\ U(t-\gamma_{mn}) \tag{3-27a}$$

for a continuously decaying source

$$\begin{aligned}{}_1Q'_{lmn}(x,t) &= b_{1l}\left\{-{}^0G\,{}^1G_{mn} + {}^2G_{mn}^+\,{}^3G_{mn}^+ + {}^2G_{mn}^-\,{}^3G_{mn}^-\right\}U(t-\gamma_{mn})\\ &+(a_{1l}-b_{1l})\left\{{}^7G_l\,{}^6G_{lmn}\,{}^5G_{lmn} - {}^3G_{mn}^+\,{}^2G_{mn}^+\,{}^4G_l^- + {}^3G_{mn}^-\,{}^2G_{mn}^-\,{}^4G_l^+\right\}U(t-\gamma_{mn})\end{aligned} \tag{3-27b}$$

$$\begin{aligned}{}_2Q'_{lmn}(x,t) &= a_{2l}\sum_{j=1}^{2}(-1)^j\left\{{}^{10}G_{jl}\,{}^9G_{jlmn}\,{}^{14}G_{jl}\,{}^8G_{jlmn}\right.\\ &\left.{}^{10}G_{jl}\left(-{}^3G_{mn}^+\,{}^2G_{mn}^+\,{}^{11}G_l^- + {}^3G_{mn}^-\,{}^2G_{mn}^-\,{}^{11}G_l^+\right)\right\}U(t-\gamma_{mn})\end{aligned} \tag{3-27c}$$

$$Q_n(x,t) = a_{2n}\sum_{j=1}^{2}(-1)^j\left\{{}^{10}G_{jn}\,{}^{14}G_{jn}\left[{}^{12}G_{jn}\,{}^{13}G_{jn} + {}^{15}G_{jn}\left({}^{16}G_{jn} - 1\right)\right]\right\}$$

$$+b_{1n}\left(\frac{1}{\lambda}-{}^{0}G\right)+\left(a_{1n}-b_{1n}\right){}^{7}G_{n}\left[{}^{17}G_{n}\,{}^{18}G_{n}+{}^{19}G_{n}-1\right] \tag{3-27d}$$

The partial derivatives of the above equation with respect to a typical parameter α at the exclusion of A^{0}, a_{1l}, a_{2l}, and b_{1l} may now be written as

$$Q_{0_{1n,\alpha}}(x,t) = A^{0}\Big\{-{}^{0}G_{,\alpha}\,{}^{1}G_{1n}-{}^{0}G\,{}^{1}G_{1n,\alpha}+\Big[{}^{3}G^{+}_{1n,\alpha}\,{}^{2}G^{+}_{1n}+{}^{3}G^{+}_{1n}\,{}^{2}G^{+}_{1n,\alpha} + {}^{3}G^{-}_{1n,\alpha}\,{}^{2}G^{-}_{1n}+{}^{3}G^{-}_{1n}\,{}^{2}G^{-}_{1n,\alpha}\Big]\Big\} \tag{3-28a}$$

$$\begin{aligned}{}_{1}Q'_{lmn,\alpha}(x,t) = {} & b_{1l}\Big\{-{}^{0}G_{,\alpha}\,{}^{1}G_{mn}-{}^{0}G\,{}^{1}G_{mn,\alpha}+{}^{2}G^{+}_{mn,\alpha}\,{}^{3}G^{+}_{mn}+{}^{2}G^{+}_{mn}\,{}^{3}G^{+}_{mn,\alpha} \\ & +{}^{2}G^{-}_{mn,\alpha}\,{}^{3}G^{-}_{mn}+{}^{2}G^{-}_{mn}\,{}^{3}G^{-}_{mn,\alpha}\Big\}U(t-\gamma_{mn}) \\ & +\left(a_{1l}-b_{1l}\right)\Big\{{}^{7}G_{l,\alpha}\,{}^{6}G_{lmn}\,{}^{5}G_{lmn}+{}^{7}G_{l}\left({}^{6}G_{lmn,\alpha}\,{}^{5}G_{lmn}+{}^{6}G_{lmn}\,{}^{5}G_{lmn,\alpha}\right) \\ & -{}^{3}G^{+}_{mn,\alpha}\,{}^{2}G^{+}_{mn}\,{}^{4}G_{l}-{}^{3}G^{+}_{mn}\,{}^{2}G^{+}_{mn,\alpha}\,{}^{4}G_{l}-{}^{3}G^{+}_{mn}\,{}^{2}G^{+}_{mn}\,{}^{4}G_{l,\alpha} \\ & +{}^{3}G^{-}_{mn,\alpha}\,{}^{2}G^{-}_{mn}\,{}^{4}G^{+}_{l}+{}^{3}G^{-}_{mn}\,{}^{2}G^{-}_{mn,\alpha}\,{}^{4}G^{+}_{l}+{}^{3}G^{-}_{mn}\,{}^{2}G^{-}_{mn}\,{}^{4}G^{+}_{l,\alpha}\Big\}U(t-\gamma_{mn})\end{aligned} \tag{3-28b}$$

$$
{}_2Q'_{lmn,_a}(x,t) = a_{2l}\sum_{j=1}^{2}(-1)^j\Big\{{}^9G_{jlmn,_a}\,{}^8G_{jlmn}\Big[{}^{10}G_{jl,_a}\,{}^{14}G_{jl} + {}^{10}G_{jl}\,{}^{14}G_{jl,_a}\Big] +
$$

$$
{}^{10}G_{jl}\,{}^{14}G_{jl}\Big[{}^9G_{jlmn,_a}\,{}^8G_{jlmn} + {}^9G_{jlmn}\,{}^8G_{jlmn,_a}\Big]
$$

$$
-\,{}^{10}G_{jl,_a}\Big[{}^3G^{+}_{mn}\,{}^2G^{+}_{mn}\,{}^{11}G^{-}_{jl} - {}^3G^{-}_{mn}\,{}^2G^{-}_{mn}\,{}^{11}G^{+}_{jl}\Big]
$$

$$
-\,{}^{10}G_{jl}\Big[{}^3G^{+}_{mn,_a}\,{}^2G^{+}_{mn}\,{}^{11}G^{-}_{jl} + {}^3G^{+}_{mn}\,{}^2G^{+}_{mn,_a}\,{}^{11}G^{-}_{jl} + {}^3G^{+}_{mn}\,{}^2G^{+}_{mn}\,{}^{11}G^{-}_{jl,_a} \tag{3-28c}
$$

$$
-\,{}^3G^{-}_{mn,_a}\,{}^2G^{-}_{mn}\,{}^{11}G^{+}_{jl} - {}^3G^{-}_{mn}\,{}^2G^{-}_{mn,_a}\,{}^{11}G^{+}_{jl} - {}^3G^{-}_{mn}\,{}^2G^{-}_{mn}\,{}^{11}G^{+}_{jl,_a}\Big]\Big\}\,U(t-\gamma_{mn})
$$

$$
Q_{n,_a}(x,t) = a_{2n}\sum_{j=1}^{2}(-1)^j\Big[{}^{10}G_{jn,_a}\,{}^{14}G_{jn} + {}^{10}G_{jn}\,{}^{14}G_{jn,_a}\Big]\Big[{}^{12}G_{jn}\,{}^{13}G_{jn} + {}^{15}G_{jn}\big({}^{16}G_{jn} - 1\big)\Big]
$$

$$
+\,{}^{10}G_{jn}\,{}^{14}G_{jn}\Big[{}^{12}G_{jn,_a}\,{}^{13}G_{jn} + {}^{12}G_{jn}\,{}^{13}G_{jn,_a} + {}^{15}G_{jn,_a}\big({}^{16}G_{jn} - 1\big) + {}^{15}G_{jn}\,{}^{16}G_{jn,_a}\Big]
$$

$$
+\,b_{1n}\left(-\frac{1}{\lambda^2}\lambda_{,a} - {}^0G_{,a}\right) + (a_{1n}-b_{1n})\Big[{}^7G_{n,_a}\big({}^{17}G_n\,{}^{18}G_n + {}^{19}G_n - 1\big) \tag{3-28d}
$$

$$
+\,{}^7G_n\big({}^{17}G_{n,_a}\,{}^{18}G_n + {}^{17}G_n\,{}^{18}G_{n,_a} + {}^{19}G_{n,_a}\big)\Big]
$$

The first order derivatives of the equations given by Equations (3-27) with respect to parameters Λ^o, a_{1l}, a_{2l}, and b_{1l} are given by

$$
Q_{o_{1n},_{\Lambda^o}}(x,t) = \frac{1}{\Lambda^o}\,Q_{o_{1n}}(x,t)\;U(t-\gamma_{1n}) \tag{3-29}
$$

$$
{}_1Q'_{lmn,_{a_{1l}}}(x,t) = \Big\{{}^7G_l\,{}^6G_{lmn}\,{}^5G_{lmn} - {}^3G^{+}_{mn}\,{}^2G^{+}_{mn}\,{}^4G^{-}_l + {}^3G^{-}_{mn}\,{}^2G^{-}_{mn}\,{}^4G^{+}_l\Big\}\,U(t-\gamma_{mn}) \tag{3-30a}
$$

$$
{}_1Q'_{lmn,b_{1l}}(x,t) = \left\{ -{}^0G\,{}^1G_{mn} + {}^2G^+_{mn}\,{}^3G^+_{mn} + {}^2G^-_{mn}\,{}^3G^-_{mn} \right\} U(t-\gamma_{mn})
$$

$$
-\left\{ {}^7G_l\,{}^6G_{lmn}\,{}^5G_{lmn} - {}^3G^+_{mn}\,{}^2G^+_{mn}\,{}^4G^-_l + {}^3G^-_{mn}\,{}^2G^-_{mn}\,{}^4G^+_l \right\} U(t-\gamma_{mn}) \qquad (3\text{-}30b)
$$

$$
{}_2Q'_{lmn,a_{2l}}(x,t) = \frac{1}{a_{2l}}\,{}_2Q'_{lmn}(x,t)\,U(t-\gamma_{mn}) \qquad (3\text{-}31)
$$

$$
Q_{n,a_{1n}}(x,t) - {}^7G_n\left[{}^{17}G_n\,{}^{18}G_n + {}^{19}G_n \quad 1 \right] \qquad (3\text{-}32a)
$$

$$
Q_{n,a_{2n}}(x,t) = \sum_{j=1}^{2} (-1)^j \left\{ {}^{10}G_{jn}\,{}^{14}G_{jn}\left[{}^{12}G_{jn}\,{}^{13}G_{jn} + {}^{15}G_{jn}\left({}^{16}G_{jn} - 1 \right) \right] \right\} \qquad (3\text{-}32b)
$$

$$
Q_{n,b_{1n}}(x,t) = \frac{1}{\lambda} - {}^0G \cdot {}^7G_n\left[{}^{17}G_n\,{}^{18}G_n + {}^{19}G_n \quad 1 \right] \qquad (3\text{-}32c)
$$

3.3. NUMERICAL DERIVATIVES

The numerically derived derivatives are based on the parameter perturbation technique (see Becker and Yeh, 1972), which uses forward or central difference schemes. In such instances, the choice of the step size (or perturbation vector) usually has an important bearing on the choice of the particular scheme. The investigator is commonly confronted with the problem of deciding upon the magnitude of this parameter, which is generally selected by means of a trial-and-error procedure.

The forward-difference approximation (FDA) is given by

$$
\frac{\partial f(A)}{\partial h} = \frac{f(A+h) - f(A)}{h} + 0(h) \qquad (3\text{-}33)
$$

and the central-difference approximation (CDA) is given by

$$
\frac{\partial f(A)}{\partial h} = \frac{f(A+h) - f(A-h)}{h} + 0(h^2) \qquad (3\text{-}34)
$$

where h is the step size. Ideally, the step size should be small enough to reduce the truncation error and large enough to cause a reasonable change in the significant figures of vector A. Following Bard (1974), we write

$$h = \epsilon A$$

where $10^{-5} < \epsilon < 10^{-2}$.

Recently, Dennis and Schnabel (1983) recommended setting ϵ equal to the square root of the relative computer precision, which in our case corresponds approximately to 10^{-16}. Note that for a typical parameter, N + 1 evaluations of the response vector are required at each iteration by the FDA (compared to 2N + 1 evaluations in the case of CDA), where N corresponds to the number of observation points.

3.4. VERIFICATION

The verification of the analytically derived local sensitivities was performed by comparison of the results yielded by this solution scheme with the ones obtained through the two finite-difference appproximations discussed earlier. The exact derivatives as well as the ones yielded by FDA and CDA were estimated, based on the data presented in Table 2-1 and values of ϵ corresponding to 10^{-16}. Figures (3-1) and (3-2) illustrate the sensitivity of the concentration and cumulative mass of Np-237 in the fracture to a selected choice of parameters (i.e., b, D_p, K_f, and K_r) in each of the five fracture layers. At the exception of the very low range of sensitivities, the numerical results are in excellent agreement with the analytical ones. Note that the values obtained from both FDA and CDA methods were identical for all the investigated test cases, when the selected values of ϵ are less than 10^{-2}. A detailed examination of the sensitivities will be presented in Part 2 of this report.

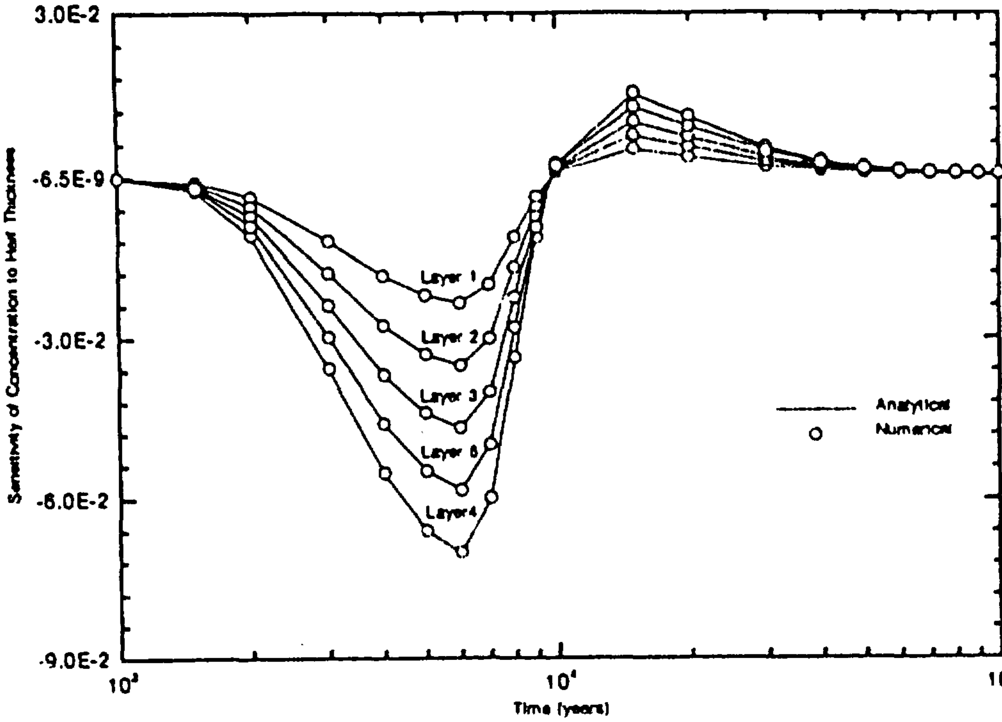

Figure 3-1a. Sensitivity of concentration to half-thickness vs. time for Np-237. (Exponentially decaying source).

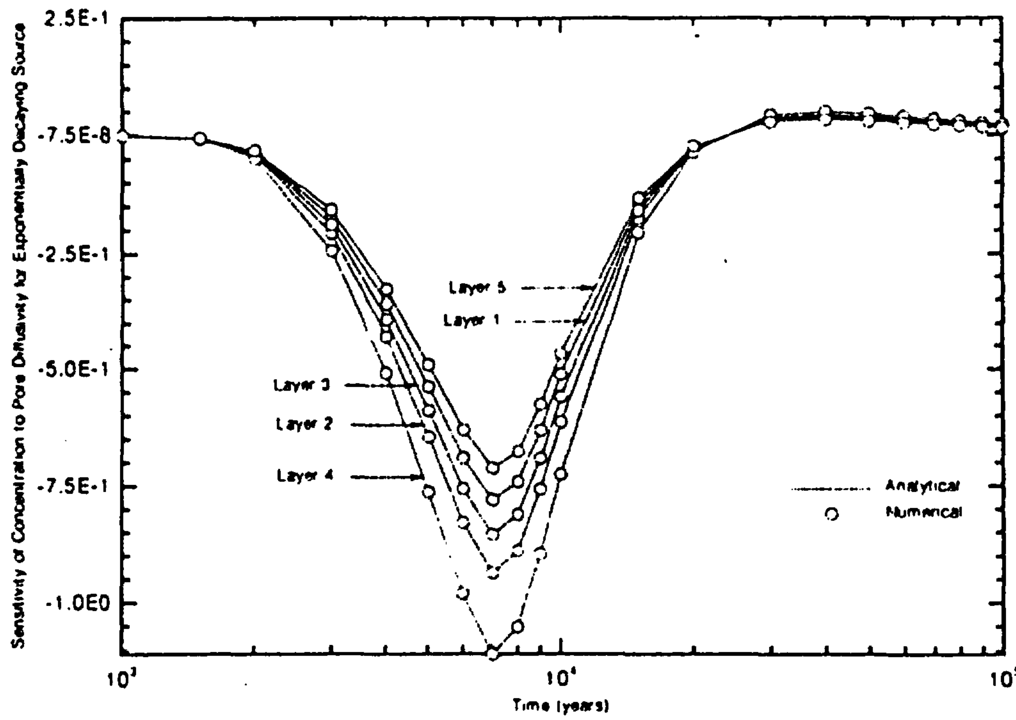

Figure 3-1b. Sensitivity of concentration to pore diffusivity vs. time for Np-237. (Exponentially decaying source).

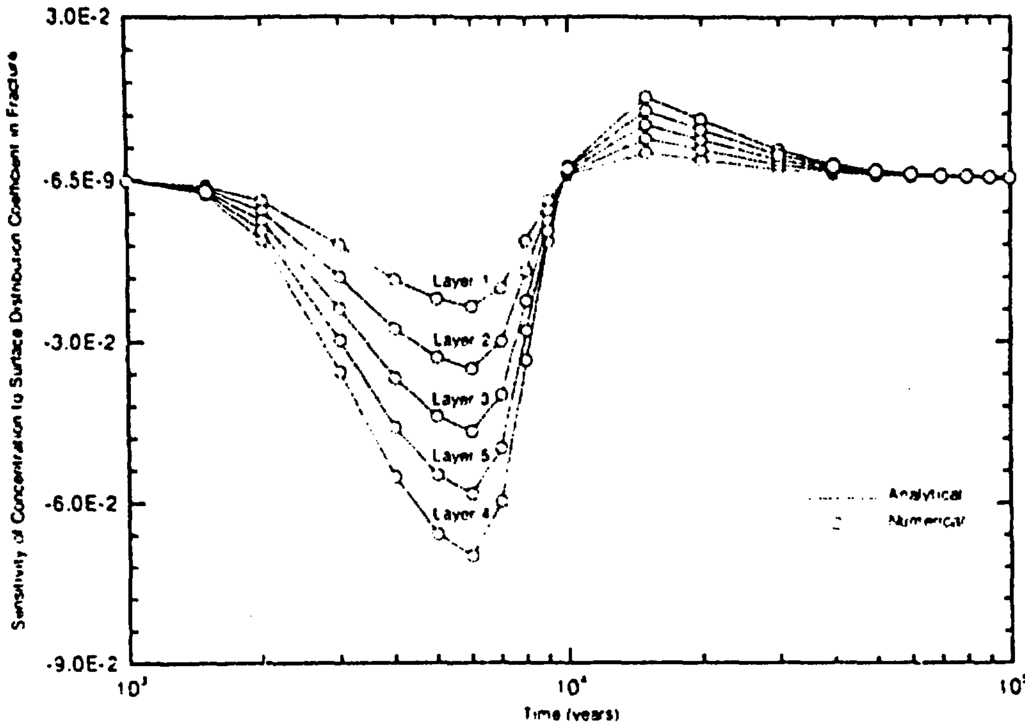

Figure 3-1c. Sensitivity of concentration to surface distribution coefficient in fracture vs. time for Np-237 (Exponentially decaying source).

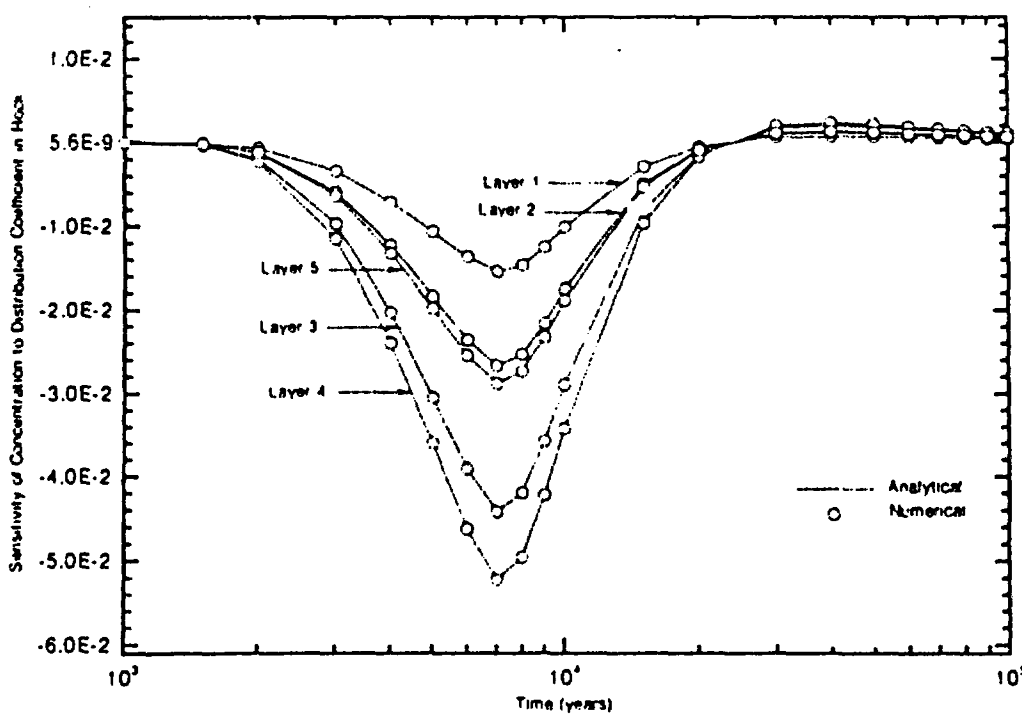

Figure 3-1d. Sensitivity of concentration to distribution coefficient in rock vs. time for Np-237 (Exponentially decaying source).

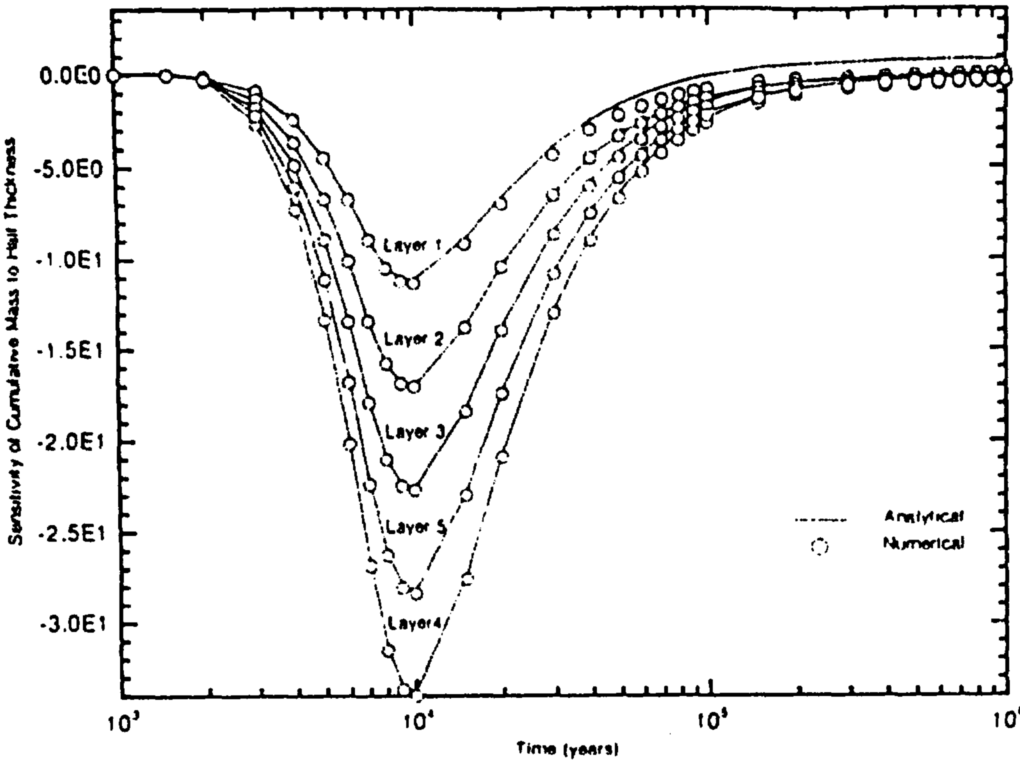

Figure 3-2a. Sensitivity of cumulative mass to half-thickness vs. time for Np-237 (Exponentially decaying source).

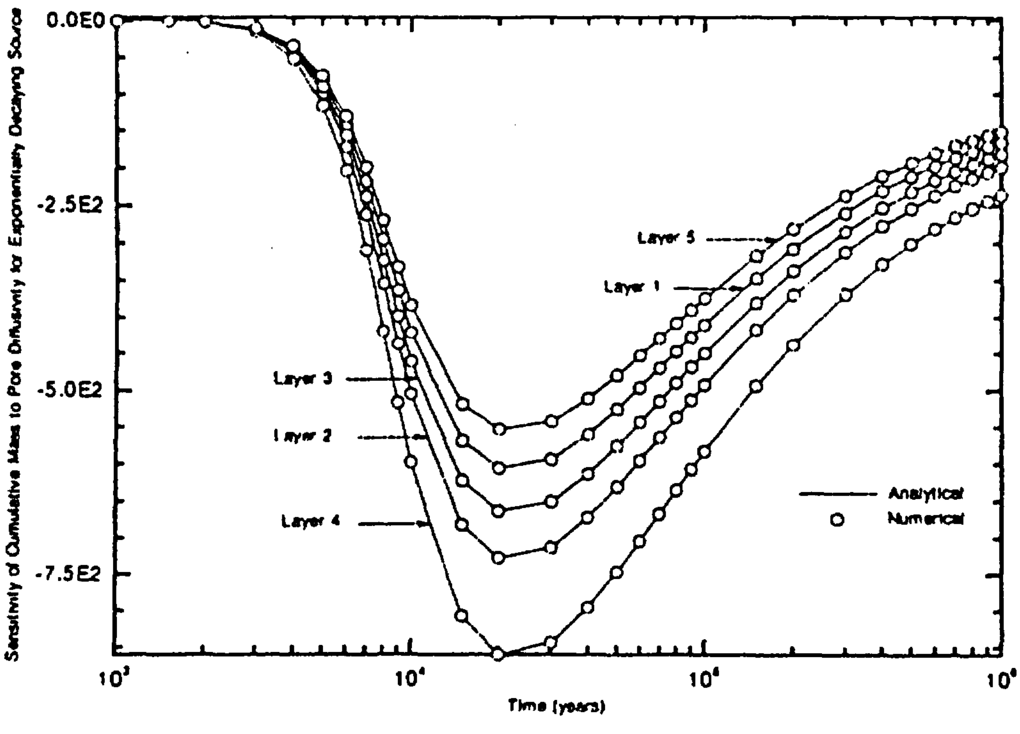

Figure 3-2b. Sensitivity of cumulative mass to pore diffusivity vs. time for Np-237 (Exponentially decaying source).

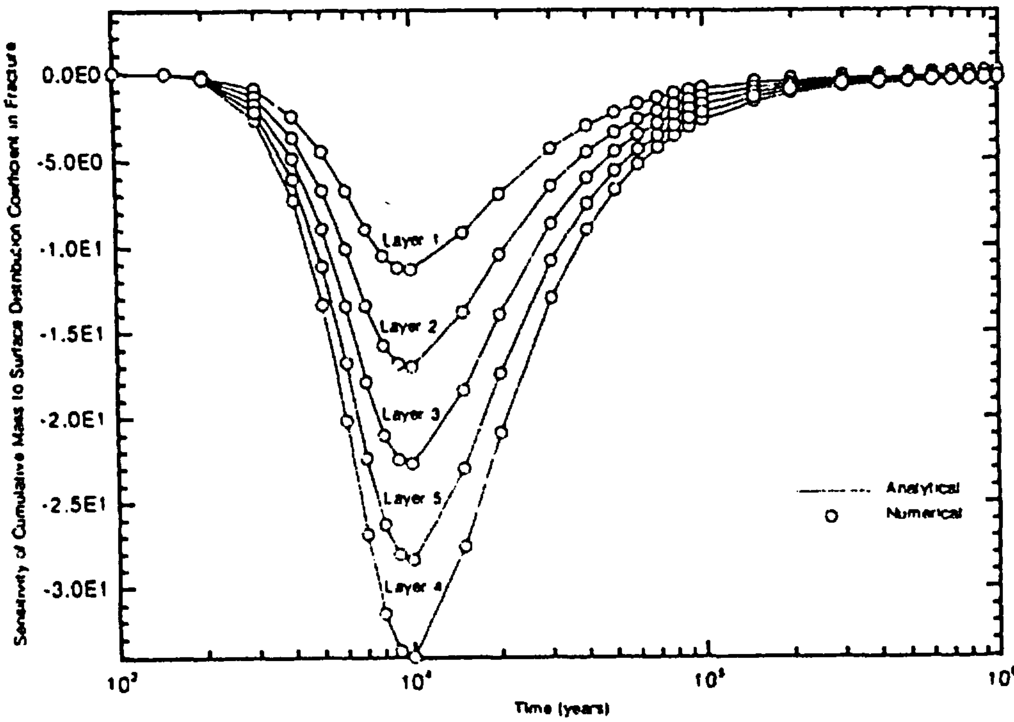

Figure 3-2c. Sensitivity of cumulative mass to surface distribution coefficient in fracture vs. time for Np-237 (Exponentially decaying source).

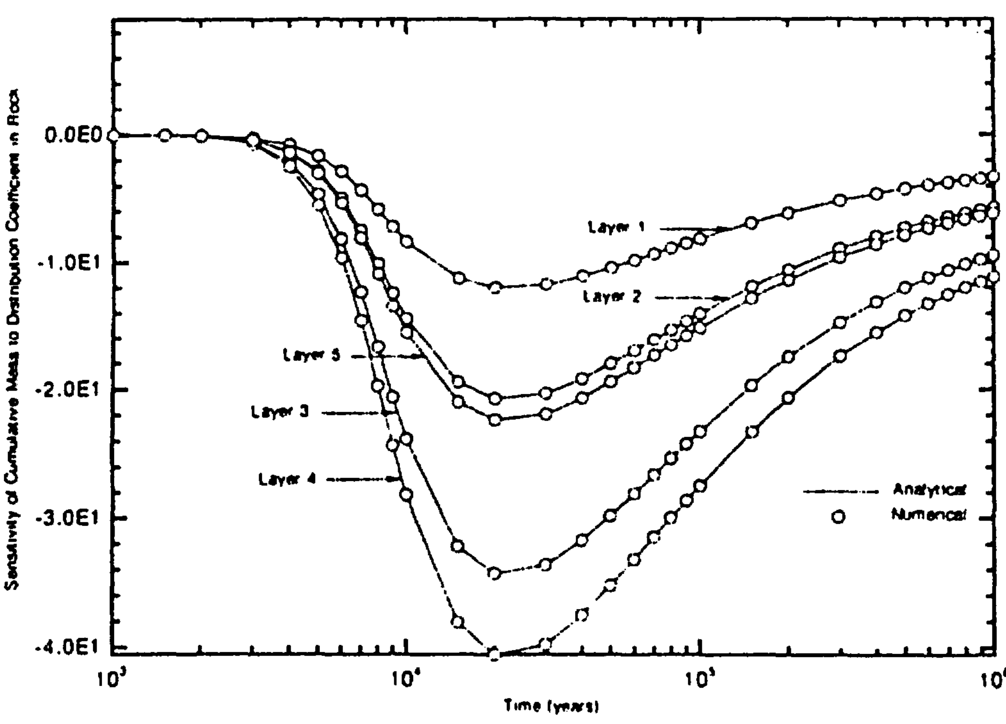

Figure 3-2d. Sensitivity of cumulative mass to distribution coefficient in rock vs. time for Np-237. (Exponentially decaying source).

4. CONCLUSIONS

Analytical solutions based on the Laplace transforms have been derived for predicting the one-dimensional non-dispersive isothermal transport of a radionuclide in a layered system of planar fractures coupled with the one-dimensional infinite diffusive transport into the adjacent rock matrix units. The solution for the cumulative mass in the fracture has also been reported.

The particular features of these solutions reside in their analytical capability designed to handle:

(a) residual concentrations in both fracture and rock matrix layers respectively. The latter are represented by a constant and/or a spatially dependent function in the case of the fracture, and a constant, in the case of the rock matrix.

(b) layered nature of the rock mass,

(c) length dependency of fracture aperture yielding a non-uniform velocity field, and

(d) both exponentially decaying and periodically fluctuating decaying source of solute at the upstream end of the fracture network, which may then be subject to either a step or band release mode.

The reported analytical solutions pertaining to the concentrations and cumulative mass were successfully verified by means of three reliable numerical methods for evaluating the inverse Laplace transform in the real and complex domain respectively. To this end, two test cases involving the migration of Np-237 and Cm-245 in a five-layered fractured rock system, using synthetic, but realistic data, were investigated. The calculated analytical local sensitivities of nuclide concentration and cumulative mass flux in fractures with respect to all of the model parameters were in excellent agreement with the ones obtained through a finite-difference method of approximation. In this particular instance, no marked evidence of a superior performance of the central over the forward finite-difference method was found as theory suggests.

In spite of some limitations (i.e., assumptions of zero dispersion in the fracture and infinite matrix diffusion), the new features embedded in the reported solutions, which allow one to deal with layered media having piece-wise constant properties, as well as non-zero initial conditions, coupled with a realistic option of a periodically fluctuating decaying source, render these solutions very useful and, above all, cost effective for performing sensitivity and uncertainty analyses of scenarios likely to be adopted in performance assessment investigations of potential nuclear waste repositories.

5. REFERENCES

Ahn, J., P. L. Chambré, and T. H. Pigford. 1986. *Radionuclide migration through fractured rock: effects of multiple fractures and two-member decay chains*. Earth Sciences Division, Lawrence Berkeley Laboratory and Department of Nuclear Engineering, University of California, Berkeley, CA.

Ahn, J., P. L. Chambré, and T. H. Pigford. 1985. *Nuclide migration through a planar fissure with matrix diffusion*. LBL-19249, Lawrence Berkeley Laboratory and Department of Nuclear Engineering, University of California, Berkeley, CA.

Bard, Y. 1974 *Nonlinear parameter estimation*. Academic Press, New York, NY

Becker, L., and W-G. Yeh. 1972. Identification of parameters in unsteady open channel flows. *Water Resour. Res.* Vol.8, No.4, pp. 956-965.

Bear, J., 1972. *Dynamics of Fluids in Porous Media*, American Elsevier Publishing Co., New York, NY.

Burkholder, H. C., M. O. Cloninger, D. A. Baker, and G. Jansen. 1976. *Incentives for partitioning high-level waste*. Nuclear Technology, Vol. 31, p. 202.

Chambré, P. L., T. H. Pigford, A. Fujita, T. Kanki, A. Kobayashi, H. Lung, D. Ting, Y. Sato, and S. J. Zavoshy. 1982. *Analytical performance models for geologic repositories*. Vol. II, LBL-14842. Lawrence Berkeley Laboratory, University of California, Berkeley, CA.

Chen, C. S. 1986. "Solutions for radionuclide transport from an injection well into a single fracture in a porous formation." *Water Resources Research*. Vol. 22, No. 4, pp. 508-518.

Dennis, Jr., J.E., and R. B. Schnabel. 1983. *Numerical methods for unconstrained optimization and nonlinear equations*. Prentice Hall, Englewood Cliffs, NJ.

Durbin, P. 1974. *Numerical inversion of Laplace transforms: an efficient improvement to Dubner and Abate's method*. Comp. J. 17, 371-376.

Foglia, M., F. Iwamoto, M. Harada, P. L. Chambré, and T. H. Pigford. 1979. "The Superposition equation for the band release of decaying radionuclides through sorbing media." UCB-NE-3335, University of California at Berkeley. *ANS Transactions*, Vol. 33, pp. 384-386.

Grisak, G. E., and J. F. Pickens. 1981. "An anlaytical solution for solute transport through fracture media with matrix diffusion." *Journal of Hydrology*. Vol. 52, pp. 47-57.

Grisak, G. E., and J. F. Pickens. 1980(a). "Solute transport through fractured media. 1. The effect of matrix diffusion." *Water Resour. Res.* 16(4): 719-730.

Grisak, G. E., Pickens, J. F., and J. A. Cherry. 1980(b). "Solute transport through fractured media, 2. Column study of fractured till." *Water Resour. Res.* 16(4): 731-739.

Gureghian, A. B. 1990a. *FRACFLO: Analytical solutions for two-dimensional transport of a decaying species in a discrete planar fracture and equidistant multiple fractures with rock matrix diffusion*. BMI/OWTD-5, p. 244. Office of Waste Technology Development, Battelle, Willowbrook, IL.

Gureghian, A. B. 1990b. *FRACVAL: Validation (nonlinear least squares method) of the solution of one-dimensional transport of a decaying species in a discrete planar fracture with rock matrix diffusion. Part I: Analytical solutions*. BMI/OWTD-8, p. 79. Office of Waste Technology Development, Battelle Energy Systems Group, Willowbrook, IL.

Gureghian, A. B. 1987. *Analytical solutions for multidimensional transport of a four-member radionuclide decay chain in ground water*. BMI/OCRD-25, p. 162. Office of Crystalline Repository Development, Battelle Memorial Institute, Columbus, OH.

Gureghian, A. B., and G. Jansen. 1985. "One-dimensional analytical solutions for the migration of a three-member radionuclide decay chain in a multilayered geologic medium." *Water Resources Research*. Vol. 21, No. 5, pp. 733-742.

Gureghian, A. B., and G. Jansen. 1983. *LAYFLO: A one-dimensional semi-analytical model for the migration of a three-member decay chain in a multilayered geologic medium*. ONWI-466, p. 87. Office of Nuclear Waste Isolation, Battelle Memorial Institute, Columbus, OH.

Hadermann, J. 1980. "Radionuclide transport through heterogeneous media." *Nuclear Technology*. Vol. 47, pp. 312-323.

Hodgkinson, D. P., and P. R. Maul. 1985. *One-dimensional modelling of radionuclide migration through permeable and fractured rock for arbitrary length decay chains using numerical inversion of Laplace transforms*. AERE-11889. AERE-Harwell, Oxfordshire, UK. p.36.

Kanki, T., A. Fujita, P. L. Chambré, and T. H. Pigford. 1981. *Transport of radionuclides through fractured media.* UCB-NE-4009. Lawrence Berkeley Laboratory, University of California, Earth Sciences Divison. Berkeley, CA.

Neretnieks, I. 1980. "Diffusion in the rock matrix: An important factor in radionuclide retardation?" *Journal of Geophysical Research.* Vol. 85, pp. 4379-4397.

Piessens, R. and R. Huysmans. 1984. *Algorithm 619: Automatic numerical inversion of the Laplace transform.* ACM Trans. Math. Softw., 10, 3, pp. 348-353.

Pigford, T. H., P. L. Chambré, M. Albert, M. Foglia, M. Harada, F. Iwamoto, T. Kanki, D. Leung, S. Masuda, S. Muraoka, and D. Ting. 1980. *Migration of radionuclides through sorbind media analytical solutions - II.* Vol. II, ONWI 360(2), LBL-11616. Lawrence Berkeley Laboratory. University of California at Berkeley.

Rasmuson, A. and I. Neretnieks. 1986. "Radionuclide transport in fast channels in crystalline rock." *Water Resources Research.* Vol. 22, pp. 1247-1256.

Rosinger, E. L. J. and K. K. R. Tremaine. 1978. *GARD2 computer program for the geochemical assessment of radionuclide disposal.* AECL-6432, Atomic Energy of Canada. Whiteshell Nuclear Research Establishment.

Shamir, U. Y. and D. R. F. Harleman. 1966. *Numerical and analytical solutions of dispersion problems in homogeneous and layered aquifers.* MIT Report No. 89, p. 206. Massachusetts Institute of Technology. Cambridge, MA.

Stefhest, H. 1970. "Numerical inversion of Laplace transforms." *Commun. ACM.* Vol. 13, No. 1, pp. 47-49.

Sudicky, E. A., and E. O. Frind. 1982. "Contaminant transport in fractured porous media: Analytical solution for a system of parallel fractures" *Water Resources Research.* Vol. 18, No. 6, pp. 1634-1642.

Sudicky, E. A. and E. O. Frind. 1984. "Contaminant transport in fractured porous media: Analytical solution for a two-member decay chain in a single fracture" *Water Resources Research.* Vol. 20, No. 7, pp. 1021-1029.

Talbot, A. 1979. *The acurate numerical inversion of Laplace's transforms.* J. Inst. Math. Applics. Vol. 23, pp. 97-120.

Tang, D. H., E. O. Frind, and E. A. Sudicky. 1981. "Contaminant transport in fractured porous media: Analytical solution for a single fracture" *Water Resources Research.* Vol. 17, No. 3, pp. 555-564.

van Genuchten, M. Th., and W. J. Alves. 1982. *Analytical solutions of the one-dimensional convective-dispersive solute transport equations*. U. S. Department of Agriculture, Technical Bulletin No. 1661.

APPENDIX A

THEOREMS AND LAPLACE TRANSFORMS

In this appendix, a selected number of theorems and inverse Laplace transforms are reported (Abramowitz and Stegun, 1972).

A.1. THEOREMS

The operations for the Laplace transformation reported in this report require, in some cases, the use of the following theorems. Note that f(s) corresponds to the Laplace transform of function F(t).

A.1.1. Translation

$$L^{-1}\left[e^{-bs}f(s)\right] = F(t-b)\,U(t-b), b>0 \qquad \text{(A.1-1)}$$

where U(t) is the Heaviside unit step function defined as

$$U(t) = \begin{cases} 0, & t<0 \\ \frac{1}{2}, & t=0 \\ 1, & t>0 \end{cases} \qquad \text{(A.1-2)}$$

A.1.2. Linear Transformation

$$L^{-1}[f(s-a)] = e^{at}F(t) \qquad \text{(A.1-3)}$$

A.1.3. Differentiation

$$L^{-1}sf(s) - F(+0) = F'(t) \qquad \text{(A.1-4)}$$

$$L^{-1}s^{n}f(s) - L^{-1}s^{n-1}F(+0) - L^{-1}s^{n-2}F'(+0) - \dots - F^{(n-1)}(+0) = F^{(n)}(t)$$

A.1.4. Convolution or Faltung

$$L^{-1}[f_1(s)f_2(s)] = \int_0^t F_1(t-\tau)F_2(\tau)d\tau = F_1 * F_2 \qquad \text{(A.1-5)}$$

In the following, the Laplace transform of the function on the right is given on the left-hand side.

Table A.1. LAPLACE TRANSFORMS

f (s)	F (t)
$\frac{1}{s+a}$	e^{-at}
$\frac{e^{-a\sqrt{s}}}{s}$	$erfc\left(\frac{a}{2\sqrt{t}}\right)$
$\frac{e^{-a\sqrt{s}}}{\sqrt{s}}$	$\frac{1}{\sqrt{\pi t}}\exp\left(-\frac{a^2}{4}t\right)$
$e^{-a\sqrt{(s)}}$	$\frac{a}{2\sqrt{\pi t^3}}\exp\left(-\frac{a^2}{4t}\right)$
$\frac{1}{\sqrt{s}(a+\sqrt{s})}$	$e^{a^2t}erfc\,a\sqrt{t}$

$\frac{e^{-k\sqrt{(s)}}}{\sqrt{s}(a+\sqrt{s})}$ $(k\geq 0)$	$e^{ak}e^{a^2t}erfc\left(a\sqrt{t}+\frac{k}{2\sqrt{t}}\right)$
$\frac{1}{\sqrt{s}+a}$	$\frac{1}{\sqrt{\pi t}} - ae^{a^2t}erfc\,a\sqrt{t}$
$\frac{e^{-k\sqrt{s}}}{a+\sqrt{s}}(k\geq 0)$	$\frac{1}{\sqrt{\pi t}}\exp\left(-\frac{k^2}{4t}\right) - ae^{ak}e^{a^2t}erfc\left(a\sqrt{t}+\frac{k}{2\sqrt{t}}\right)$
$\frac{e^{-k\sqrt{s}}}{s(a+\sqrt{s})}$	$\frac{1}{a}\left[erfc\left(\frac{k}{2\sqrt{t}}\right) - e^{ak}e^{a^2t}erfc\left(a\sqrt{t}+\frac{k}{2\sqrt{t}}\right)\right]$
$\frac{1}{s(a+\sqrt{s})}$	$\frac{1}{a}\left[1 - e^{a^2t}erfc(a\sqrt{t})\right]$
$\frac{b}{(s+a)^2+b^2}$	$e^{-at}\sin bt$

The inverse Laplace transform of the product of $1/(s^2 + a^2)$ and $e^{-a\sqrt{s}}$ may be obtained using their respective inverse transforms given in Table A.1 and applying the convolution theorem, Equation (A.1-5), to yield

$$L^{-1}\frac{e^{-a\sqrt{s}}}{s - ib} = \frac{a}{2\sqrt{\pi}}\int_0^t e^{ib(t-\tau)}\frac{e^{-\frac{a^2}{4\tau}}}{\tau^{3/2}}d\tau$$

$$= \frac{a e^{ibt}}{2\sqrt{\pi}}\int_0^t \frac{1}{\tau^{3/2}} e^{-ib\tau - \frac{a^2}{4\tau}} d\tau \qquad \text{(A.2-1)}$$

$$= \frac{a e^{ibt}}{\sqrt{\pi}}\int_{t^{-1/2}}^{\infty} e^{-\frac{a^2}{4}\tau^2 - \frac{ib}{\tau^2}}d\tau$$

Using the integral given by Equation (C-1) we get

$$L^{-1}\frac{e^{-a\sqrt{s}}}{s^2 + b^2} = L^{-1}\frac{e^{-a\sqrt{s}}}{2ib}\left[\frac{1}{s - ib} - \frac{1}{s + ib}\right] \qquad \text{(A.2-2)}$$

$$= \frac{1}{4ib}[E(t,a,ib) - E(t,a,-ib)]$$

where

$$E(t,a,ib) = e^{ibt}\left(e^{a\sqrt{ib}}\,erfc\left(\frac{a}{2\sqrt{t}} + \sqrt{ibt}\right) + e^{-a\sqrt{ib}}\,erfc\left(\frac{a}{2\sqrt{t}} - \sqrt{ibt}\right)\right) \qquad \text{(A.2-3)}$$

Substituting for $\sqrt{i}$ in Equation (A.2-3) using the following relations

$$\sqrt{i} = \left(e^{(\pi/2)i}\right)^{1/2} = \cos\frac{\pi}{4} + i\sin\frac{\pi}{4} = \frac{1 + i}{\sqrt{2}} \qquad \text{(A.2-4)}$$

yields

$$E(t,a,ib) = \exp\left[a\left(\frac{b}{2}\right)^{\frac{1}{2}} + i\left(bt + a\left(\frac{b}{2}\right)^{\frac{1}{2}}\right)\right] erfc\left[\frac{a}{2\sqrt{t}} + \left(\frac{bt}{2}\right)^{\frac{1}{2}} + i\left(\frac{bt}{2}\right)^{\frac{1}{2}}\right]$$

$$+ \exp\left[-a\left(\frac{b}{2}\right)^{\frac{1}{2}} + i\left(bt - a\left(\frac{b}{2}\right)^{\frac{1}{2}}\right)\right] erfc\left[\frac{a}{2\sqrt{t}} - \left(\frac{bt}{2}\right)^{\frac{1}{2}} - i\left(\frac{bt}{2}\right)^{\frac{1}{2}}\right] \quad \text{(A.2-5)}$$

A similar expression to the above may be obtained for E (t, a, -ib) after substituting for $\sqrt{-i}$ the following relation

$$\sqrt{-i} = \left(e^{-(\pi/2)i}\right)^{1/2} = \frac{1-i}{\sqrt{2}} \quad \text{(A.2-6)}$$

Hence

$$E(t,a,ib) - E(t,a,-ib) =$$

$$\exp(A + iB) erfc(C + iD) - \exp(A - iB) erfc(C - iD) + \quad \text{(A.2-7)}$$

$$\exp(\bar{A} + i\bar{B}) erfc(\bar{C} + i\bar{D}) - \exp(\bar{A} - i\bar{B}) erfc(\bar{C} - i\bar{D})$$

where

$$A = a\left(\frac{b}{2}\right)^{\frac{1}{2}};\ B = bt + a\left(\frac{b}{2}\right)^{\frac{1}{2}};\ C = \frac{a}{2\sqrt{t}} + \left(\frac{bt}{2}\right)^{\frac{1}{2}};\ D = \left(\frac{bt}{2}\right)^{\frac{1}{2}}$$

$$\bar{A} = -a\left(\frac{b}{2}\right)^{\frac{1}{2}};\ \bar{B} = bt - a\left(\frac{b}{2}\right)^{\frac{1}{2}};\ \bar{C} = \frac{a}{2\sqrt{t}} - \left(\frac{bt}{2}\right)^{\frac{1}{2}};\ \bar{D} = -\left(\frac{bt}{2}\right)^{\frac{1}{2}} \quad \text{(A.2-8)}$$

APPENDIX B

EVALUATION OF ERROR FUNCTION AND PRODUCT OF EXPONENTIAL AND COMPLEMENTARY ERROR FUNCTION TERMS

B.1. Error Function

The error or probability function is defined as

$$erf(x) = \frac{2}{\sqrt{\pi}} \int_0^x e^{-\xi^2} d\xi \qquad \text{(B.1-1)}$$

with

$$erf(-x) = -erf(x) \qquad \text{(B.1-2)}$$

this may be expressed in terms of the complementary error function erfc(x) written as

$$erf(x) = 1 - erfc(x) \qquad \text{(B.1-3)}$$

where

$$erfc(x) = \frac{2}{\sqrt{\pi}} \int_x^\infty e^{-\xi^2} d\xi \qquad \text{(B.1-4)}$$

and

$$erfc(-x) = 2 - erfc(x) \qquad \text{(B.1-5)}$$

Note that when x is small the integrand in Equation (B.1-1) may be conveniently expanded in a power series convergent everywhere and integrated term by term to yield

$$erf(x) = \frac{2}{\sqrt{\pi}} \left[x - \frac{x^3}{3 \cdot 1!} + \frac{x^5}{5 \cdot 2!} - \frac{x^7}{7 \cdot 3!} + \ldots + (-1)^{n+1} \frac{x^{2n+1}}{(2n+1) \cdot n!} + \ldots \right] \qquad \text{(B.1-6)}$$

A few terms in the expansion are necessary to determine the value of erf(x) to a given number of decimal places. However, as x becomes large, the loss in accuracy must be compensated by a large number of terms which renders the calculation tedious and impractical. A rational Chebysheb approximation may be used to alleviate this problem when $x \geq 4$ (see Cody, 1969). Alternatively, the asymptotic expansion reported by Abramowitz and Stegun (1972) expressed in terms of the complementary error function erfc(x) (see Equation (B.2-3)) is used. The derivative of the error function may be written as

$$\frac{d}{d\alpha}[erf(x)] = \frac{2}{\sqrt{\pi}}\exp(-x^2)\frac{dx}{d\alpha} \tag{B.1-7}$$

B.2. Formulae of Error Functions with Complex Arguments

Let z be the complex argument written as

$$z = x \pm iy \tag{B.2-1}$$

and Euler's formula written as

$$e^{iz} = \cos z + i\sin z \tag{B.2-2}$$

Note that the evolution of the error function for a real argument was based on Cody (1969).

B.2-1. Asymptotic Expansion $|z| > 2$ and $x < 1$ and $|y| \geq 6$

In this case, the asymptotic expansion of erfc(z) as given by Abramowitz and Stegun (1972) may be written as

$$erfc(z) = \frac{e^{-z^2}}{z\sqrt{\pi}}\left[1 + \sum_{n=1}^{\infty}(-1)^n\frac{1.3...(2n-1)}{(2z^2)^n}\right] + R_n(x) \tag{B.2-3}$$

where R (x) is the remainder after n terms.

B.2-2. Confluent Hypergeometric Function $|z| < 2$

In this case, the error function is evaluated from the confluent hypergeometric function (see Abramowitz and Stegun (1972) Equation (7.1.21), written as

$$erfz = \frac{2z}{\pi}M(\frac{1}{2},\frac{3}{2},-z^2) = \frac{2z}{\pi}e^{-z^2}M(1,\frac{3}{2},z^2) \tag{B.2-4}$$

where M is the Kummer's function (see Abramowitz and Stegun (1972), p.504, Equation

(13.1.2)), written as

$$M(a,b,z) = 1 + \frac{az}{b} + \frac{(a)_2 z^2}{(b)_2 2!} + \cdots \frac{(a)_n z^n}{(b)_n n!} + \cdots \qquad \text{(B.2-5a)}$$

with

$$(a)_n = a(a+1)(a+2) \cdots (a+n-1),\ (a)_0 = 1 \qquad \text{(B.2.5b)}$$

B.2-3. Continued Fraction Approximation | z | > 2 and x > 1

In this case, the error function is evaluated from the continued fractions approximations (see Abramowitz and Stegun (1972) p.298, Equation (7.1.14)), written as

$$erfc(z) = \frac{e^{-z^2}}{\sqrt{\pi}}\left[\frac{1}{z^\cdot}\,\frac{1/2}{z^\cdot}\,\frac{1}{z^\cdot}\,\frac{3/2}{z^\cdot}\,\frac{2}{z^\cdot}\cdots\right] (\mathcal{R}z > 0) \qquad \text{(B.2-6)}$$

B.2-4. Infinite Series Expansion | z | > 2, 0 ≤ x ≤ 1, y < 6

In this case, the eror function is evaluated from the infinite series approximation (see Abramowitz and Stegun (1972), p. 299, Equation (7.1.29)), written as

$$erf(x + iy) = erfx + \frac{e^{-x^2}}{2\pi x}[(1 - \cos 2xy) + i\sin 2xy]$$
$$+ \frac{2}{\pi}e^{-x^2}\sum_{n=1}^{\infty}\frac{e^{-n^2/4}}{n^2 + 4x^2}[f_n(x,y) + ig_n(x,y)] + \epsilon(x,y) \qquad \text{(B.2-7)}$$

where

$$f_n(x,y) = 2x - 2x\cosh ny\cos 2xy + n\sinh ny\sin 2xy \qquad \text{(B.2-8a)}$$

$$g_n(x,y) = 2x\cosh ny\sin 2xy + n\sinh ny\cos 2xy \qquad \text{(B.2-8b)}$$

$$|\epsilon(x,y)| \approx 10^{-16}|erf(x + iy)| \qquad \text{(B.2-8c)}$$

B.3. Evaluation of Product of Exponential and Complementary Error Function with Complex Arguments

Functions involving the product of exponential and complementary error functions may witness two types of arguments inherent to such functions, i.e., real or complex.

When the arguments of the exponential and complementary functions are both real, the scheme reported in Appendix C of Gureghian (1990) is the one adopted in this work. However, in the event where the arguments of these functions are of the complex form, the typical model for the complementary error function as reported in the preceding sections is selected based upon its adequacy to cope with the magnitude of the complex argument of interest. In the case where an infinite series approximation model for the complex error function, such as given by Equation (B.2-7) is adopted, it will be subsequently shown that expressions similar to one given by Equation A.2-7, which display a combination of products of complex exponential and complementary error functions, may yield either a real or an imaginary number.

Writing

$$F^{+}(t,A,iB,C,iD) = \exp(A + iB)\,erfc(C + iD) + \exp(A - iB)\,erfc(C - iD) \qquad \text{(B.3-1)}$$

and using Equations (B.2-2) and (B.2-7), it may be shown that the result is a real number given by

$$\begin{aligned} F^{+}(t,A,iB,C,iD) = 2\exp(A)\Bigg[\cos B\Bigg(& erfc(C) - u(C)(1 - \cos 2CD) - v(C)\sum_{n}^{\infty} r_n(C)\, f_n(C,D)\Bigg) \\ &+ \sin B\left(u(C)\sin 2CD + v(C)\sum_{n}^{\infty} r_n(C)\, g_n(C,D)\right)\Bigg] \\ &+ \epsilon(A,B,C,D) \end{aligned} \qquad \text{(B.3-2)}$$

Similarly, writing

$$F^{-}(t,A,iB,C,iD) = \exp(A + iB)\,erfc(C + iD) - \exp(A - iB)\,erfc(C + iD) \qquad \text{(B.3-3)}$$

it may be shown that the result is an imaginary number given by

$$
\begin{aligned}
F^{*}(t,A,iB,C,iD) = i2\exp(A)\Big[\sin B\Big(&erfc(C) - \\
&u(C)(1 - \cos 2CD) - v(C)\sum_{n}^{\infty} r_n(C) f_n(C,D)\Big) \\
- \cos B\Big(&u(C)\sin 2CD + v(C)\sum_{n}^{\infty} r_n(C)\, g_n(C,D)\Big)\Big] \\
&+ \epsilon(A,B,C,D)
\end{aligned}
\tag{B.3-4}
$$

where

$$
u(C) = \frac{e^{C^2}}{2\pi C} \tag{B.3-5a}
$$

$$
v(C) = \frac{2e^{-C^2}}{\pi} \tag{B.3-5b}
$$

$$
r_n(C) = \frac{e^{-\frac{n^2}{4}}}{n^2 + 4C^2} \tag{B.3-5c}
$$

and f_n, g_n and ε are given by Equations (B.2-8a) through (B.2-8c).

Equations (B.3-2) and (B.3-4) may be written in a more explicit form as

$$
\begin{aligned}
F^{+}(t,A,iB,C,iD) &= 2\Big[\cos B \, \exp(A)\, erfc(C) \\
&+ \frac{\exp(A - C^2)}{2\pi C}\left[- \cos B + \cos(B - 2CD)\right] \\
&- \frac{2}{\pi}\sum_{n=1}^{\infty} \frac{1}{n^2 + 4C^2}\Big[-n \left[E_2 - E_3\right] \sin(B - 2CD) \\
&+ 2C\left(E_1 \cos B - \cos(B - 2CD)\left(E_2 + E_3\right)\right)\Big]\Big]
\end{aligned}
\qquad \text{(B.3-6)}
$$

$$
\begin{aligned}
F^{-}(t,A,iB,C,iD) &= 2i\Big[\sin B \, \exp(A)\, erfc(C) \\
&+ \frac{\exp(A - C^2)}{2\pi C}\left[- \sin B + \sin(B - 2CD)\right] \\
&- \frac{2}{\pi}\sum_{n=1}^{\infty} \frac{1}{n^2 + 4C^2}\Big[n \left[E_2 - E_3\right] \cos(B - 2CD) \\
&+ 2C\left(E_1 \sin B - \sin(B - 2CD)\left(E_2 + E_3\right)\right)\Big]\Big]
\end{aligned}
\qquad \text{(B.3-7)}
$$

where

$$E_1 = \exp\left(A - C^2 - \frac{n^2}{4}\right) \qquad \text{(B.3-8a)}$$

$$E_2 = \frac{1}{2}\exp\left(A - C^2 - \frac{n^2}{4} + nD\right) \qquad \text{(B.3-8b)}$$

$$E_3 = \frac{1}{2}\exp\left(A - C^2 - \frac{n^2}{4} - nD\right) \qquad \text{(B.3-8c)}$$

REFERENCES:

Abramowitz, M., and I. A. Stegun. 1972. *Handbook of Mathematical Functions.* Dover Publications, Inc., New York, NY.

Cody, W. J. 1969. *Rational Chebyshev Approximation for the Error Function.* Mathematics of Computation. Vol. 23, No. 107, pp.631-637.

Gureghian, A. B. 1990. *FRACVAL Validation (Nonlinear Least Squares Method) of the Solution of One-Dimensional Transport of Decaying Species in a Discrete Planar Fracture with Rock Matrix Diffusion Part I: Analytical Solutions.* BMI/OWTD-8 Battelle Energy Systems Group, OWTD, Willowbrook, IL.

APPENDIX C

SOME INTEGRALS INVOLVING THE ERROR FUNCTION AND OTHER FUNCTIONS

This appendix reports the derivation of a number of integrals involving products of exponential and complementary error functions which are required for an exact evaluation of the cumulative mass flux presented in section 2.3.

From Abramowitz and Stegun (1972) (p.304, Eqn. 7.4.33), we have the following indefinite integral:

$$\int e^{-a^2x^2 - \frac{b^2}{x^2}} dx = \frac{\sqrt{\pi}}{4a}\left[e^{2ab} erf(ax + \frac{b}{x}) + e^{-2ab} erf(ax - \frac{b}{x})\right], \ (a \neq 0) \qquad (C.1)$$

C.1.1

Writing

$$I_1(t,\alpha,\beta,\gamma) = \int_\gamma^t e^{-\alpha\tau} erfc\left[\frac{\beta}{(\tau - \gamma)^{1/2}}\right] d\tau \qquad (C.1\text{-}1)$$

Integrating this equation by parts gives

$$I_1(t,\alpha,\beta,\gamma) = I_{11} + I_{12} \qquad (C.1\text{-}2)$$

where

$$I_{11} = \frac{e^{\alpha t}}{\alpha} erfc\left[\frac{\beta}{(t - \gamma)^{1/2}}\right] \qquad (C.1\text{-}3)$$

$$I_{12} = -\frac{2}{\alpha\sqrt{\pi}}\int_\gamma^t e^{-\alpha\tau - \frac{\beta^2}{(\tau - \gamma)}} d\left[\frac{\beta}{(\tau - \gamma)^{1/2}}\right] \qquad (C.1\text{-}4)$$

$$I_{12} = \frac{\beta e^{-\gamma\alpha}}{\alpha\sqrt{\pi}}\int_0^{t-\gamma} \frac{1}{\sqrt{\tau^3}} e^{-\alpha\tau - \frac{\beta^2}{\tau}} d\tau \qquad (C.1\text{-}5)$$

subsituting $\eta = 1/\tau^{1/2}$ in the above, and using Equation (C.1), will then yield

$$I_{12} = \frac{e^{-\alpha\gamma}}{2\alpha}\left(e^{2\beta\sqrt{\alpha}} erfc\left(\frac{\beta}{\sqrt{t - \gamma}} + \sqrt{\alpha(t - \gamma)}\right) + e^{-2\beta\sqrt{\alpha}} erfc\left(\frac{\beta}{\sqrt{t - \gamma}} - \sqrt{\alpha(t - \gamma)}\right)\right) \tag{C.1-6}$$

C.2

Writing

$$I_2(t,\alpha,\beta_1,\beta_2,\gamma) = \int_{\gamma}^{t} e^{\alpha\tau} erfc\left[\beta_1(\tau - \gamma)^{1/2} + \frac{\beta_2}{(\tau - \gamma)^{1/2}}\right] d\tau \tag{C.2-1}$$

Integration by parts gives

$$I_2(t,\alpha,\beta_1,\beta_2,\gamma) = I_{21} + I_{22} \tag{C.2-2}$$

where

$$I_{21} = \frac{e^{\alpha t}}{\alpha} erfc\left[\beta_1(t - \gamma)^{1/2} + \frac{\beta_2}{(t - \gamma)^{1/2}}\right] \tag{C.2-3}$$

and

$$I_{22} = -\frac{2}{\sqrt{\pi}\,\alpha}\int_{\gamma}^{t} e^{\alpha\tau - \left[\beta_1(\tau - \gamma)^{1/2} + \frac{\beta_2}{(\tau - \gamma)^{1/2}}\right]^2} d\left[\beta_1(\tau - \gamma)^{1/2} + \frac{\beta_2}{(\tau - \gamma)^{1/2}}\right] \tag{C.2-4}$$

substitution of $\eta = \tau - \gamma$ in the above equation gives

$$I_{22} = I_{221} + I_{222} \tag{C.2-5}$$

where

$$I_{221} = \frac{\beta_1 e^{\alpha\gamma - 2\beta_1\beta_2}}{\sqrt{\pi}\,\alpha}\int_{0}^{t-\gamma} \frac{1}{\eta^{1/2}} e^{-(\beta_1^2 - \alpha)\eta - \frac{\beta_2^2}{\eta}} d\eta \tag{C.2-6}$$

and

$$I_{222} = -\frac{\beta_2 e^{\alpha\gamma - 2\beta_1\beta_2}}{\sqrt{\pi}\,\alpha}\int_0^{t-\gamma}\frac{1}{\eta^{3/2}}e^{-(\beta_1^2 - \alpha)\eta - \frac{\beta_2^2}{\eta}}\,d\eta \qquad \text{(C.2-7)}$$

substitution of $\tau = \eta^{1/2}$ in I_{221} and $\tau = 1/\eta^{1/2}$ in I_{222} respectively, gives

$$I_{221} = 2\beta_1 \frac{e^{\alpha\gamma - 2\beta_1\beta_2}}{\sqrt{\pi}\,\alpha}\int_0^{(t-\gamma)^{1/2}} e^{-(\beta_1^2 - \alpha)\tau^2 - \frac{\beta_2^2}{\tau^2}}\,d\tau \qquad \text{(C.2-8)}$$

$$I_{222} = -2\beta_2 \frac{e^{\alpha\gamma - 2\beta_1\beta_2}}{\sqrt{\pi}\,\alpha}\int_{(t-\gamma)^{-1/2}}^{\infty} e^{-\beta_2^2\tau^2 - \frac{(\beta_1^2 - \alpha)}{\tau^2}}\,d\tau \qquad \text{(C.2-9)}$$

Using the results given by Equation (C.1), we then have

$$I_{221} = -\frac{\beta_1 e^{\alpha\gamma - 2\beta_1\beta_2}}{2\alpha(\beta_1^2-\alpha)^{1/2}}\left[e^{2\beta_2(\beta_1^2-\alpha)^{1/2}} erfc\left((\beta_1^2-\alpha)^{1/2}(t-\gamma)^{1/2} + \frac{\beta_2}{(t-\gamma)^{1/2}}\right) - e^{-2\beta_2(\beta_1^2-\alpha)^{1/2}} erfc\left(-(\beta_1^2-\alpha)^{1/2}(t-\gamma)^{1/2} + \frac{\beta_2}{(t-\gamma)^{1/2}}\right)\right]$$

(C.2-10)

$$I_{222} = -\frac{e^{\alpha\gamma - 2\beta_1\beta_2}}{2\alpha}\left[e^{2\beta_2(\beta_1^2-\alpha)^{1/2}} erfc\left(\frac{\beta_2}{(t-\gamma)^{1/2}} + (\beta_1^2-\alpha)^{1/2}(t-\gamma)^{1/2}\right) + e^{-2\beta_2(\beta_1^2-\alpha)^{1/2}} erfc\left(\frac{\beta_2}{(t-\gamma)^{1/2}} - (\beta_1^2-\alpha)^{1/2}(t-\gamma)^{1/2}\right)\right]$$

(C.2-11)

$$I_{22} = -\frac{e^{\alpha\gamma - 2\beta_1\beta_2}}{2\alpha}\left[e^{2\beta_2(\beta_1^2-\alpha)^{1/2}} erfc\left((\beta_1^2-\alpha)^{1/2}(t-\gamma)^{1/2} + \frac{\beta_2}{(t-\gamma)^{1/2}}\right)\cdot \right.$$

$$\left(\frac{\beta_1}{(\beta_1^2-\alpha)^{\frac{1}{2}}} + 1\right) - e^{-2\beta_2(\beta_1^2-\alpha)^{1/2}} \tag{C.2-12}$$

$$\left. erfc\left(-(\beta_1^2-\alpha)^{1/2}(t-\gamma)^{1/2} + \frac{\beta_2}{(t-\gamma)^{1/2}}\right)\left(\frac{\beta_1}{(\beta_1^2-\alpha)^{\frac{1}{2}}} - 1\right)\right]$$

C.3

Writing

$$I_3(t_1,t_2,\alpha,\beta) = \int_{t_1}^{t_2} e^{\alpha\tau} erfc(\beta\tau^{1/2})d\tau \tag{C.3-1}$$

Integration by parts yields

$$I_3(t_1,t_2,\alpha,\beta) = \frac{1}{\alpha}\sum_{i=1}^{2}(-1)^i\left[e^{\alpha t_i} erfc\left(\beta t_i^{1/2}\right) + \right.$$

$$\left.\frac{\beta}{(\beta^2-\alpha)^{1/2}} erf\left(\sqrt{(\beta^2-\alpha)t_i}\right)\right] \tag{C.3-2}$$

C.4

Writing

$$I_4(t,a,ib,\lambda,\gamma) = \int_{\gamma}^{t}\frac{e^{-\lambda\tau}}{4ib}[E(\tau-\gamma,a,ib) - E(\tau-\gamma,a,-ib)]d\tau \tag{C.4-1}$$

where E (t, a, ib) is given by Equation (A.2-3). Integration by parts gives

$$I_4(t,a,ib,\lambda,\gamma) = I_{41} + I_{42} \tag{C.4-2}$$

using the following definitions

$$E_1(t,a,ib) = e^{-ibt}E(t,a,ib) \tag{C-4.3a}$$

and

$$E_2(t,a,-ib) = e^{-ibt}E(t,a,-ib) \tag{C.4-3b}$$

I_{41} may then be written as

$$I_{41} = \frac{1}{4ib}\left[-\frac{e^{-(\lambda-ib)t}}{\lambda-ib}E_1(t-\gamma,a,ib) + \frac{e^{-(\lambda+ib)t}}{\lambda+ib}E_2(t-\gamma,a,-ib)\right] \tag{C.4-4}$$

multiplying the first and second terms in square brackets in the above equation, by the conjugate of their respective denominators, we then get

$$I_{41} = -\frac{e^{-\lambda t}}{4(\lambda^2+b^2)}\Big[(E_1(t-\gamma,a,ib) + E_2(t-\gamma,a,-ib)) + \frac{\lambda}{ib}(E_1(t-\gamma,a,ib) - E_2(t-\gamma,a,-ib))\Big] \tag{C.4-5}$$

Note that I_{41} corresponds to a real number, since it has been shown earlier (see Section B.3) that the sum and difference of $E_1[\,\cdot\,]$ and $E_2[\,\cdot\,]$ will yield a real and an imaginary number respectively.

$$I_{42} = \frac{1}{4ib(\lambda-ib)}\int_\gamma^t e^{-(\lambda-ib)\tau}\, d\big[E_1(\tau-\gamma,a,ib)\big] - \frac{1}{4ib(\lambda+ib)}\int_\gamma^t e^{-(\lambda+ib)\tau} d\big[E_2(\tau-\gamma,a,-ib)\big] \tag{C.4-6}$$

substituting $\tau' = \tau - \gamma$ in the above equation and after some simplifications leads to

$$I_{42} = \frac{1}{4\sqrt{\pi}ib}\left[\frac{e^{(\lambda - ib)\gamma}}{(\lambda - ib)} - \frac{e^{-(\lambda + ib)\gamma}}{(\lambda + ib)}\right]\int_0^{t-\gamma}\frac{a}{\tau'^{3/2}}e^{-\lambda\tau' - \frac{a^2}{4\tau'}}d\tau' \qquad \text{(C.4-7)}$$

substituting $\eta = 1/\tau'^{1/2}$ in the above equation yields

$$I_{42} = \frac{ae^{-\lambda\gamma}}{2\sqrt{\pi}ib}\left[\frac{e^{ib\gamma}}{(\lambda - ib)} - \frac{e^{-ib\gamma}}{(\lambda + ib)}\right]\int_{(t-\gamma)^{-\frac{1}{2}}}^{\infty}\exp\left[-\frac{a^2}{4}\eta^2 - \frac{\lambda}{\eta^2}\right]d\eta \qquad \text{(C.4-8)}$$

Using the integral given by Equation (C.1) and the following properties of a complex variable

$$\sin z = \frac{e^{iz} - e^{-iz}}{2i} \qquad \text{(C.4-9a)}$$

$$\cos z = \frac{e^{iz} + e^{-iz}}{2} \qquad \text{(C.4-9b)}$$

we then get

$$I_{42} = \frac{e^{-\lambda\gamma}(\lambda\sin b\gamma + b\cos b\gamma)}{2b(\lambda^2 + b^2)}\left[e^{a\sqrt{\lambda}}erfc\left(\frac{a}{2\sqrt{t-\gamma}} + \sqrt{\lambda(t-\gamma)}\right) + e^{-a\sqrt{\lambda}}erfc\left(\frac{a}{2\sqrt{t-\gamma}} - \sqrt{\lambda(t-\gamma)}\right)\right]$$

(C.4-10)

REFERENCES:

Abramowitz, M., and I.A. Stegun. 1972. *Handbook of Mathematical Functions*. Dover Publications, Inc. New York, NY.

APPENDIX D

FIRST ORDER DERIVATIVES OF THE COMPONENTS OF THE CONCENTRATION SOLUTION IN THE FRACTURE LAYERS

This appendix reports the first order derivatives of the components of the solution of the concentration in the fracture layers as reported in Section 3.2.2 of Chapter 3.

$$ {}^{1}P_{mn} = erfc({}^{1}f_{mn}) \tag{D-1a} $$

$$ {}^{1}f_{mn} = \frac{\theta_{mn}}{2(t - \gamma_{mn})^{1/2}} \tag{D-1b} $$

$$ {}^{1}P_{mn,_{a}} = {}^{1}_{1}P_{mn}\,{}^{1}f_{mn,_{a}} \tag{D-1c} $$

$$ {}^{1}f_{mn,_{a}} = \frac{1}{2(t-\gamma_{mn})^{1/2}}\left[\theta_{mn,_{a}} + \frac{{}^{1}f_{mn}\gamma_{mn,_{a}}}{(t - \gamma_{mn})^{1/2}}\right] \tag{D-1d} $$

$$ {}^{1}_{1}P_{mn} = -\frac{2}{\sqrt{\pi}}\exp[-{}^{1}f_{mn}^{2}] \tag{D-1e} $$

$$ {}^{2}P_{lmn} = erfc[{}^{1}f_{mn} + {}^{2}f_{lmn}] \tag{D-2a} $$

$$ {}^{2}f_{lmn} = \left(\frac{c_{fl}}{R_{l}}\right)(t - \gamma_{mn})^{1/2} \tag{D-2b} $$

$$ {}^{2}P_{lmn,_{a}} = {}^{2}_{1}P_{lmn}[{}^{1}f_{mn,_{a}} + {}^{2}f_{lmn,_{a}}] \tag{D-2c} $$

$$ {}^{2}_{1}P_{lmn} = -\frac{2}{\sqrt{\pi}}\exp\left[-({}^{1}f_{mn} + {}^{2}f_{lmn})^{2}\right] \tag{D-2d} $$

$$ {}^{2}f_{lmn,_{a}} = -\frac{c_{fl}}{2R_{l}(t - \gamma_{mn})^{1/2}}\gamma_{mn,_{a}} + \frac{(t - \gamma_{mn})^{1/2}}{R_{l}}c_{fl,_{a}} - \frac{c_{fl}(t - \gamma_{mn})^{1/2}}{R_{l}^{2}}R_{l,_{a}} \tag{D-2e} $$

$$^{3}P_{tmn} = \exp(^{3}f_{tmn}) \qquad \text{(D-3a)}$$

$$^{3}f_{tmn} = \frac{\theta_{mn} c_{ft}}{R_t} \qquad \text{(D-3b)}$$

$$^{3}P_{tmn_a} = {}^{3}P_{tmn}\, {}^{3}f_{tmn_a} \qquad \text{(D-3c)}$$

$$^{3}f_{tmn_a} = \frac{c_{ft}}{R_t}\theta_{mn_a} + \frac{\theta_{mn}}{R_t} c_{ft_a} - c_{ft}\frac{\theta_{mn}}{R_t^2} R_{t_a} \qquad \text{(D-3d)}$$

$$^{4}P_{tmn} = \exp\left[\,^{2}f_{tmn}^{2}\right] \qquad \text{(D-4a)}$$

$$^{4}P_{tmn_a} = 2\,{}^{4}P_{tmn}\, {}^{2}f_{tmn}\, {}^{2}f_{tmn_a} \qquad \text{(D-4b)}$$

$$^{5}P_{t} = \exp\left[\,^{5}f_{t}^{2}\right] \qquad \text{(D-5a)}$$

$$^{5}f_{t} = \frac{c_{ft}}{R_t} t^{1/2} \qquad \text{(D-5b)}$$

$$^{5}P_{t_a} = 2\,{}^{5}P_{t}\, {}^{5}f_{t}\, {}^{5}f_{t_a} \qquad \text{(D-5c)}$$

$$^{5}f_{t_a} = \frac{t^{1/2}}{R_t} c_{ft_a} - \frac{c_{ft}}{R_t^2} t^{1/2} R_{t_a} \qquad \text{(D-5d)}$$

$$^{6}P_{t} = erfc(^{5}f_{t}) \qquad \text{(D-6a)}$$

$$^{6}P_{t_a} = {}^{6}_{1}P_{t}\, {}^{5}f_{t_a} \qquad \text{(D-6b)}$$

$$ {}^6_1P_l = -\frac{2}{\sqrt{\pi}} \exp[-{}^5f_l^2] \tag{D-6c} $$

$$ {}^7P_{jkmn} = erfc({}^7f_{jkmn} + {}^1f_{mn}) \tag{D-7a} $$

$$ {}^7f_{jkmn} = \beta_{jk}(t - \gamma_{mn})^{1/2} \tag{D-7b} $$

$$ {}^7P_{jkmn_{,\alpha}} = {}^7_1P_{jkmn}\left(f_{jkmn_{,\alpha}} + f_{mn_{,\alpha}}\right) \tag{D-7c} $$

$$ {}^7f_{jkmn_{,\alpha}} = \beta_{jk_{,\alpha}}(t-\gamma_{mn})^{1/2} - \frac{\beta_{jk}}{2(t-\gamma_{mn})^{1/2}}\gamma_{mn_{,\alpha}} + {}^1f_{mn_{,\alpha}} \tag{D-7d} $$

$$ {}^7_1P_{jkmn} = -\frac{2}{\sqrt{\pi}}\exp\left[-\left({}^7f_{jkmn} + {}^1f_{mn}\right)^2\right] \tag{D-7e} $$

$$ {}^8P_{jkmn} = \exp[{}^8f_{jkmn}] \tag{D-8a} $$

$$ {}^8f_{jkmn} = \beta_{jk}\theta_{mn} + \beta_{jk}^2(t-\gamma_{mn}) \tag{D-8b} $$

$$ {}^8P_{jkmn_{,\alpha}} = {}^8P_{jkmn}\,{}^8f_{jkmn_{,\alpha}} \tag{D-8c} $$

$$ {}^8f_{jkmn_{,\alpha}} = \beta_{jk_{,\alpha}}\theta_{mn} + \beta_{jk}\theta_{mn_{,\alpha}} + 2\beta_{jk}\beta_{jk_{,\alpha}}(t-\gamma_{mn}) - \beta_{jk}^2\gamma_{mn_{,\alpha}} \tag{D-8d} $$

$$ {}^9P_{jk} = \frac{\beta_{jk}}{q_l} \tag{D-9a} $$

$$ {}^9P_{jk_{,\alpha}} = \frac{q_l\beta_{jk_{,\alpha}} - \beta_{jk}q_{l_{,\alpha}}}{q_l^2} \tag{D-9b} $$

$$^{10}P_{bn} = \exp\left[\,^{10}f_{bn}\right] \qquad \text{(D-10a)}$$

$$^{10}f_{bn} = -\alpha_n \chi_n + \beta_{bn}{}^2 t \qquad \text{(D-10b)}$$

$$^{10}P_{bn_a} = {}^{10}P_{bn}\ {}^{10}f_{bn_a} \qquad \text{(D-10c)}$$

$$^{10}f_{bn_a} = -\alpha_{n_a}\chi_n - \alpha_n \chi_{n_a} + 2\beta_{bn}\beta_{bn_a} t \qquad \text{(D-10d)}$$

$$^{11}P_{bn} = erfc(\,^{11}f_{bn}) \qquad \text{(D-11a)}$$

$$^{11}f_{bn} = \beta_{bn} t^{1/2} \qquad \text{(D-11b)}$$

$$^{11}P_{bn_a} = {}^{11}_{1}P_{bn}\ {}^{11}f_{bn_a} \qquad \text{(D-11c)}$$

$$^{11}f_{bn_a} = \beta_{bn_a} t^{1/2} \qquad \text{(D-11d)}$$

$$^{11}_{1}P_{bn} = -\frac{2}{\sqrt{\pi}}\exp\left[-\,{}_{11}f_{bn}{}^2\right] \qquad \text{(D-11e)}$$

APPENDIX E

FIRST ORDER DERIVATIVES OF THE COMPONENTS OF THE CUMULATIVE MASS SOLUTION IN THE FRACTURE LAYERS

This appendix reports the first order derivatives of the cumulative mass in the fracture layers as reported in Section 3.2.3 of Chapter 3.

$$ {}^{0}G = \frac{e^{-\lambda t}}{\lambda} \tag{E-1a} $$

$$ {}^{0}G_{,\alpha} = -\,{}^{0}G\left(t + \frac{1}{\lambda}\right)\lambda_{,\alpha} \tag{E-1b} $$

$$ {}^{1}G_{mn} = erfc({}^{1}h_{mn}) \tag{E-2a} $$

$$ {}^{1}h_{mn} = \frac{\theta_{mn}}{2(t - \gamma_{mn})^{1/2}} \tag{E-2b} $$

$$ {}^{1}G_{mn,\alpha} = {}^{1}_{1}G_{mn}\,{}^{1}h_{mn,\alpha} \tag{E-2c} $$

$$ {}^{1}h_{mn,\alpha} = \frac{1}{2(t-\gamma_{mn})^{1/2}}\left[\theta_{mn,\alpha} + \frac{{}^{1}h_{mn}\gamma_{mn,\alpha}}{(t - \gamma_{mn})^{1/2}}\right] \tag{E-2d} $$

$$ {}^{1}_{1}G_{mn} = -\frac{2}{\sqrt{\pi}}\exp[-\,{}^{1}h^{2}_{mn}] \tag{E-2e} $$

$$ {}^{2}G^{\pm}_{mn} = erfc[\,{}^{1}h_{mn} \pm {}^{2}h_{mn}] \tag{E-3a} $$

$$ {}^{2}h_{mn} = \sqrt{\lambda(t - \gamma_{mn})} \tag{E-3b} $$

$$ {}^{2}G^{\pm}_{mn,\alpha} = {}^{2}_{1}G^{\pm}_{mn}[\,{}^{1}h_{mn,\alpha} + {}^{2}h_{mn,\alpha}] \tag{E-3c} $$

$$ {}^{2}_{1}G^{\pm}_{mn} = -\frac{2}{\sqrt{\pi}}\exp\left[-\left({}^{1}h_{mn} \pm {}^{2}h_{mn}\right)^{2}\right] \tag{E-3d} $$

$$ {}^{2}h_{mn,_\alpha} = \frac{\lambda_{,_\alpha}(t-\gamma_{mn}) - \lambda\gamma_{mn,_\alpha}}{2[\lambda(t-\gamma_{mn})]^{1/2}} \tag{E-3c} $$

$$ {}^{3}G^{\pm}_{mn} = \frac{1}{2\lambda}\exp({}^{3}h^{\pm}_{mn}) \tag{E-4a} $$

$$ {}^{3}h^{\pm}_{mn} = -\lambda\gamma_{mn} \pm \theta_{mn}\sqrt{\lambda} \tag{E-4b} $$

$$ {}^{3}G^{\pm}_{mn,_\alpha} = {}^{3}G^{\pm}_{mn}\left[{}^{3}h^{\pm}_{mn,_\alpha} - \frac{\lambda_{,_\alpha}}{\lambda}\right] \tag{E-4c} $$

$$ {}^{3}h^{\pm}_{mn,_\alpha} = -\lambda\gamma_{mn,_\alpha} - \gamma_{mn}\lambda_{,_\alpha} \pm \left(\theta_{mn,_\alpha}\sqrt{\lambda} + \frac{\theta_{mn}}{2\sqrt{\lambda}}\lambda_{,_\alpha}\right) \tag{E-4d} $$

$$ {}^{4}G^{\pm}_{l} = \left(\frac{c_{fl}}{R_l\sqrt{\lambda}} \pm 1\right)^{-1} \tag{E-5a} $$

$$ {}^{4}G^{\pm}_{l,_\alpha} = -\,{}^{4}G^{\pm 2}_{l}\left(\frac{R_l\left(c_{fl,_\alpha}\sqrt{\lambda} - \frac{c_{fl}}{2\sqrt{\lambda}}\lambda_{,_\alpha}\right) - c_{fl}\sqrt{\lambda}R_{l,_\alpha}}{R_l^2\lambda}\right) \tag{E-5b} $$

$$ {}^{5}G_{lmn} = erfc[\,{}^{1}h_{mn} + {}^{5}h_{lmn}] \tag{E-6a} $$

$$ {}^{5}h_{lmn} = \left(\frac{c_{fl}}{R_l}\right)(t - \gamma_{mn})^{1/2} \tag{E-6b} $$

$$ {}^{5}G_{lmn,_\alpha} = {}^{5}_{1}G_{lmn}\left[{}^{1}h_{mn,_\alpha} + {}^{5}h_{lmn,_\alpha}\right] \tag{E-6c} $$

$$ {}^{5}_{1}G_{lmn} = -\frac{2}{\sqrt{\pi}} \exp\left[-\left({}^{1}h_{mn} + {}^{5}h_{lmn} \right)^2 \right] \qquad \text{(E-6d)} $$

$$ {}^{5}h_{lmn_{,\alpha}} = -\frac{c_{fl}}{2R_l(t - \gamma_{mn})^{1/2}} \gamma_{mn_{,\alpha}} + \frac{(t - \gamma_{mn})^{1/2}}{R_l} c_{fl_{,\alpha}} - \frac{c_{fl}(t - \gamma_{mn})^{1/2}}{R_l^2} R_{l_{,\alpha}} \qquad \text{(E-6e)} $$

$$ {}^{6}G_{lmn} = \exp\left[{}^{6}h_{lmn} \right] \qquad \text{(E-7a)} $$

$$ {}^{6}h_{lmn} = \frac{c_{fl}}{R_l}\left[\theta_{mn} + \left(\frac{c_{fl}}{R_l} \right)(t - \gamma_{mn}) \right] - \lambda t \qquad \text{(E-7b)} $$

$$ {}^{6}G_{lmn_{,\alpha}} = {}^{6}G_{lmn} \, {}^{6}h_{lmn_{,\alpha}} \qquad \text{(E-7c)} $$

$$ {}^{6}h_{lmn_{,\alpha}} = \frac{\theta_{mn}}{R_l} c_{fl_{,\alpha}} + \frac{c_{fl}}{R_l}\left[\theta_{mn_{,\alpha}} - \frac{\theta_{mn}}{R_l} R_{l_{,\alpha}} \right] + \frac{2c_{fl}}{R_l^3}\left(R_l c_{fl_{,\alpha}} - c_{fl} R_{l_{,\alpha}} \right)(t - \gamma_{mn}) - \left(\frac{c_{fl}}{R_l} \right)^2 \gamma_{mn_{,\alpha}} - \lambda_{,\alpha} t \qquad \text{(E-7d)} $$

$$ {}^{7}G_l = \left(\left(\frac{c_{fl}}{R_l} \right)^2 - \lambda \right)^{-1} \qquad \text{(E-8a)} $$

$$ {}^{7}G_{l_{,\alpha}} = -\,{}^{7}G_l^2 \left\{ 2\frac{c_{fl}}{R_l^3}\left(R_l c_{fl_{,\alpha}} - c_{fl} R_{l_{,\alpha}} \right) - \lambda_{,\alpha} \right\} \qquad \text{(E-8b)} $$

$$ {}^{8}G_{flmn} = erfc\left({}^{8}h_{flmn} + {}^{1}h_{mn} \right) \qquad \text{(E-9a)} $$

$$ {}^{8}h_{\beta mn} = \beta_{\beta}(t - \gamma_{mn})^{1/2} \tag{E-9b} $$

$$ {}^{8}G_{\beta mn_{,a}} = {}^{8}_{1}G_{\beta mn}\left({}^{8}h_{\beta mn_{,a}} + {}^{1}h_{mn_{,a}}\right) \tag{E-9c} $$

$$ {}^{8}h_{\beta mn_{,a}} = \beta_{\beta_{,a}}(t - \gamma_{mn})^{1/2} - \frac{\beta_{\beta}}{2(t-\gamma_{mn})^{1/2}}\gamma_{mn_{,a}} \tag{E-9d} $$

$$ {}^{8}_{1}G_{\beta mn} = -\frac{2}{\sqrt{\pi}}\exp\left[-\left({}^{8}h_{\beta mn} + {}^{1}h_{mn}\right)^{2}\right] \tag{E-9e} $$

$$ {}^{9}G_{\beta mn} = \exp[\,{}^{9}h_{\beta mn}] \tag{E-10a} $$

$$ {}^{9}h_{\beta mn} = \beta_{\beta}\theta_{mn} + \beta_{\beta}^{2}(t-\gamma_{mn}) - \lambda t \tag{E-10b} $$

$$ {}^{9}G_{\beta mn_{,a}} = {}^{9}G_{\beta mn}\,{}^{9}h_{\beta mn_{,a}} \tag{E-10c} $$

$$ {}^{9}h_{\beta mn_{,a}} = \beta_{\beta_{,a}}\theta_{mn} + \beta_{\beta}\theta_{mn_{,a}} + 2\beta_{\beta}\beta_{\beta_{,a}}(t-\gamma_{mn}) - \beta_{\beta}^{2}\gamma_{mn_{,a}} - t\lambda_{,a} \tag{E-10d} $$

$$ {}^{10}G_{\beta} = \frac{\beta_{\beta}}{q_{l}} \tag{E-11a} $$

$$ {}^{10}G_{\beta_{,a}} = \frac{q_{l}\beta_{\beta_{,a}} - \beta_{\beta}q_{l_{,a}}}{q_{l}^{2}} \tag{E-11b} $$

$$ {}^{11}G_{\beta}^{*} = \left(\frac{\beta_{\beta}}{\sqrt{\lambda}} \pm 1\right)^{-1} \tag{E-12a} $$

$$ {}^{11}G^{*}_{\ell,\alpha} = - {}^{11}G^{*2}_{\ell} \left(\frac{\sqrt{\lambda}\,\beta_{\ell,\alpha} - \frac{\beta_{\ell}}{2\sqrt{\lambda}}\lambda_{,\alpha}}{\lambda} \right) \tag{E-12b} $$

$$ {}^{12}G_{\ell n} = \exp\left[{}^{12}h_{\ell n} \right] \tag{E-13a} $$

$$ {}^{12}h_{\ell n} = -\alpha_{n}\chi_{n} + \beta^{2}_{\ell n}t - \lambda t \tag{E-13b} $$

$$ {}^{12}G_{\ell n,\alpha} = {}^{12}G_{\ell n}\; {}^{12}h_{\ell n,\alpha} \tag{E-13c} $$

$$ {}^{12}h_{\ell n,\alpha} = -\alpha_{n,\alpha}\chi_{n} - \alpha_{n}\chi_{n,\alpha} + 2t\beta_{\ell n}\beta_{\ell n,\alpha} - t\lambda_{,\alpha} \tag{E-13d} $$

$$ {}^{13}G_{\ell n} = erfc\left({}^{13}h_{\ell n} \right) \tag{E-14a} $$

$$ {}^{13}h_{\ell n} = \beta_{\ell n}t^{1/2} \tag{E-14b} $$

$$ {}^{13}G_{\ell n,\alpha} = {}^{13}_{1}G_{\ell n}\; {}^{13}h_{\ell n,\alpha} \tag{E-14c} $$

$$ {}^{13}h_{\ell n,\alpha} = \beta_{\ell n,\alpha}t^{1/2} \tag{E-14d} $$

$$ {}^{13}_{1}G_{\ell n} = -\frac{2}{\sqrt{\pi}}\exp\left[- {}^{13}h_{\ell n}^{2} \right] \tag{E-14e} $$

$$ {}^{14}G_{\ell} = \frac{1}{\beta^{2}_{\ell} - \lambda} \tag{E-15a} $$

$$ {}^{14}G_{\ell,\alpha} = - {}^{14}G^{2}_{\ell}\left(2\beta_{\ell}\beta_{\ell,\alpha} - \lambda_{,\alpha} \right) \tag{E-15b} $$

$$ {}^{15}G_{l} = e^{-\alpha_{l}\chi_{l}} \tag{E-16a} $$

$$ {}^{15}G_{l_{w_e}} = {}^{15}G_{l}\left(-\alpha_{l_{w_e}}\chi_{l} - \alpha_{l}\chi_{l_{w_e}}\right) \tag{E-16b} $$

$$ {}^{16}G_{tn} = {}^{16}_{1}h \; {}^{16}_{2}h_{tn} \tag{E-17a} $$

$$ {}^{16}_{1}h = erf\left[(\lambda t)^{1/2}\right] \tag{E-17b} $$

$$ {}^{16}_{2}h_{tn} = \frac{\beta_{tn}}{\sqrt{\lambda}} \tag{E-17c} $$

$$ {}^{16}G_{tn_{w_e}} = {}^{16}_{1}h_{w_e} \; {}^{16}_{2}h_{tn} + {}^{16}_{1}h \; {}^{16}_{2}h_{tn_{w_e}} \tag{E-17d} $$

$$ = {}^{16}_{1}h_{w_e} = \sqrt{\frac{t}{\lambda\pi}}\exp(-\lambda t)\lambda_{w_e} \tag{E-17e} $$

$$ {}^{16}_{2}h_{tn_{w_e}} = \frac{\beta_{tn_{w_e}}}{\sqrt{\lambda}} - \frac{1}{2}\frac{\beta_{tn}}{\lambda^{3/2}}\lambda_{w_e} \tag{E-17f} $$

$$ {}^{17}G_{n} = \exp\left({}^{17}h_{n}\right) \tag{E-18a} $$

$$ {}^{17}h_{n} = \left[\left(\frac{c_{fn}}{R_{n}}\right)^{2} - \lambda\right]t \tag{E-18b} $$

$$ {}^{17}h_{R_{n,\alpha}} = \left[\frac{2c_{fn}t\left(R_n c_{fn_{,\alpha}} - c_{fn}R_{n_{,\alpha}}\right)}{R_n^3} - \lambda_{,\alpha}t\right] \tag{E-18c} $$

$$ {}^{17}G_{R_{n,\alpha}} = {}^{17}G_n \; {}^{17}h_{R_{n,\alpha}} \tag{E-18d} $$

$$ {}^{18}G_n = erfc\left[{}^{18}h_n\right] \tag{E-19a} $$

$$ {}^{18}h_n = \frac{c_{fn}}{R_n}t^{1/2} \tag{E-19b} $$

$$ {}^{18}G_{R_{n,\alpha}} = -\frac{2}{\sqrt{\pi}}\exp\left(-{}^{18}h_n^2\right) {}^{18}h_{R_{n,\alpha}} \tag{E-19c} $$

$$ {}^{18}h_{R_{n,\alpha}} = \left(\frac{R_n c_{fn_{,\alpha}} - c_{fn}R_{n_{,\alpha}}}{R_n^2}\right)t^{1/2} \tag{E-19d} $$

$$ {}^{19}G_n = {}_1^{16}h \; {}^{19}h_n \tag{E-20a} $$

$$ {}^{19}h_n = \frac{c_{fn}}{R_n\sqrt{\lambda}} \tag{E-20b} $$

$$ {}^{19}G_{R_{n,\alpha}} = {}_1^{16}h_{,\alpha} \; {}^{19}h_n + {}_1^{16}h \; {}^{19}h_{R_{n,\alpha}} \tag{E-20c} $$

where ${}_1^{16}h$ is given by Equation (E-17b), and its derivative by Equation (E-17e)

$$ {}^{19}h_{R_{n,\alpha}} = \frac{\left(R_n\sqrt{\lambda}\,c_{fn'_{\alpha}} - c_{fn}\left(R_{n_{,\alpha}}\sqrt{\lambda} + \frac{R_n}{2\sqrt{\lambda}}\lambda_{,\alpha}\right)\right)}{R_n^2\lambda} \tag{E-20d} $$

APPENDIX F

NOTATIONS

a_{1i}, a_{2i}, α_i	constants in the model for residual concentrations in the ith fracture layer i
A_i	concentration of the species in the ith fracture layer
A^o	concentration of the species at the source at time equals to zero
b_i	half-thickness of the ith fracture layer
b_{1i}	residual concentration in the ith rock matrix layer
B_i	concentration of the species in the ith rock matrix layer
D_{ei}	effective diffusivity in the ith rock matrix layer
D_d	molecular diffusion of nuclide in water
D_{pi}	pore diffusivity in the ith rock matrix layer
g_{fi}	geometric factor of the ith rock matrix layer
J_i	diffusive rate of nuclide at surface of ith fracture layer per unit area of fracture surface
K_{fi}	surface distribution in the ith fracture layer
K_{ri}	distribution coefficient in the ith rock matrix layer
L_i	thickness of ith rock matrix layer
n	total number of layers
Q	steady water flow rate in fracture
R_i	retardation factor in the ith fracture layer
R'_i	retardation factor in the ith rock matrix layer
t	time
T	leaching time
T_p	time period of a complete cycle ($2\pi/\omega$)
$T_{1/2}$	half-life

u_i	average fluid velocity in the ith fracture layer
x	position vector in the fracture
z	position vector in the rock matrix
α_i	constant in model of initial concentration in the ith fracture layer
δ_{di}	constrictivity for diffusion in the ith rock layer
λ	first-order rate constant for decay
ν_1	constants in model of periodically fluctuating decaying source
ν_2	constants in model of periodically fluctuating decaying source
ρ_{ri}	rock density in the ith layer
τ_{ri}	tortuosity of the ith rock layer
Φ_i	porosity of the ith rock layer
ω	frequency of oscillation

Abbreviated Forms

$$c_{fi} = \frac{\phi_i}{b_i}(R'_i D_{pi})^{1/2}$$

$$c_{ri} = \left(R'_i / D_{pi}\right)^{1/2}$$

$$D_{ei} = \phi_i D_{pi}$$

$$\bar{L}_i = \begin{cases} L_i, & i < n \\ x - x_{i-1}, & i = n \end{cases}$$

$$p_l = u_l \alpha_l$$

$$q_l = 2\left[\left(\frac{c_{fl}}{2R_l}\right)^2 + \frac{p_l}{R_l}\right]^{1/2}$$

$$Q = 2u_l b_l$$

$$R_l = 1 + \frac{K_{fl}}{b_l}$$

$$R'_l = 1 + [(1-\Phi_l)/\Phi_l]\rho_{rl} K_{rl}$$

$$\beta_{1l} = \frac{c_{fl}}{2R_l} - \frac{q_l}{2}$$

$$\beta_{2l} = \frac{c_{fl}}{2R_l} + \frac{q_l}{2}$$

$$\overline{\eta}_l = \frac{L_l}{u_l}$$

$$\eta_l = \frac{x - x_{l-1}}{u_l}$$

$$\theta_{mn} = \sum_{l=m}^{n-1} c_{fl}\overline{\eta}_l + c_{fn}\eta_n$$

$$\theta'_n = \theta_{mn} + c_{rn}(z - b_n)$$

$$\gamma_{mn} = \sum_{i=m}^{n-1} R_i \overline{\eta}_i + R_n \eta_n$$

$$x_i = \begin{cases} x, & i = 1 \\ x - x_i, & i > 1 \end{cases}$$

APPENDIX G

MODEL PARAMETERS

The following parameters are used in the computer code (written in ANSI Standard FORTRAN 77) that implements the analytic solutions described in Section 2.

FORTRAN NAME	EXPLANATION
ALFA(I)	Constant alpha in the exponential term in residual concentration mode in the ith fracture layer (1/L)
CC0	Concentration of the species at the source at time equals zero (units of activity/L^3)
CINF(1,I)	Constant in residual concentration model in the ith fracture (units of activity/L^3)
CINF(2,I)	Coefficient of exponential term in residual concentration model in the ith fracture (units of activity/L^3)
CINR(I)	Residual concentration in the ith rock matrix layer (units of activity/L^3)
CNS(1)	Constant in periodically fluctuating decaying source term model (NPERIOD = 1)
CNS(2)	Coefficient of sine function term in periodically fluctuating decaying source term model (NPERIOD = 1)
DENSR(I)	ith Rock matrix layer bulk density (M/L^3) (used if IDIST(1) = 2)
DIFFR(I)	Pore diffusivity (L^2/T)
DIMENS(I,J)	Dimensions used in the problem; each must be ≤ 12 characters in length. (1,J) = Species name (2,J) = Time (year) (3,J) = Length (meter) (4,J) = L/T (meter/year) (5,J) = L^2/T (m^2/year) (6,J) = Mass/Volume (g/cc) (7,J) = Volume/Mass (cc/g) (8,J) = 1/Time (1./year) (9,J) = Units of Activity/Volume (UA/L^3) (10,J) = 1/L (1./meter)

FORTRAN NAME	EXPLANATION
DISTX(I)	Thickness of ith fracture or rock layer (L)
DISTRB_F(I)	ith Fracture layer surface distribution coefficient (L) (IDIST(1) = 1)
DISTRB_R(I)	ith Rock matrix layer distribution coefficient (L^3/M) (IDIST(2) = 1)
EXMAX	Largest allowed magnitude for exponential arguments (machine dependent)
FLOWR	Steady water flow rate per unit width of fracture (L^3/T)
HALFL	Half-life of species (T)
HALF_THICK(I)	Half-thickness of the ith fracture layer (L)
IAUTO	= 0 User supplies arrays REFX, REFZ, and TIME including parameters NX, NZ and NT = 1 Automatic generation of arrays REFX, REFZ and
TIME	including parameters NX, NZ and NT (see Note)
IBAND	= 0 Step release mode at source = 1 Band release mode at source
ICONCF	= 0 Do not calculate fracture concentrations = 1 Do calculate fracture concentrations
ICONCR	= 0 Do not calculate rock concentrations = 1 Do calculate rock concentrations
ICUMF	= 0 Do not calculate cumulative mass flux = 1 Do calculate cumulative mass flux
IDIST(1)	= 0 RETARD_F corresponds to retardation factor in fracture = 1 RETARD_F corresponds to surface distribution coefficient in fracture (i.e., DISTRB_F)

FORTRAN NAME	EXPLANATION
IDIST(2)	= 0 RETARD_R corresponds to retardation factor in rock matrix = 1 RETARD_R corresponds to distribution coefficient in rock matrix (i.e., DISTRB_R)
IGRAPH	= 0 Graphics output disabled = 1 Graphics output enabled; formatted graphics written to logical unit 30, 31, 32, 35, 36 Logical Unit 30: Concentrations in Fracture " " 31: Concentrations in Rock Matrix " " 32: Cumulative Mass " " 35: Concentration Sensitivities " " 36: Cumulative Mass Sensitivities
INDEX(I)	= 1 Evaluate sensitivity computation related to parameter i (i.e., NCONC_SENSIT ≥ 2) = 0 Skip
LAYER	Number of fracture/rock matrix layers
NCONC_SENSIT	= 1 Execute Module 1 (i.e., calculate concentrations and cumulative mass in the fractures and concentrations in the rock matrix = 2 Execute Module 2 (calculate sensitivity coefficients, relative sensitivies and variance = 3 Execute both Modules 1 and 2
NPERIOD	= 0 Continuously Decaying Source = 1 Periodically Fluctuating Decaying Source
NRUNMAX	Number of data sets to be run
NT	≤ 500, number of time values to be evaluated (skip if IAUTO = 1)
NVAL	Index for selecting solution module = 0 Option for analytical solutions = 1 Option for sensitivity module

FORTRAN NAME	EXPLANATION
NX	≤ 500, number of positions to be evaluated in x direction (skip if IAUTO = 1)
NZ	≤ 500, number of positions to be evaluated in x direction (skip if IAUTO = 1)
PERIOD	Time period for a complete cycle of variation in periodically fluctuating decaying source term model (NPERIOD = 1)
POROSR(I)	Average porosity in ith rock matrix layer
REFX(I)	x-position in space (L) (read if IAUTO = 0)
REFZ(I)	z-position in space (L) (read if IAUTO = 0)
RETARD_F(I)	Retardation factor in the ith fracture layer (IDIST(1) = 0) or Surface distribution coefficient (i.e., DISTRB_F) in the ith fracture layer (IDIST(1) = 1)
RETARD_R(I)	Retardation factor in the ith rock matrix layer (IDIST(2) = 0) or Distribution coefficient (i.e., DISTRB_R) in the ith rock matrix layer(IDIST(2) = 1)
STDV(I)	Standard deviation of parameter I (i.e., NCONC_SENSIT ≥ 2)
TIME(I)	Position in time (T) (read if IAUTO = 0)
TIML	Leaching time (T) (used if IBAND = 1)
TITLE	2 Lines, ≤ 80 characters per line, title of data set
VELX(I)	Average fluid velocity in the ith fracture layer (L/T)

Note: The following parameters are read-in if IAUTO = 1 in order to generate arrays REFX, REFZ and TIME and their associated parameters NX, NZ and NT.

X0	First value of spatial coordinate X = REFX(1)
DX	Spatial increment along X-axis
ENDX	Final value of spatial coordinate X = REFX(NX)

Z0	First value of spatial coordinate Z = REFZ(1)
DZ	Spatial increment along Z-axis
ENDZ	Final value of spatial coordinate Z = REFZ(NZ)
T0	First value of simulation time = TIME(1)
DT	Time increment
ENDT	End value of simulation time = TIME(NT)
NLOG	= 0 Position in space or time are equally spaced = 1 Log scale used for splitting space or time arrays: REFX, REFZ and TIME (i.e., 10 divisions per log cycle)